



## Durham E-Theses

---

### *Dielectric properties of some oxide and oxynitride glasses*

Kenmuir, S.V.J

#### How to cite:

---

Kenmuir, S.V.J (1986) *Dielectric properties of some oxide and oxynitride glasses*, Durham theses, Durham University. Available at Durham E-Theses Online: <http://etheses.dur.ac.uk/7083/>

#### Use policy

---

The full-text may be used and/or reproduced, and given to third parties in any format or medium, without prior permission or charge, for personal research or study, educational, or not-for-profit purposes provided that:

- a full bibliographic reference is made to the original source
- a [link](#) is made to the metadata record in Durham E-Theses
- the full-text is not changed in any way

The full-text must not be sold in any format or medium without the formal permission of the copyright holders.

Please consult the [full Durham E-Theses policy](#) for further details.

The copyright of this thesis rests with the author.  
No quotation from it should be published without  
his prior written consent and information derived  
from it should be acknowledged.

(1)

DIELECTRIC PROPERTIES OF SOME OXIDE

AND

OXYNITRIDE GLASSES

by

S.V.J.Kenmuir, B.Sc.(Belfast), M.Sc.(Dunelm)

Graduate Society

A Thesis submitted to the University of Durham in  
candidature for the degree of Doctor of Philosophy

May, 1986



-1. DEC. 1986

Theris  
1986/KEN

ABSTRACT

The main part of this thesis describes dielectric studies on a series of oxynitride glasses prepared at Wolfson Centre for High Strength Materials, University of Newcastle upon Tyne.

Bridge techniques were used to determine the room temperature values of permittivity ( $\epsilon'$ ) and dielectric loss ( $\epsilon''$ ) for some Y-Al-Si and Nd-Al-Si oxynitride glasses and for further compositions in the Mg-Al-Si and Ca-Al-Si systems. Over the range 500 Hz to 10 KHz the frequency dependencies of  $\epsilon'$  and conductivity ( $\sigma$ ) were found to be in good agreement with the Universal law of dielectric response

$$\text{i.e. } (\epsilon' - \epsilon_{\infty}) \propto \omega^{(n-1)}$$

$$\text{and } \sigma(\omega) \propto \omega^n$$

giving  $n = 1.0 \pm 0.1$  for all compositions examined. In all four systems the addition of nitrogen increased the permittivity while, at each concentration of nitrogen (including the oxide glasses) the permittivity increased with cation type in the order magnesium, yttrium, calcium, neodymium.

As regards the higher frequency regime coaxial line techniques were used to determine, at room temperature, both  $\epsilon'$  and  $\epsilon''$  for some Mg-Al-Si, Ca-Al-Si and Y-Al-Si oxynitride glasses over the frequency range 500 MHz to 5 GHz. Here the frequency dependencies of  $\epsilon'$  and  $\epsilon''$  are also consistent with the Universal Law of dielectric response in that  $(\epsilon' - \epsilon_{\infty}) \propto \omega^{(n-1)}$  and  $\epsilon'' \propto \omega^{(n-1)}$  for all glass compositions. The high experimental value of the exponent ( $n = 1.0 \pm 0.1$ ) suggested the limiting form of lattice loss situation. In this frequency range (as

(iii)

also at the lower frequencies) the addition of nitrogen increased the permittivity and it was confirmed that in both the oxide and oxynitride glasses  $\epsilon'$  is influenced by the cation, being increased with cation type in the order magnesium, yttrium, calcium as at lower frequencies. At still higher frequencies, in the microwave region, special cavity perturbation methods of measurement were developed and used.

Preliminary studies are also reported on the temperature dependencies of  $\epsilon'$  and  $\epsilon''$  for a similar range of glass compositions and on the optical behaviour of the oxynitride glasses both in the visible and infra-red regions of the spectrum.

In the Appendices summaries are given of published papers on oxynitride glasses (Appendix I) and also on single crystal MgO, Fe/MgO, Cr/MgO and Co/MgO (Appendix II) a study which formed an addendum to the main work.

ACKNOWLEDGEMENTS

I wish to express my sincere thanks to my Supervisors, Dr.J.S.Thorp and Dr.B.L.J.Kulesza, for their guidance and assistance ; to Professor G.C.Roberts for providing access to the facilities of the Department of Applied Physics and Electronics ; to members of the technical staff, particularly Messers R.T.Harcourt and C.Savage for their help in the sample preparation and construction of apparatus, and not least to Mrs.S.Mellanby and Mr.N.Thompson for the typing and artwork of thesis material.

I also wish to record my thanks to the Science and Engineering Research Council for the award of a postgraduate studentship.

CONTENTS

	Pages
ABSTRACT	ii
ACKNOWLEDGEMENTS	iv
CHAPTER 1 Introduction	1
CHAPTER 2 The Measurement of Permittivity and Dielectric Loss : I Low Frequency Techniques	10
2.1 Introduction	10
2.2 Bridge Methods	11
2.2.1 General features	11
2.2.2 Specimen preparation	14
2.2.3 Apparatus and procedure	14
2.2.4 Calculation of permittivity	16
2.2.5 Calculation of the dielectric loss	17
2.3 High Temperature Low Frequency Technique	18
2.4 Coaxial Line Methods	20
2.4.1 General comments	21
2.4.2 Principles of Methods	22
2.4.3 Coaxial Line Sample Holder	23
2.4.4 The Matched Termination Method	24
2.4.5 The Resonant Line Method	26
2.4.6 Conclusions	28

CHAPTER	3	The Measurement of Permittivity and Dielectric Loss ; II Microwave Techniques	30
	3.1	Choice of Experimental Technique	30
	3.2	Perturbation Theory of Resonant Cavities	33
	3.3	Specimen Preparation	39
	3.4	The Resonant Cavities	39
	3.5	Positioning the Specimen	43
	3.6	Measurement of Resonance Frequency	44
	3.7	The 9.4 GHz System	44
	3.7.1	The waveguide circuit	44
	3.7.2	Initial adjustments	46
	3.7.3	Measurement of $\epsilon'$ and $\epsilon''$ at 9.4 GHz	47
	3.8	The 2.9 GHz System	48
	3.8.1	The waveguide circuit	48
	3.8.2	Initial adjustments	48
	3.8.3	Measurement of $\epsilon'$ and $\epsilon''$	49
	3.9	Conclusion	49
CHAPTER	4	The Dielectric Behaviour of Oxynitride Glasses in the A.F. and R.F. Ranges	50
	4.1	Introduction	50
	4.2	Results in the A.F. Range	51
	4.2.1	Glass compositions	51
	4.2.2	Experimental data at A.F.	51
	4.2.3	Discussion of A.F. Data	53
	4.3	Results in the R.F. Range	56
	4.3.1	Measurement methods	56
	4.3.2	Glass compositions	57
	4.3.3	Experimental data at R.F.	58
	4.3.4	Discussion of R.F. data	59

CHAPTER	5	The Dielectric Behaviour of Oxynitride Glasses in the Microwave Frequency Range	63
	5.1	Introduction	63
	5.2	Glass Composition	63
	5.3	Specimen Dimensions and Associated Errors	63
	5.4	Experimental Microwave Data	65
	5.5	Comparison with Lower Frequency Results	66
	5.6	Discussion of Microwave Data	67
	5.7	Comparison of Cavity Perturbation and Coaxial Line Measurement Techniques	69
	5.8	The Perturbation Method at Higher Frequencies	71
CHAPTER	6	The Temperature Variations of Permittivity and Dielectric Loss	74
	6.1	Introduction	74
	6.2	Temperature Dependence of Permittivity ; Experimental Data	74
	6.3	Temperature Dependence of Dielectric Loss; Experimental Data	75
	6.4	Discussion	76
CHAPTER	7	Some Optical Properties of Oxynitride Glasses	79
	7.1	Introduction	79
	7.2	Visible/UV Absorption Spectra	80
	7.3	Infra-Red Spectra	82
APPENDIX	I	Publications Based on Studies of Oxynitride Glasses	87
APPENDIX	II	Publications Based on Work on Magnesium Oxide	88

## CHAPTER 1

## INTRODUCTION

Over the past two decades there has been a steadily increasing interest in the development of new engineering materials suitable for the wide-ranging and demanding needs of the aerospace and nuclear industries. In most of these applications several physical parameters - rather than a single one - must be optimised simultaneously because the material will be used in extreme conditions, for example of temperature and environment. Thus, using ceramic components for gas turbine engines as an example, it can be seen that engineering ceramics of this kind must combine high strength at elevated temperatures ( $\sim 1400^{\circ}\text{C}$  in the turbine) with good thermal shock properties, negligible creep, high oxidation resistance and the ability to withstand corrosive environments. In addition to areas where high strength is the first priority there has (over the same period of time) been sustained interest in some of the electrical properties of the new ceramics, particularly in regard to materials for electromagnetic windows and radome applications ; here the primary requirement is for low absorption at the electromagnetic frequency concerned (which is usually in the microwave region) but the other features listed above, particularly the strength, thermal shock resistance and thermal conductivity, are also very important.

Any material has a useful strength which may be taken as the stress that it can withstand at small strains which are usually less than about



0.1%. A strong ceramic is necessarily required to have a high value of the elastic modulus, but since many of the materials in question have potential applications in space where weight must be minimised, a better criterion is to have a high specific modulus, i.e. a high value of the ratio of elastic modulus to specific gravity. Until a few years ago the main refractory, high specific modulus materials were silicon nitride, silicon carbide, aluminium oxide, aluminium nitride, beryllium oxide and carbon fibre, all of which have specific moduli at least three times larger than the more old-established steel, glass or aluminium materials at temperatures exceeding 1900°C, (i.e. their specific moduli lie in the range  $9 \times 10^4 \text{ MNm}^{-2}$  to  $42 \times 10^4 \text{ MNm}^{-2}$  as compared with  $3 \times 10^4 \text{ MNm}^{-2}$  for steel). It is worth noting here that the combination of a high elastic constant and a low density (required to give a high specific modulus) means that the interatomic bond strength in the material must be high and that the atomic weights and co-ordination numbers must be small, a set of conditions satisfied by co-valent bonding.

Even the use of its specific modulus however is not a sufficient criterion for the overall behaviour and suitability of a particular ceramic. It is found that aluminium oxide has poor thermal shock properties while aluminium nitride is easily hydrolysed ; beryllium oxide is very toxic and carbon is also easily oxidised. Thus the choice is further restricted leaving, until relatively recently, silicon nitride as the most promising material for a high temperature ceramic because it had a unique combination of desirable properties including high strength, good wear resistance, a high decomposition temperature, good oxidation resistance, a low coefficient of friction, high resistance to attack in corrosive environments and, (by no means least

important) excellent thermal shock properties.

Although studies of glass manufacturing processes led to the discoveries that nitrogen can be chemically incorporated into oxide glasses [1.1, 1.2, 1.3, 1.4] and that quantities as small as 1% improved certain physical properties [1.5, 1.6, 1.7], much recent interest in oxynitride glasses as a class of materials with wide industrial potential has arisen from their connection with modern high-performance engineering ceramics. Intensive research on the preparation and properties of silicon nitride had been initiated at many laboratories, including The Crystallography Laboratory, University of Newcastle-upon-Tyne, and work on the development of silicon nitride ceramics led Wild, Grievson and Jack to predict in 1968 [1.8] that, just as wide ranges of aluminosilicates are formed from the basic  $(SiO_4)$  and  $(AlO_4)$  tetrahedra, so corresponding ranges of new materials both crystalline and non-crystalline could be formed from  $(Si, Al)(O, N)_4$  tetrahedra. They were given the name "Sialons" by Jack [1.9]. Ceramic materials of this type were discovered independently in Japan [1.10, 1.11] and in England [1.12]; the vitreous materials were found to occur on the manufacture of silicon nitride. When silicon nitride is made by hot pressing with additives (included to improve densification) a liquid phase formed at high temperatures can be cooled to an oxynitride glass, rather than to an oxide glass as first thought. More importantly, the finished ceramic contains a glassy grain boundary phase which greatly influences its mechanical properties at high temperatures, and this has also been identified as an oxynitride glass [1.13, 1.14]. The initial researches on the three fabrication techniques of hot-pressing, reaction bonding

and pressureless sintering led to a broader interest in the general field of nitrogen ceramics. This interest was in turn further extended by the discovery made by Jack and Wilson [1.12] and independently by Oyama and Kamigaito [1.10] that in silicon nitride it was possible to replace silicon by aluminium and also to replace nitrogen by oxygen without changing the structure. This led to the realisation that there was a very wide field of nitrogen ceramics able to be formed by alloying silicon nitride with alumina and other metal oxides and nitrides. The name "sialon" [ Jack, 1.9 ] has become a generic term for phases in the Si-Al-O-N and related systems which are primarily alumino-silicates in which oxygen is partially or completely replaced by nitrogen and which may be either crystalline or vitreous in nature. Again the sialons showed advantages over silicon nitride as regards their physical properties particularly in respect of specific modulus, and high temperature strength.

About eight years ago it was found, within the general framework of research into sialon structures, that bulk nitrogen glasses could be made in the magnesium-silicon-oxygen-nitrogen system and also in the yttrium and magnesium sialon systems [ Jack, 1.16]. Glassy phases had been previously observed during densification of silicon nitride by hot-pressing or pressureless-sintering with an oxide additive, which can provide suitable conditions for liquid phase sintering. Magnesium, for example, reacts with the surface layer of silicon which is always present on the surface of the silicon nitride, resulting in a glass with a low softening temperature occurring at grain boundaries ; in this instance the inter-granular vitreous phase is deleterious since the creep resistance of the high density silicon nitride decreases rapidly

above 1000°C. A different type of result occurs when hot-pressing silicon nitride with yttria ; a Y-Si-O-N liquid forms which reacts with more nitride to give a very refractory complex oxynitride glass which improves the high temperature properties of the silicon nitride. It is now generally accepted that these glassy phases are in fact oxy-nitrides [Jack, 6.9, Drew et al 1.19].

The importance of these glasses in the performance of silicon nitride ceramics, the realisation that appropriate oxynitride glasses might result in glass ceramics which could be shaped in the glassy phase before devitrification to crystalline phases of highly refractory nitrides and oxynitrides together with the indications from the earlier work that the inclusion of nitrogen might produce glasses with technologically useful properties, has led to increased interest in the preparation and properties of oxynitride glasses. Jack et al [ 1.15, 1.16 ] reported Mg-Si-Al-O-N, Y-Si-Al-O-N and Li-Si-Al-O-N glasses containing 10-12 atomic % nitrogen. Shillito [ 1.17 ] achieved up to 5 atomic % nitrogen in Y-Si-Al-O-N glasses. Loebman [ 1.18 ] prepared Y-Si-Al-O-N glasses containing up to 7 atomic % nitrogen and mentioned that some La-Si-Al-O-N and Ca-Si-Al-O-N glasses had also been made. Ca-Si-Al-O-N and Nd-Si-Al-O-N glasses with 10-12 atomic % have been reported by Jack, Thompson, Hampshire and Drew [1.19, 1.20, 1.21].

One of the first systematic attempts to fabricate a series of bulk specimens of oxy-nitride glasses was made by Drew [ 1.21 ] working at the Crystallography Laboratory, University of Newcastle-upon-Tyne and all the specimens examined in the work described in this thesis came from

that source. The details of the preparative methods adopted have been discussed at length by Drew [Drew, Ph.D.Thesis 1.21]. In most instances silicon nitride was used as a starting nitride although some compositions used aluminium nitride or a mixture of aluminium nitride and silicon nitride. Compositions in the Magnesium-aluminium-silicon, the calcium-aluminium-silicon, the yttrium-aluminium-silicon and the neodymium-aluminium-silicon oxy-nitride glass systems were made, starting from mixtures of powders of the appropriate components subsequently formed into pellets which, after being introduced into either a high alumina or boron nitride crucible, were fired at about 1700°C in a tungsten resistance furnace or at higher temperatures in an inductively heated graphite furnace. The design of the furnaces available to Drew limited the fusions to batches of about 20 gm in weight when preparing specimens for property measurement but despite restrictions imposed by the dimensions of the hot zones of the various furnaces - usually only a few centimetres long at maximum - it was possible for specimens of about 1 cm diameter and up to 1 cm thick to be produced in most instances. The availability of specimens of this order of size was essential - as will become evident later - in order to enable the dielectric measurement programme forming the bulk of the work described in the present thesis to be undertaken.

At the time when the present work was commenced there was already a strong interest in the Department of Applied Physics and Electronics at Durham University both in the development of precision techniques for the measurement of permittivity and dielectric loss and in the study of the dielectric behaviour of ceramics. Low frequency bridge techniques

had been applied to the study of doped calcium tungstate [Thorp and Ammar, 1.22], a material used in single crystal form for laser rods, and yttria stabilised zirconia [Thorp and Buckley, 1.23] whose potential as a refractory electrode in magneto-hydrodynamic generators was being assessed; while the former study provided an example of a precise measurement on several single, chemically well-defined materials, the latter illustrated the use of dielectric measurement in identifying impurities, in this instance colloidal zirconium formed by solid state electrolysis. Later similar precise low frequency bridge methods were employed in an extensive study of doped magnesium oxide single crystals [Thorp and Rad 1.24] where it was shown that the effects due to different substitutional dopants could be followed at dopant concentrations of as little as a few hundred ppm. The specific interest in the behaviour of oxy-nitride glasses arose from two main considerations. In the first- and more general- instance there had become available a new group of materials and it was of scientific importance to assess whether their dielectric properties fitted the general pattern found for oxide glasses with particular regard to the conductivity mechanisms involved and to the changes in behaviour, if any, caused by the introduction of nitrogen. In the second place there was an interest in the potential use of oxy-nitride glasses as electro-magnetic window and radome materials as alternatives to silicon nitride, alumina or oxide glass ceramics. This second interest highlighted the area of measurement techniques where additional effort was required. Since the relevant frequency range of operation for window and radome materials is, broadly, in the microwave region (typically

around 9 GHz) there was a need to develop suitable techniques not only at these microwave frequencies but also, in order to follow the frequency variation of permittivity and dielectric loss and to allow detailed comparison with low frequency data, at some or all of the intermediate positions over this wide range of nearly seven decades of frequency. In this situation it quickly became apparent that, although there were many possible techniques listed in the literature, there were very few which appeared capable (without further refinement) of the accuracies required when dealing with loss-loss material. Furthermore, an additional interest in the radome context lay in the infra-red absorbtive properties of the oxy-nitride glasses, since in modern applications radomes may be used to house both microwave radar and *infra-red* sensing equipment simultaneously.

As a result of these considerations the work described in this thesis was arranged so as to cover both research into experimental methods for the precise determination of permittivity and dielectric loss of low loss materials over a very wide range of frequencies and the application of these general methods to the specific study of oxy-nitride glasses. In summary, Chapter 2 outlines low frequency techniques for the measurement of permittivity and dielectric loss, giving details of the requirements on specimen geometry, the apparatus and experimental procedure and the methods of calculating the permittivity ( $\epsilon'$ ) and dielectric loss ( $\epsilon''$ ) concluding with a discussion of the modifications in technique required to enable low frequency measurements to be made at high temperatures of up to 1000°C. The extension of measurement techniques to the microwave region is discussed in Chapter 3 which describes the perturbation theory of resonant

cavities, and the constructional and operational features of measurement systems operating at 2.9 GHz and 9.4 GHz respectively. The dielectric behaviour of oxy-nitride glasses in the audio-frequency (A.F.) region is described in Chapter 4 which details the experimental results for a number of glasses of different compositions and interprets the data in terms of a hopping conductivity model fitting the Universal Law of dielectric response. Chapter 5 extends this discussion to the higher frequency range by giving the microwave data obtained and comparing it with that obtained at lower frequencies. The temperature dependence of the permittivity and dielectric loss is reported and analysed in terms of loss peaks in Chapter 6. Finally an account of preliminary optical (infra-red) studies of the  $\lambda$ .r.spectra and absorption properties of the oxy-nitride glasses is given in Chapter 7 while the Appendices include reprints of published papers on the dielectric behaviour of doped magnesium oxide, which were also completed during the period of the main research.

## CHAPTER 1

### REFERENCES

- 1.1 H. O. Mulfinger and H. Meyer, *Glastech. Ber.* 36 [1963] 481.
- 1.2 H. O. Mulfinger and H. Franz, *Glastech. Ber.* 38 [1965] 235.
- 1.3 H. O. Mulfinger, *J. Amer.Ceram. Soc.* 49 [1966] 462.
- 1.4 V. T. Kelen and H. O. Mulfinger, *Glastech. Ber.* 41 [1968] 230.
- 1.5 T. H. Elmer and M. G. Nordberg, 7th Int.Cong.Glass, Brussels (1965) 30.
- 1.6 T. H. Elmer and M. G. Nordberg, *J. Amer.Ceram.Soc.* 50 (1967) 275.
- 1.7 F. L. Harding and R. J. Ryder, *Glass Tech.* 11 [1970] 54.
- 1.8 S. Wild, P. Grievson and K.H.Jack, 1968 Progress Report No.1, Ministry of Defence Contract N/Cp.61/9411/67/4B/Mp, 387.  
S. Wild, P. Grievson and K.H.Jack, "Special Ceramics 5" Ed. P. Popper (1972) 289.
- 1.9 K. H. Jack, *Trans. J. Brit.Ceram.Soc.* 72 (1973) 376.
- 1.10 Y. Oyama and O. Kamigaito, *Japan J. Applied Phys.* 10 (1971) 1637.
- 1.11 Y. Oyama, *Japan J. Applied Phys.* 11 (1972) 760.
- 1.12 K.H.Jack and W.I.Wilson, *Nature* 238 (1972) 28.
- 1.13 K. Nuttall and D.P.Thompson, *J. Mater.Sci.* 9 (1974) 850.
- 1.14 S. Wild, P. Grievson, K.H.Jack and M.J.Latimer, "Special Ceramics 5", Ed. P.Popper (1972) 377.
- 1.15 K.H.Jack, *Proc.Nato Adv.Study Inst. "Nitrogen Ceramics"*, Canterbury 1976, 257.
- 1.16 K.H.Jack, *J.Mater.Sci.* 11 (1976) 1135.
- 1.17 K.R.Shillito, R.R.Wills and R.B.Bennett, *J.Amer.Ceram.Soc.* 61 (1978) 537.

- 1.18 R.E.Loehman, J. Amer.Ceram.Soc., 62 (1979) 491.
- 1.19 K.H.Jack, D.P.Thompson, S. Hampshire, R.A.L. Drew, private communications 1980.
- 1.20 S. Hampshire, Ph.D.Thesis 1980, University of Newcastle upon Tyne.
- 1.21 R.A.L.Drew, Ph.D.Thesis 1980, University of Newcastle upon Tyne.
- 1.22 J.S.Thorp, E.A.E.Ammar, J. Mat.Sci 10, (1975), 918.
- 1.23 J.S.Thorp and H.P.Buckley, J.Mat.Sci 8 (1973), 1401.
- 1.24 J.S.Thorp, N.E.Rad, J.Mat.Sci 16, (1981), 255.

## CHAPTER 2

## THE MEASUREMENT OF PERMITTIVITY AND DIELECTRIC LOSS ;

## I LOW FREQUENCY TECHNIQUES

2.1 INTRODUCTION

In general, the dielectric properties of solids are measured by constructing part of an electric component or circuit from the solid and measuring its properties. The finite bandwidths of practical components and circuits means that measurement over a wide frequency range requires the use of more than one technique.

The group at Durham has been building a capability for very broad band dielectric measurement by designing a range of compatible techniques. These have been designed to accept small specimens so that new materials can be investigated on becoming available in laboratory quantities.

This work involved the development of techniques which could detect small differences in dielectric constants between different materials, in order to study relationships between dielectric constants and composition when composition is changed by small amounts. Of the techniques developed, the low frequency and radio frequency techniques are described in this chapter, and the microwave techniques are described in Chapter 3.

Other techniques used without additional development are also described briefly in this chapter.

## 2.2 BRIDGE METHODS

### 2.2.1 General features

For frequencies in the range 500 Hz to 20 KHz, specimen material was used as the dielectric of a parallel plate capacitor whose capacitance  $C$  and conductance  $G$  were measured with a transformer ratio arm bridge. From these and the capacitor dimensions  $\epsilon'$  and  $\epsilon''$  were calculated.

If the parallel plate capacitor were 'ideal', as in Fig 2.1a,  $\epsilon'$  and  $\epsilon''$  could be calculated simply from

$$C = \frac{\epsilon' \epsilon_0 A}{d} \quad (2.1)$$

and

$$G = \frac{\omega C \epsilon''}{\epsilon'} \quad (2.2)$$

where  $A$  is the electrode area,  $d$  the electrode separation and  $\epsilon'$ ,  $\epsilon''$  the characteristics of the material between the plates. These equations hold exactly if the electric field is everywhere perpendicular to the electrodes and does not extend beyond them, the contact between electrode and dielectric is perfect, and all current flow is through the bulk of the dielectric. In practice this is seldom true and additional terms are required, giving equations whose form depends on the details of the apparatus and the technique employed.

In a real parallel plate capacitor (Fig 2.1b) the electric field extends beyond the electrode edges giving an actual value of capacitance greater than the ideal value of  $(\epsilon_0 \epsilon' A/d)$  by an amount  $C_e$ , known as the edge or fringe capacitance. Its magnitude is determined by the

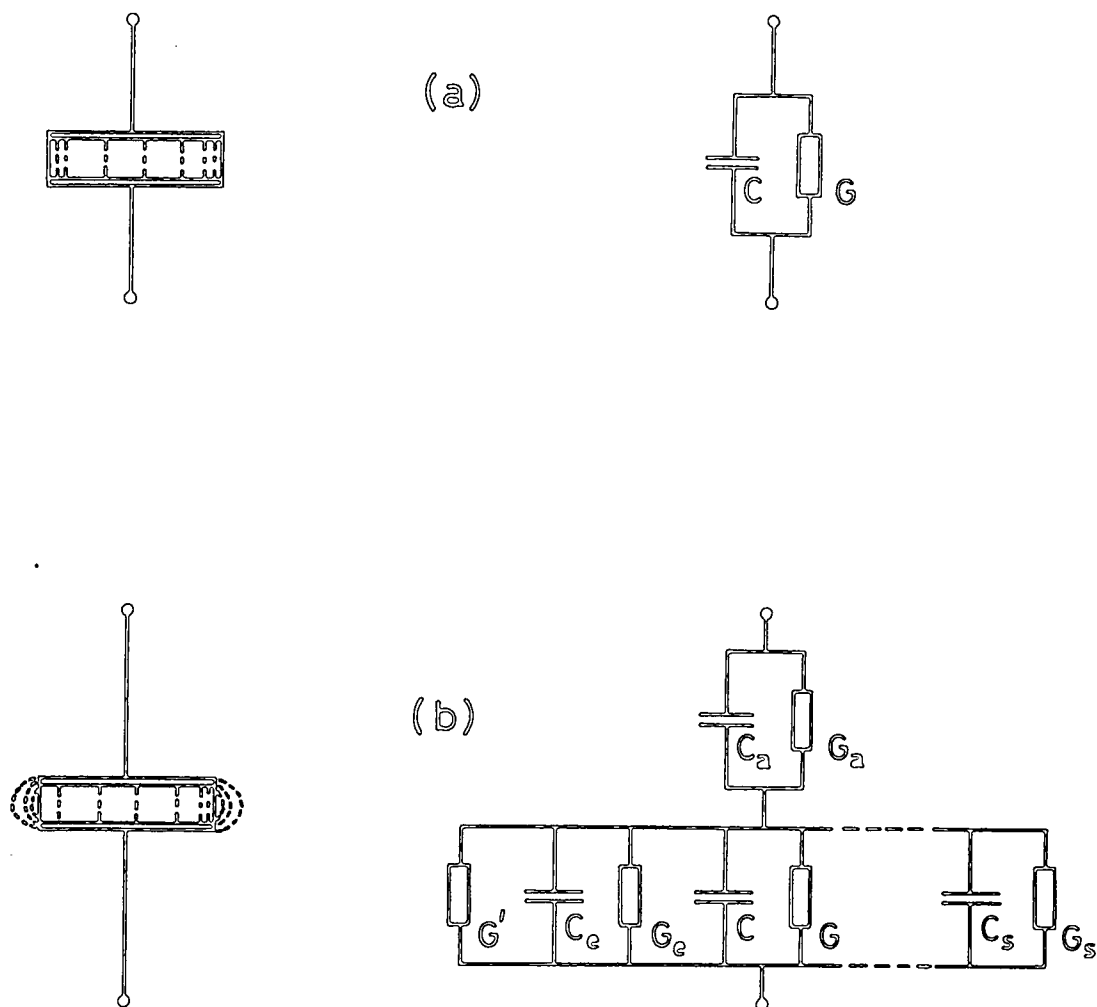


FIG.2.1. THE ELECTRIC FIELDS ON a) AN IDEAL AND b) A REAL PARALLEL PLATE CAPACITOR, AND THE EQUIVALENT CIRCUITS.

$C$  ,  $G$  ARE 'IDEAL' VALUES

$C_a$  ,  $G_a$  THE AIR GAP CONTRIBUTIONS

$C_e$  ,  $G_e$  THE EDGE EFFECTS

$G'$  THE SURFACE LEAKAGE AND

$C_s$  ,  $G_s$  THE STRAYS IN THE CONNECTING LEADS AND APPARATUS.

electrode dimensions. It can be calculated for most electrode configurations [Scott and Curtis, 2.1, Lynch 2.2] and can be as much as 10% of the total capacitance.

Gaps between the electrodes and the specimen surfaces form small air-dielectric capacitors in series with the test capacitor, and so introduce errors into both capacitance and conductance. As small values of capacitance and conductance have a large effect on total performance when connected in series, even very small airgaps produce serious errors. These must be reduced, either by eliminating the airgaps by the prior application of thin metal secondary electrodes to the dielectric surface, or by using a deliberate airgap.

The use of a deliberate airgap is the recommended standard technique in both Britain and America. Detailed descriptions are given for this frequency range in Lynch [2.3, 2.4], British Standards Institute (B54542 1970) and ASTM (D-9), and for slightly higher frequencies in Hartshorn and Ward [2.5], BS2067 [1953] and ERA [1973]. The parallel plate capacitor is measured firstly with the specimen placed loosely between the plates, and secondly without a specimen.

Although experimentally quick and convenient for comparing different specimens, and with accurately calculable edge capacitance [Lynch 2.2, Blanco White 2.6], preliminary tests showed that the small sizes and low dielectric losses of the oxynitride specimens produced changes in conductance too small for accurate measurement by this method. Secondary electrodes were therefore used.

The configuration of the secondary electrodes affects both the accuracy of the conductance measurement and the value of the edge capacitance.

For the conductance measurement to be accurate, surface conduction over the edges of the dielectric must be small in comparison with the conduction through the bulk material. If electrodes smaller than the specimen can be used, the increase in the length of the surface path increases surface resistance and reduces surface conductance [Hartshorn and Ward 2.5, Blumenthal and Seitz 2.7]. This technique was used here, as electrodes small enough to reduce the surface conduction to acceptable levels also gave satisfactory values of capacitance and conductance. Edge capacitances were calculated from the formulae of Scott and Curtis [2.1].

The alternative technique of using a third guard electrode was experimentally more complicated and offered little advantage in accuracy. In such an arrangement the guard electrode is connected to earth. Current paths exist between each large electrode and the guard electrode but not between the large electrodes, thus preventing surface conduction contributing to the conductance measurement. Edge capacitance can be reduced by suitable design of the guard electrode [Van Hippel 2.8]. If the guard is at least twice as wide as the specimen is thick, the extent of the fringing field and hence the magnitude of the edge capacitance is determined by the width of the gap, and can be made small.

Gold was used for the secondary electrodes. It does not tend to diffuse into glassy materials under electric fields except at high temperatures. Aluminium, copper and silver diffuse more readily and oxidise more quickly [Dalton 2.9, Kim and Tomozawa 2.10]. The conductivity of gold at these frequencies is high enough for the rather thin electrodes produced by evaporation to be satisfactory. Evaporation with suitable masks has the advantage of producing well defined electrodes with sharp edges, whose area can be measured accurately.

Although thick, higher conductivity electrodes can be obtained by using metal foils, these have to be rolled onto the material with low electrical loss adhesive such as silicon grease, and then trimmed to size. Metal paints have lower conductivities but contain solvents which must be removed by baking.

### 2.2.2 Specimen Preparation

Specimens 0.5 mm thick were cut from the bulk material on a diamond wheel cutting machine. Diameters were limited to about 10 mm by the size of the bulk pieces. Care was taken to make the large surfaces flat and parallel. They were polished with diamond paste to a  $0.25 \mu$  finish. Circular gold electrodes 6mm in diameter were evaporated onto the flat surfaces. The specimens were cleaned and dried before applying the gold films. After the evaporation they were handled with degreased tweezers to avoid surface contamination which might increase surface conduction. The electrode diameters were measured with a travelling microscope, and as the specimens were not opaque this was also used to check the electrode alignment.

### 2.2.3 Apparatus and Procedure

The main electrode system which formed the parallel plate capacitor is shown in Fig.2.2. The electrodes were brass, electrically isolated by perspex mountings. The specimen with gold secondary electrodes was placed on the lower electrode, which was fixed. The upper electrode whose vertical position was controlled by a micrometer head was lowered to make firm contact with the specimen. The brass electrodes were made slightly smaller than the gold electrodes, so that the gold defined the area of material to which the electric field was applied. The resistance of the gold film at these frequencies was too small for the projection of the gold beyond the main electrode to cause significant

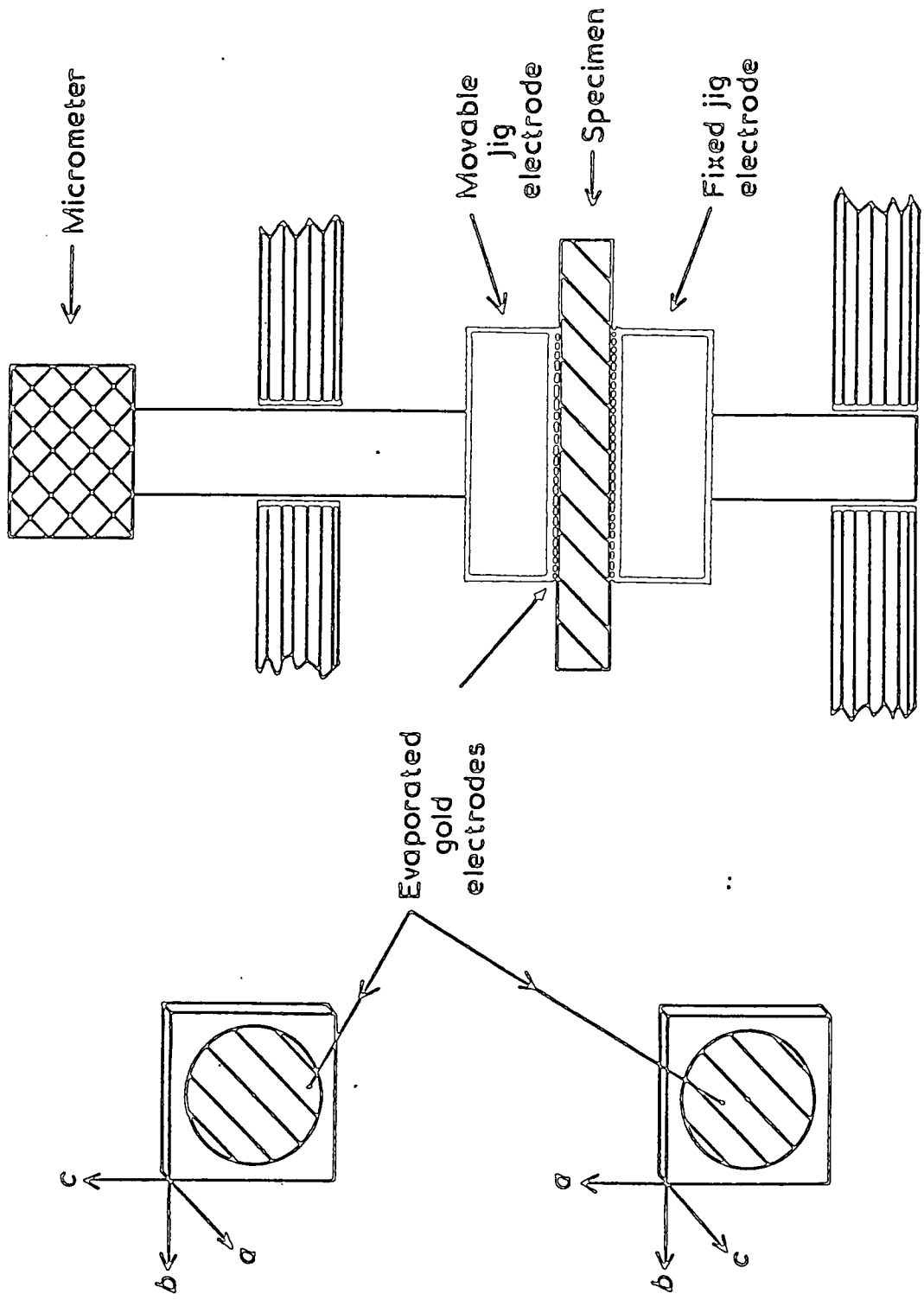


FIG.2.2. General form of specimen and dielectric testing jig.

errors : test measurements on one set of gold electrodes with brass electrodes of large and small diameters showed no measurable difference. The system was enclosed in a metal box, isolated from both electrodes and earthed to bridge earth, thus providing good electromagnetic screening. Bridge connections were made by screened leads. A standard Wayne Kerr B224 bridge was used. At balance this gave direct readings of capacitance and conductance. With the specimen in position, a tray of dry silica gel was placed inside the screened enclosure, about 20 minutes before taking measurements. This ensured that the specimen was measured in a dry atmosphere, and prevented condensation on the specimen surface and the perspex mountings forming leakage current paths. The bridge was first trimmed with neither apparatus nor leads connected to it. The apparatus containing the specimen was then connected, and the bridge was balanced, giving the total capacitance  $C_1$  and the total conductance  $G_1$ .  $C_1$  and  $G_1$  were noted at several frequencies in the range. The specimen was removed, the upper electrode was reset to the same position, and the bridge was rebalanced at the same frequencies, giving  $C_2$  and  $G_2$ . These values allowed the stray capacitance and conductance to be estimated. For each specimen, measurements were made at least twice with each set of evaporated gold electrodes, and with at least two different sets of evaporated gold electrodes. This was essential as occasionally poor evaporation, although visually perfect, gave results which were in error by 50%-100%. This was thought to be caused by contamination of the specimen immediately before the evaporation.

#### 2.2.4 Calculation of permittivity

The relative dielectric constant (permittivity) is given by the ratio

$$\epsilon' = \frac{C}{C_0} \quad (2.3)$$

where  $C$  = the capacitance of a capacitor with the material as dielectric.

$C_0$  = the capacitance of the same capacitor with air as dielectric.

As the dielectric constant of air,  $\epsilon_0$ , is known,  $C_0$  can be calculated from the electrode dimensions and measurement of  $C$  therefore gives  $\epsilon'$ .

The measured value  $C_1$  comprises the capacitance of the specimen capacitor,  $C$ , and the stray capacitance in the apparatus,  $C_s$ .

$$C_1 = C + C_s \quad (2.4)$$

The value  $C_2$  comprises the capacitance of the capacitor formed by the main electrodes with air as dielectric,  $C_m$ , and the same stray capacitance.

$$C_2 = C_m + C_s \quad (2.5)$$

Subtracting eliminates  $C_s$ , which is not calculable.

$$C = C_1 - C_2 + C_m \quad (2.6)$$

The dielectric constant is given by

$$\epsilon' = \frac{C}{C_g} = \frac{C_1 - C_2 + C_m}{C_g} \quad (2.7)$$

where  $C_g$  is the capacitance of the capacitor formed by the gold

secondary electrodes with air as dielectrics.  $C_1$  and  $C_2$  are known ;  $C_m$  and  $C_g$  are calculable.

$C$  includes a contribution due to edge capacitance which is not cancelled when  $C_2$  is subtracted from  $C_1$  as its magnitude is different in each case : for  $C_2$  the fringing electric field is in air, while for  $C_1$  it is mostly in the part of the specimen material which extends beyond the electrodes. As  $C$  includes edge capacitance,  $C_m$  and  $C_g$  must also include the appropriate edge capacitance contributions if the formula for  $\epsilon'$  is to be valid. Following Scott and Curtis [2.1], the corrected values were calculated from :

$$C_m = \frac{\epsilon_o A_m}{d} + \left( \frac{1.113 D_m}{8\pi} \right) \left[ \ln \left( \frac{8\pi D_m}{d} \right) - 3 \right] \quad (2.8)$$

$$C_g = \frac{\epsilon_o A_g}{d} + \left( \frac{1.113 D_g}{8\pi} \right) \left[ \ln \left( \frac{8\pi D_g}{d} \right) - 3 \right] \quad (2.9)$$

where  $A_m$ ,  $D_m$  are the area and diameter of the gold secondary electrodes, and  $A_g$ ,  $D_g$ , those of the main electrodes of the apparatus.  $d$  is the electrode separation.

#### 2.2.5 Calculation of the dielectric loss

The measured value  $G_1$  includes the stray conductance in the apparatus,  $G_2$ . Taking the conductance of dry air as negligible, the value  $G_2$  gives the stray conductance directly. The conductance of the specimen material is therefore

$$G = G_1 - G_2 \quad (2.10)$$

The loss factor  $\epsilon''$ , loss tangent  $\tan \delta$ , and conductivity  $\sigma$  were calculated from the standard dielectric formulae

$$\tan \delta = \frac{G}{\omega C} \quad (2.11)$$

$$\epsilon'' = \epsilon' \tan \delta \quad (2.12)$$

$$\sigma = \frac{d G}{A g} \quad (2.13)$$

where  $\omega$  is the angular frequency at which  $C_1$ ,  $G_1$ ,  $C_2$  and  $G_2$  were measured.

### 2.3 HIGH TEMPERATURE LOW FREQUENCY TECHNIQUE

Measurements were made over the frequency range 500 Hz to 20 KHz at temperatures up to 500°C by suspending the same plate specimens measured at room temperature inside a vertical furnace, and measuring capacitance and conductance on the Wayne Kerr B224 bridge. Gold electrodes were evaporated onto the specimen as before. Short platinum wires were cemented to the gold with platinum paste.

The furnace arrangement is shown in Fig 2.3. The specimen was suspended from platinum wires threaded through a silica tube and leading to the bridge connections. A thermocouple monitored the temperature near the specimen. A steel furnace tube was used, earthed to provide electromagnetic screening of the specimen area. The top of the furnace was also shielded and all leads entering the shielded area were screened. The furnace heating current and controller were switched off while each measurement was being made. A water-cooled collar at the top of the furnace tube kept the area outside the tube at room temperature, providing a constant ambient temperature for connections and equipment.

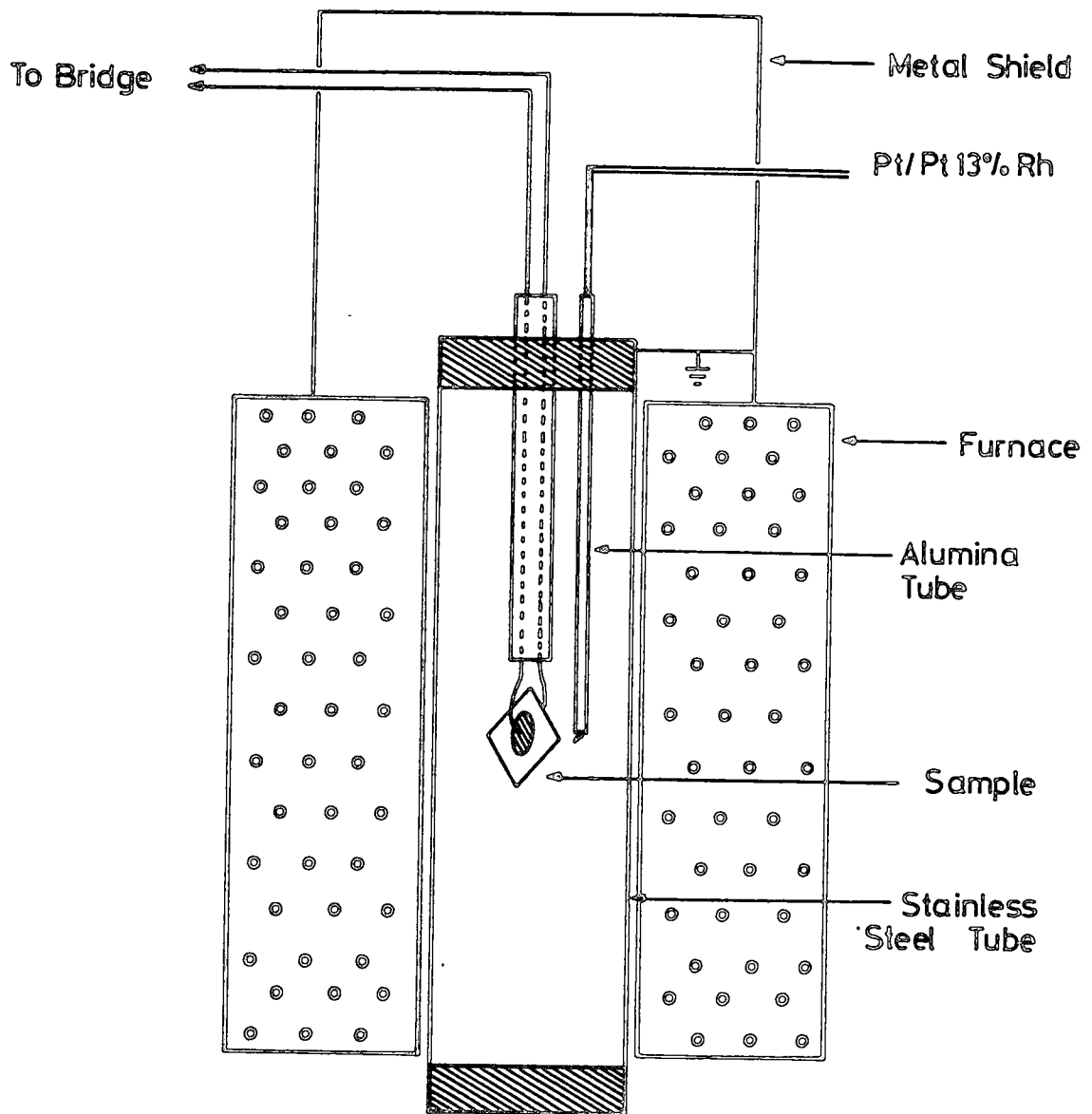


FIG.2-3. Schematic arrangement for measuring permittivity at high temperatures.

An inert atmosphere of argon was maintained in the specimen area. The maximum temperature of 500°C was chosen to be well below the glass transition temperature  $T_g$ , reported by Drew [2.11,2.12] to be in the range 800°C to 1000°C, in order that structural changes in the material would not occur as the temperature was raised.

Two other possible causes of change in the specimen material at high temperature are diffusion of electrode material into the material, and reaction with the surrounding atmosphere. The use of gold electrodes and an upper temperature limit of 500°C should prevent the first, and the inert argon atmosphere the second, but as these oxynitrides were new materials no experimental data was available. As a check therefore, after the measurements at each of the selected temperatures in the range, the specimen was returned to room temperature and the values of capacitance and conductance measured at a few frequencies. No measurable change in the room temperature values was observed.

At each temperature, capacitance  $C_T$  and conductance  $G_T$  were measured at the same frequencies as in the room temperature measurements.  $\epsilon'$  and  $\epsilon''$  were calculated from

$$\epsilon'_T = \frac{C_T}{C_o + C_e} \quad (2.14)$$

where  $C_o = \frac{\epsilon_o A_g}{d}$

and  $C_e = \left( \frac{1.113 D_g}{8\pi} \right) \left[ \ln \left( \frac{8\pi D_g}{d} \right) - 3 \right]$

$$\epsilon''_T = \epsilon'_T (\tan\delta)_T \quad (2.15)$$

$$(\tan\delta)_T = \frac{G_T}{\omega C_T} \quad (2.16)$$

$$\sigma_T = \frac{dG_T}{A} \quad (2.17)$$

#### 2.4 COAXIAL LINE METHODS

Measurements over the frequency range 500 MHz to 5 GHz were facilitated by the development of precision coaxial line techniques which were themselves initiated by the need encountered in earlier work on doped magnesium oxide for greater precision in the dielectric constant measurements with low loss materials.

The measurements were made using coaxial line methods in which a disc-shaped sample is fitted in a coaxial holder terminated by either a short circuit, a matched termination or a resonance circuit; the details of these techniques have been described recently by Kulesza et al [2.13]. For these measurements circular samples of about 6.5 mm diameter and 0.5 mm thick were cut from the bulk oxynitride glasses using conventional diamond cutting methods and polished with diamond paste to 0.25  $\mu\text{m}$  finishes. The coaxial line with short-circuit termination proved most suitable for the determination of  $\epsilon'$  in the frequency range 500 MHz to 5 GHz while the coaxial line resonance method was found to be preferable for  $\epsilon''$  determination. The matched termination method gave reliable answers only below about 1 GHz and was more suitable for the lower dielectric constant compositions. Above 5 GHz the voltage standing wave ratio (VSWR) measured by the coaxial line resonance method becomes very high, thus effectively setting an upper frequency limit of about 5 GHz for the loss measurements on those glasses.

## 2.4 COAXIAL LINE METHODS

### 2.4.1 General Comments

Measurements over the frequency range 500 MHz to 5 GHz were facilitated by the development of precision coaxial line techniques which were themselves initiated by the need encountered in earlier work on doped magnesium oxide for greater precision in the dielectric constant measurements with low loss materials.

The measurements were made using coaxial line methods in which a disc-shaped sample is fitted in a coaxial holder terminated by either a short circuit, a matched termination or a resonance circuit; the details of these techniques have been described recently by Kulesza, Thorp and Ahmad [2.13].

For these measurements circular samples of about 6.5 mm diameter and 0.5 mm thick were cut from the bulk oxynitride glasses using conventional diamond cutting methods and polished with diamond paste to 0.25  $\mu\text{m}$  finishes. The coaxial line with short-circuit termination proved most suitable for the determination of  $\epsilon'$  in the frequency range 500 MHz to 5 GHz while the coaxial line resonance method was found to be preferable for  $\epsilon''$  determination. The matched termination method gave reliable answers only below about 1 GHz and was more suitable for the lower dielectric constant compositions. Above 5 GHz the voltage standing wave ratio (VSWR) measured by the coaxial line resonance method

becomes very high, thus effectively setting an upper frequency limit of about 5 GHz for the loss measurements on those glasses. The following sections summarise the main features of the theory and experimental procedures.

#### 2.4.2 Principles of Methods

Two coaxial line techniques for the determination of complex permittivities of solids and liquids were developed. Both methods use a coaxial sample holder especially designed for this purpose, incorporating a parallel plate capacitor in series with the inner conductor.

The first, the matched termination method, is essentially a comparison technique using air as the reference dielectric. In this case, the changes in the voltage standing wave pattern are recorded when the sample material is inserted. Precise measurements of the reflection coefficient and shift in the standing wave minimum are of importance, as the following theory will show. In order to improve further the accuracy of measuring the voltage standing wave ratio, VSWR, its values are lowered by terminating the sample holder with the characteristic impedance,  $Z_0$ .

In the second method, the resonant line method, the characteristic impedance termination is replaced by an adjustable short circuit known as the reactive stub. After the test material is placed in the sample holder the VSWR readings are taken and plotted against the varying stub lengths. Maximum occurs at resonance when the termination of the line is resistive and this value of VSWR,  $VSWR_{MAX}$ , is related to the loss tangent of the material, i.e.  $\tan \delta = \epsilon''/\epsilon'$ . The procedure can be successfully employed for low loss materials when the value of  $\epsilon'$  is known; possibly determined by the former matched-termination technique.

Both methods can be used for frequencies in the 200 MHz to 9 GHz range and normally require only conventional apparatus. It will be apparent from the following paragraphs, however, that better results are achievable with more sensitive instruments and higher precision components.

#### 2.4.3 Coaxial Line Sample Holder

The external and cross-sectional views of the sample holder are shown in Fig 2.4a and 2.4b. It was made from brass with the internal and external diameters chosen to give theoretically a characteristic impedance,  $Z_0$ , of 50 ohms. The design was based dimensionally on the connector assembly of the General Radio slotted line system used in the measurements. Part of the inner conductor was made replaceable both to allow different sample thicknesses to be inserted and for possible spring removal. The access to the gap is through a cutout window on the outer conductor. When the sample holder is in use a slide-on close-fitting ring clamps the window cover in place. A functional representation of the gap is given in Fig 2.4c.

The performance of the sample holder was examined by measuring its VSWR over the operational frequency range when terminated with  $Z_0$ . The resulting plot in Fig 2.5a for the unit with the gap closed satisfied the requirements adequately. Further, the deviation of VSWR from the calculated values as a function of the air gap spacing in Fig 2.5b gave an additional check on the possible errors introduced by the sample holder. These measurements helped in estimating the tolerances in the values of the reflection coefficient and later the accuracy of  $\epsilon'$  and  $\epsilon''$  components of the complex permittivity constant. Such plots would normally be required at the frequencies of interest and for each sample holder design. Calibration of sample holders does not need any additional equipment nor different procedures from those used in the

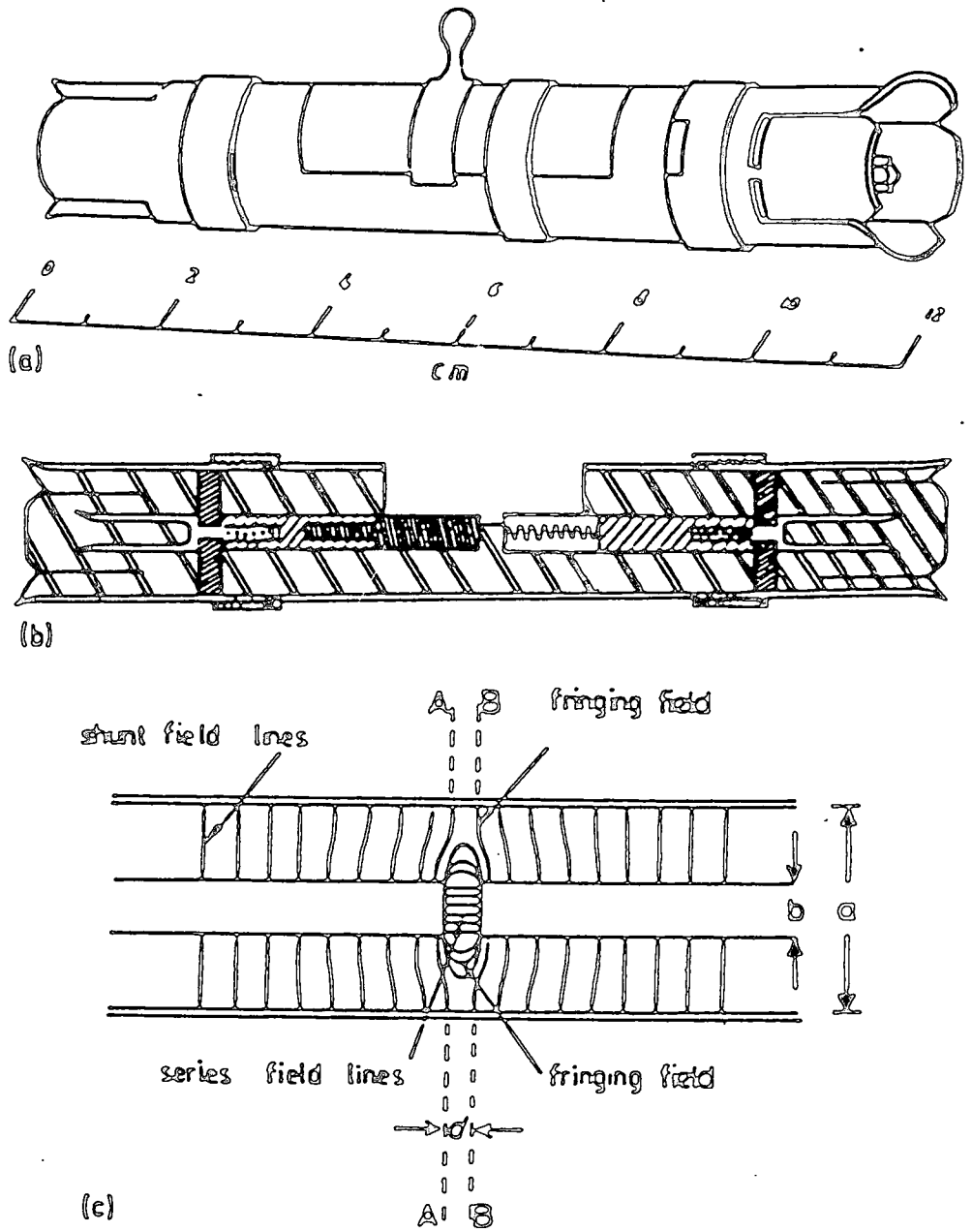


FIG. 2-4. (a) External view and (b) cross-section of sample holder. (c) Electric field distribution.

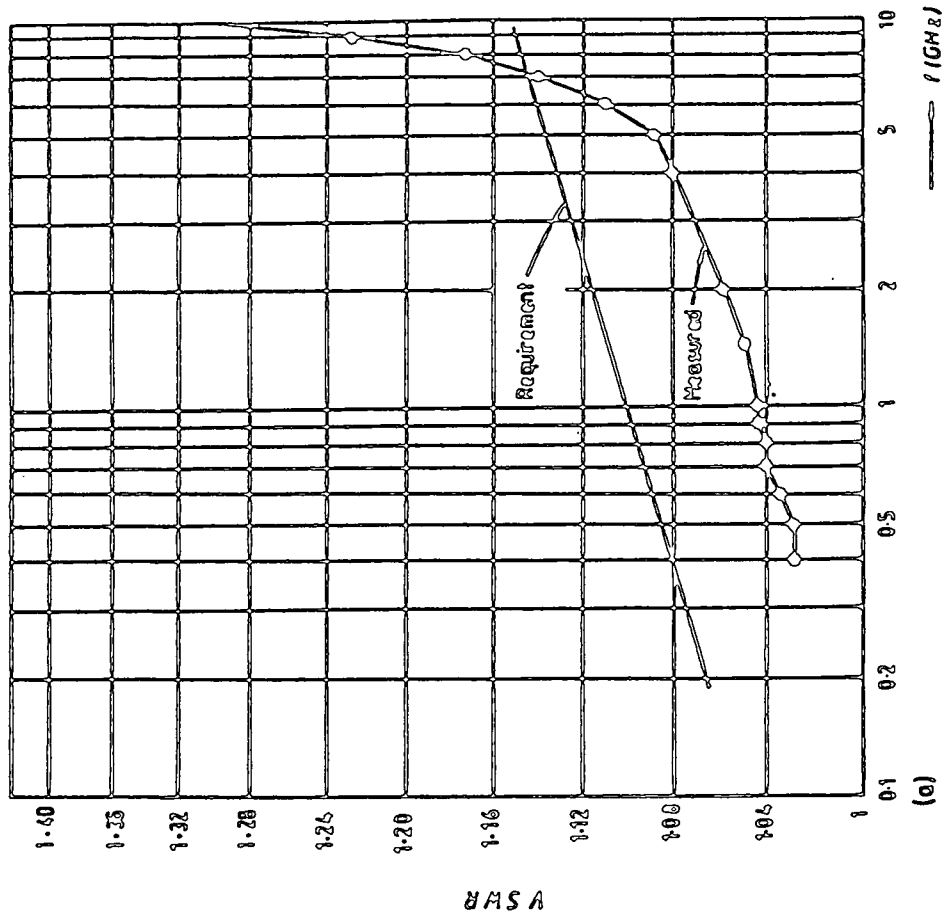
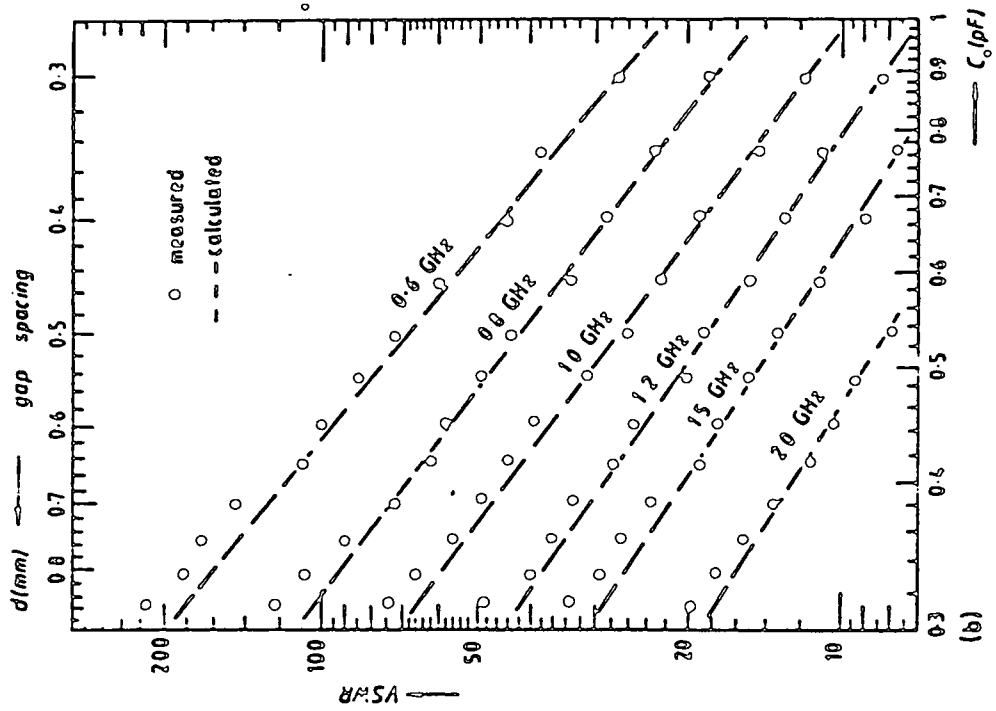


FIG. 2.5. VSWR of the sample holder terminated with  $50 \Omega$  at various frequencies for (a) gap closed and (b) different gap spacing.

actual dielectric measurements. The block diagram in Fig 2.6 shows the experimental apparatus and arrangements for the two methods.

#### 2.4.4 The Matched Termination Method

The sample holder with the material under test placed in the gap may be represented by the equivalent circuit of Fig 2.7. The series capacitance is given by  $C_o \epsilon_r^*$ , where  $\epsilon_r^*$  is the relative complex permittivity of the material,  $\epsilon' - j\epsilon''$ , and  $C_o$  (in farads) is a function of the air permittivity,  $\epsilon_o$ , and the ratio of the cross-sectional area of the inner conductor,  $A$ , and the gap spacing,  $d$ , i.e.  $\epsilon_o A/d$ . The fringing field capacitance,  $C_f$ , is associated with the inner conductor discontinuities (2.14, 2.15).

When the sample holder is terminated with the characteristic impedance, the resulting line load may be approximated to (2.16, 2.17),

$$Z_L \approx \frac{1 + j\omega(C_o \epsilon_r^* + C_f)Z_o}{j\omega(C_o \epsilon_r^* + C_f)} \quad (2.18)$$

where  $\omega$  is the radian frequency.

The reflection coefficient at A-A' may be expressed in terms of impedance (2.17) as

$$\Gamma_L = |\Gamma_L| \exp(-j\theta_L) = \frac{Z_L - Z_o}{Z_L + Z_o} \quad (2.19)$$

which for air dielectric, i.e.  $\epsilon_r^* = 1$ , may be written as

$$|\Gamma_a| \exp(-j\theta_a) = \frac{1}{1 + j2\omega Z_o (C_o + C_f)} \quad (2.20)$$

$$|\Gamma_s| \exp(-j\theta_s) = \frac{1}{1 + j2\omega Z_o (C_o \epsilon_r^* + C_f)} \quad (2.21)$$

Combining Equations (2.20) and (2.21) gives

$$\frac{|\Gamma_a|}{|\Gamma_s|} \exp[j(\theta_s - \theta_a)] = \frac{1 + 2\omega Z_o C_o \epsilon'' + j2\omega Z_o C_o \left( \epsilon' + \frac{C_f}{C_o} \right)}{1 + j2\omega Z_o C_o \left( 1 + \frac{C_f}{C_o} \right)} \quad (2.22)$$

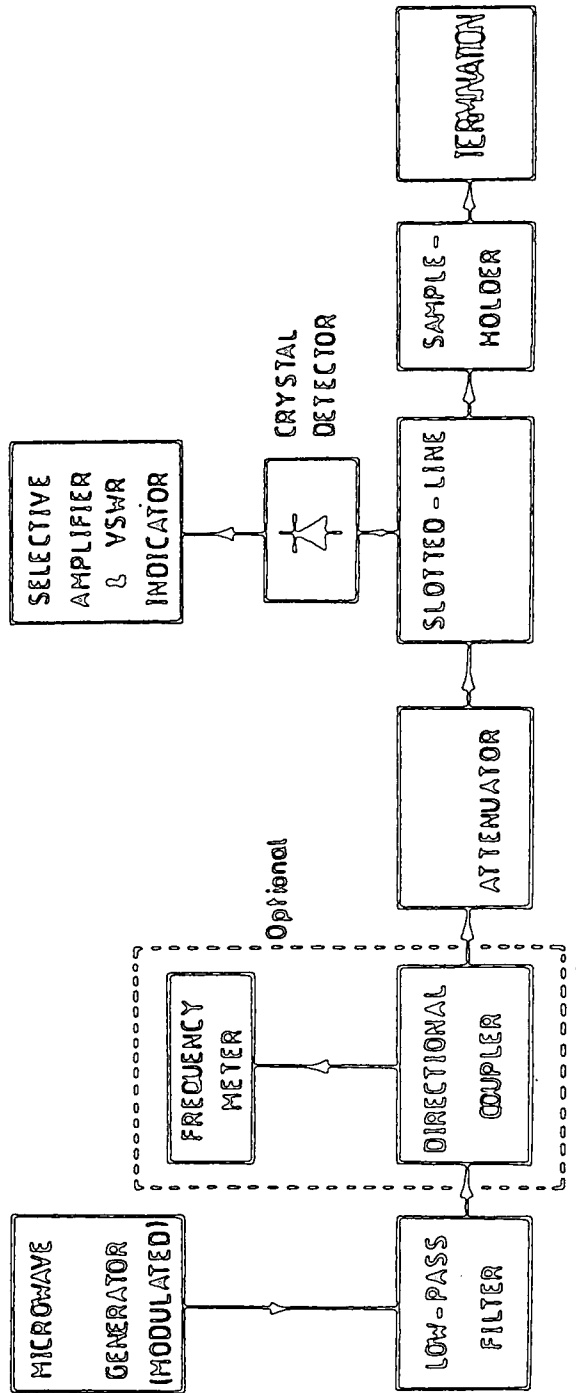


FIG.2-6. BLOCK DIAGRAM OF THE COAXIAL LINE EXPERIMENTAL BENCH

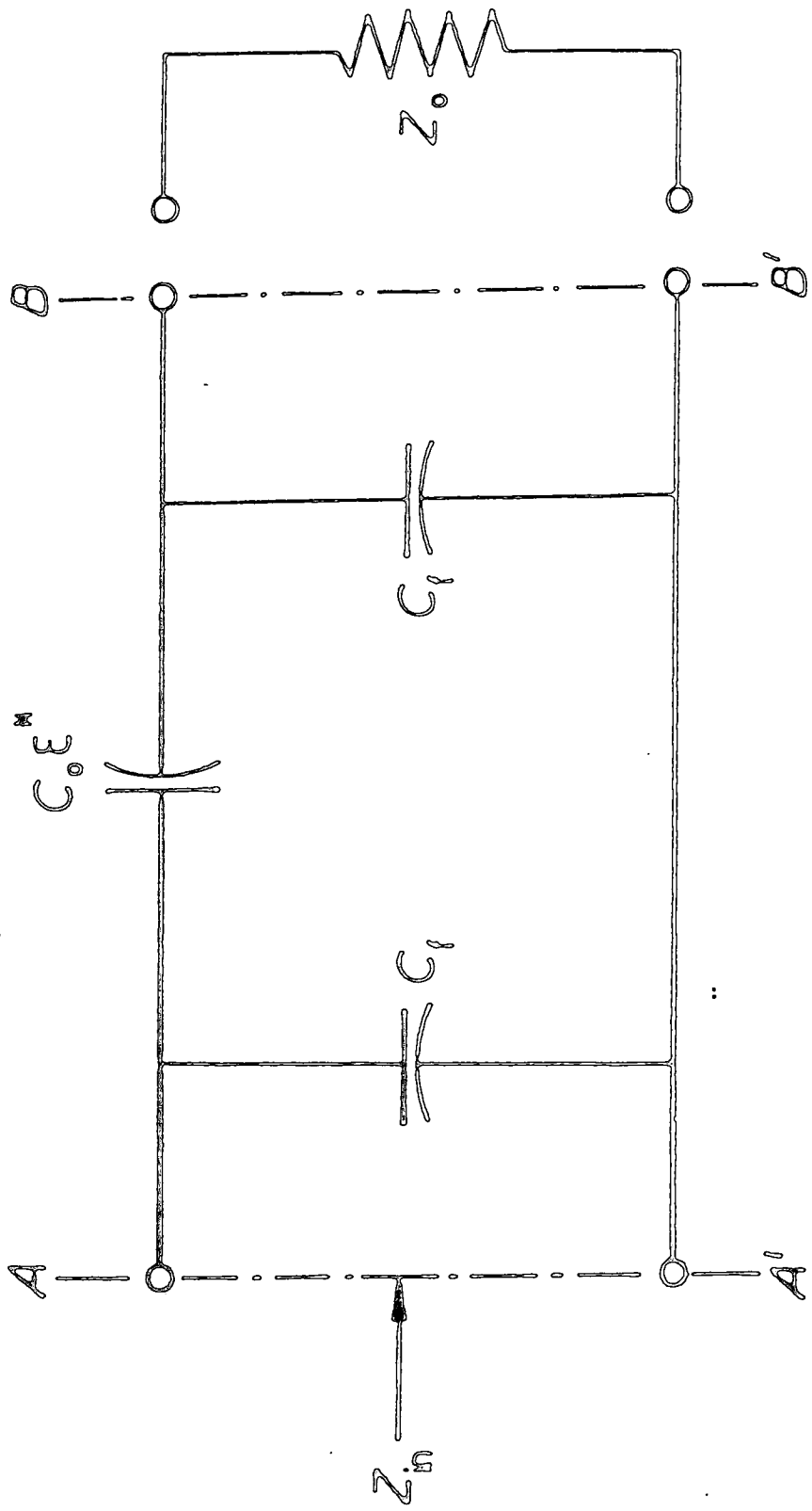


FIG. 2.7. THE EQUIVALENT CIRCUIT FOR THE MATCHED TERMINATION METHOD

On equating the real and imaginary parts and solving explicitly for  $\epsilon'$  and  $\epsilon''$  we finally obtain

$$\epsilon' = \frac{|\Gamma_a|}{|\Gamma_s|} \left\{ \left[ \left( 1 + \frac{C_f}{C_o} \right)^2 + \left( \frac{1}{2\omega Z_o C_o} \right)^2 \right]^{\frac{1}{2}} \sin\theta_s \right\} - \frac{C_f}{C_o} \quad (2.23)$$

and

$$\epsilon'' = \frac{|\Gamma_a|}{|\Gamma_s|} \left\{ \left[ \left( 1 + \frac{C_f}{C_o} \right)^2 + \left( \frac{1}{2\omega Z_o C_o} \right)^2 \right]^{\frac{1}{2}} \cos\theta_s \right\} - \frac{1}{2\omega Z_o C_o} \quad (2.24)$$

where  $\theta_s = 2\beta l_s$ ,  $l_s$  being the standing wave minima location with the sample material as the dielectric and  $\beta = 2\pi/\lambda_g$ ,  $\lambda_g$  being the wavelength.

Using Equations (2.23) and (2.24) or directly from Equation (2.21), we can get the following implicit relationship:

$$\frac{\epsilon' + C_f/C_o}{\epsilon'' + 1/2\omega Z_o C_o} = \tan\theta_s \quad (2.25)$$

leading to an approximation

$$\epsilon' \approx \frac{1}{2\omega Z_o C_o} \tan\theta_s \quad (2.26)$$

if  $\frac{C_f}{C_o} \ll \epsilon'$

and  $\epsilon'' \ll \frac{1}{2\omega Z_o C_o}$

The relationships between the reflection coefficient and the dielectric properties of the material under test, for a particular set of dimensions and frequency, are shown in Fig 2.8. The plots were obtained using Equations (2.21) and (2.25), and require only the experimental values and the reflection coefficient magnitude and its angle to determine  $\epsilon'$  and  $\tan \delta$  for the sample material.

#### 2.4.5 The Resonant Line Method

If the line is terminated with a reactance instead of the characteristic impedance,  $Z_0$ , standing waves will be produced along its length. Such termination can be achieved by using an adjustable lossless stub connected to the line as the load. The line, incorporating the sample holder with air or the material under test in the gap, presents a capacitive impedance (R and C in series). By varying the stub length a maximum reading in the voltage standing wave ratio, VSWR, will be observed when the inductance of the stub cancels the reactive part (C) of the line impedance. This condition of resonance results in a pure resistance (R) which can be related to and deduced from the normalized minimum impedance value given by

$$\frac{R}{Z_0} = \frac{1}{\text{VSWR}_{\text{MAX}}} \quad (2.27)$$

according to transmission line theory (2.18). The equivalent circuit of the arrangement is shown in Fig 2.9 and produces the following relationships.

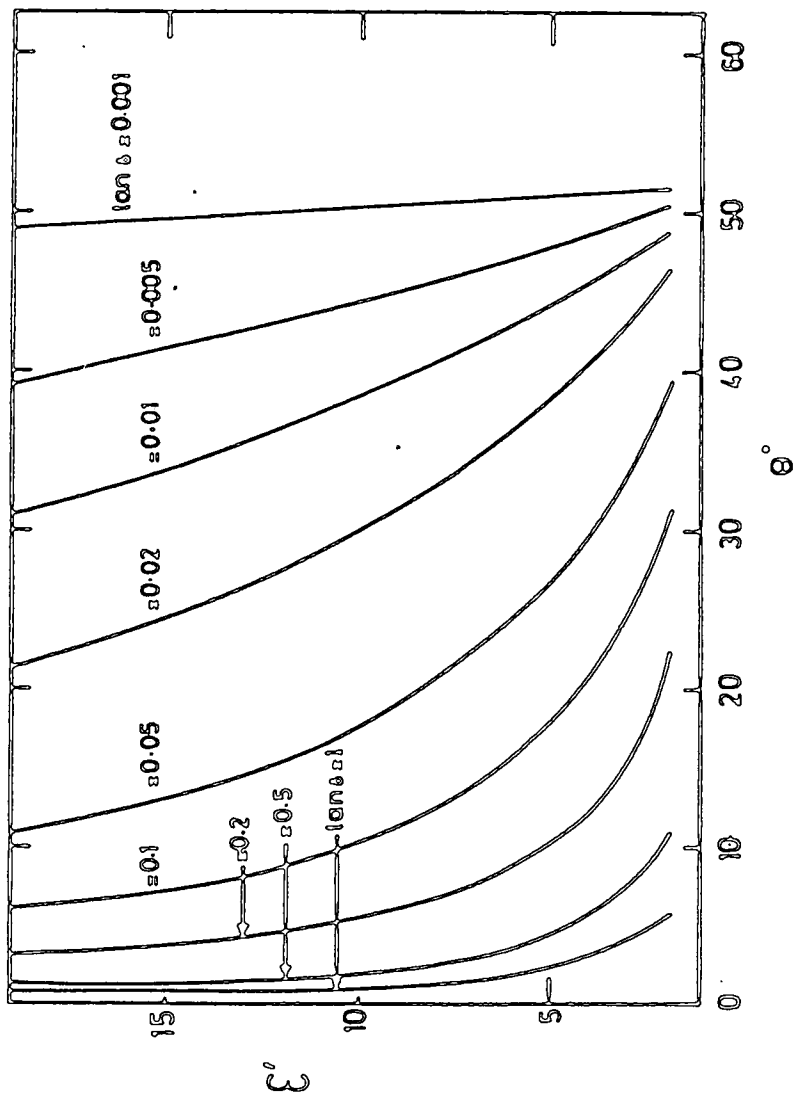


FIG.2.8. Interdependence of parameters in Equation 8 for 0.5 mm gap at 500 MHz with  $C_1/C_0 = 0.112$ .

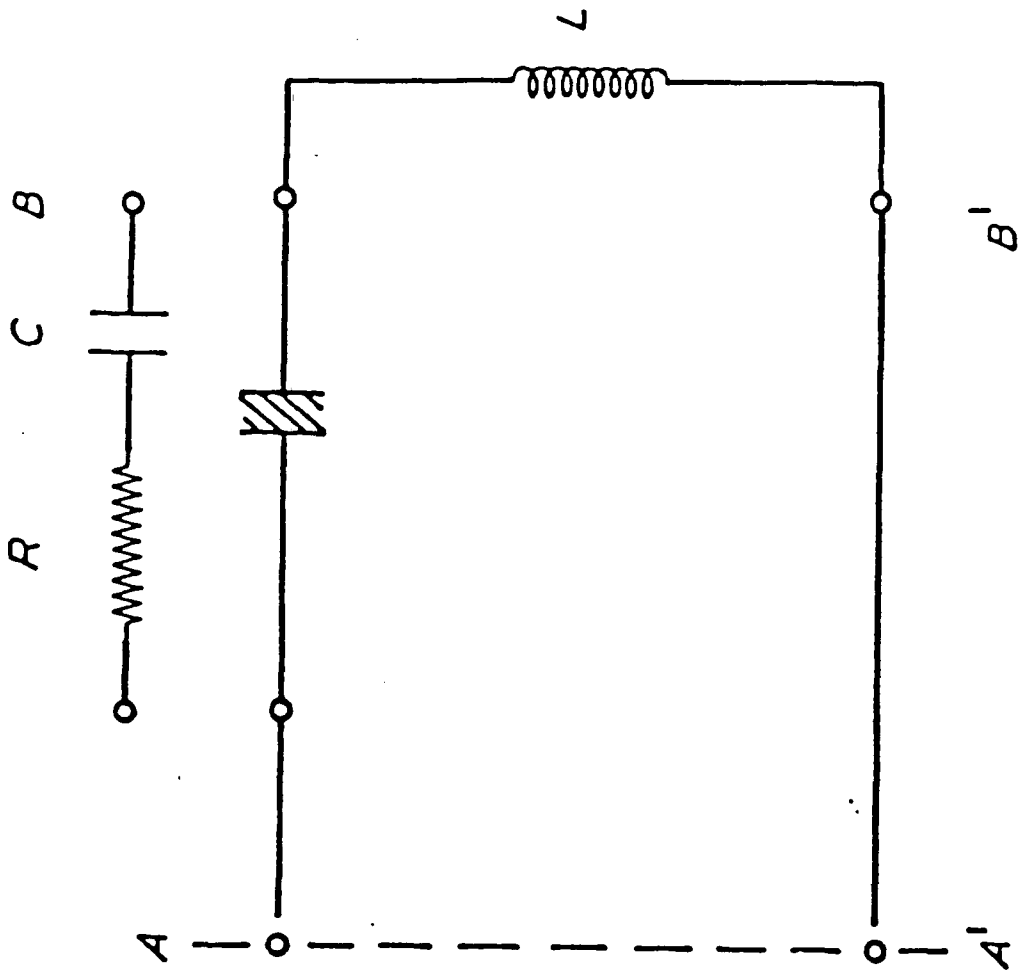


FIG. 2·9. The equivalent circuit for the resonant line method.

The impedance of the material sample may be written as

$$Z = \frac{1}{j\omega C_0 \epsilon_r^*} \quad (2.28)$$

where the symbols have the meanings previously defined.

On substitution for the complex permittivity

$$\epsilon_r^* = \epsilon' - j\epsilon''$$

results in

$$Z = \frac{\epsilon'' - j\epsilon'}{\omega C_0 (\epsilon'^2 + \epsilon''^2)} \quad (2.29)$$

which at resonance with the variable terminating stub gives, on equating the real and imaginary parts,

$$\frac{\epsilon''}{\omega C_0 (\epsilon'^2 + \epsilon''^2)} = R = \frac{Z_0}{VSWR_{MAX}} \quad (2.30)$$

and

$$\frac{\epsilon'}{\omega C_0 (\epsilon'^2 + \epsilon''^2)} = Z_0 \tan \beta l_r \quad (2.31)$$

where  $l_r$  is the stub length at resonance.

Combining equations (2.30) and (2.31) leads to

$$\tan \delta = \frac{\epsilon''}{\epsilon'} = \frac{1}{VSWR_{MAX} \tan \beta l_r} \quad (2.32)$$

If  $\epsilon'' \ll \epsilon'$ , approximations may be obtained, namely

$$\epsilon' \approx \frac{1}{\omega C_o Z_o \tan \beta l_r} \quad (2.33)$$

and

$$\tan \delta \approx \epsilon' C_o \frac{Z_o}{VSWR_{MAX}} \quad (2.34)$$

or

$$\epsilon'' \approx \frac{1}{\omega C_o Z_o VSWR_{MAX} \tan^2 \beta l_r} \quad (2.35)$$

As can be seen from the above,  $\epsilon'$  may be determined from the resonant condition knowing only the relevant stub length,  $l_r$ . However, to determine  $\epsilon''$  it is also necessary to know the maximum value of VSWR measured at resonance. The value of  $\tan \delta$  is given without any approximations by Equation (2.32) involving both parameters,  $VSWR_{MAX}$  and  $l_r$ .

#### 2.4.6 Conclusions

The two methods just described, are independent and may be used for complementary measurements or mutual verification of results. These aims can be carried out with ease since the only difference between the two sets of apparatus is in the termination, that is, matched load or variable short circuit stub.

The matched termination method produces reasonably accurate values of  $\epsilon'$  as can be deduced from equation (2.27) and were supported by the results obtained for chlorobenzene and PMMA perspex. The values for  $\epsilon''$ , on the other hand, were not in such a good agreement with the published information for both materials, although still very comparable. It

suggests that the method using matched termination may be used with some confidence for finding  $\epsilon'$ .

The resonant line method was developed primarily for the purpose of determining the values of  $\tan\delta$  in materials having moderate or low dielectric loss. There are two parameters involved as shown by Equation (2.34) - the maximum or the resonant value of VSWR and the resultant stub length. Some difficulty may arise in measuring the high VSWR values expected in the case of good insulators. Highly sensitive quality standing wave meters will normally have the range of 80 dB, 60 dB attenuator plus 20 dB on the meter scale. This would imply a VSWR range of up to  $10^4$  (20 dB  $\equiv$  a factor of 10) which, however, cannot be fully realized in practice due to overloading and noise-at-minima problems. A VSWR of  $10^3$  is possible with care, allowing  $\tan\delta$  of  $10^{-3}$  or less to be measured. There may also be additional difficulty in establishing graphically the actual  $VSWR_{MAX}$ . If precise measurements are not possible around the peak, extrapolation of the slopes could give an estimate of the maximum value and error involved.

## CHAPTER 2

### REFERENCES

- 2.1 A.H.Scott, and H.L.Curtis, J.Res.Nat.Bur.Stan., 22, (1939), 747.
- 2.2 A.C.Lynch, Proc.I.E.E., 120, (1973), 934.
- 2.3 A.C.Lynch, Proc.I.E.E., 104, Part B, (1956), 359.
- 2.4 A.C.Lynch, Proc.I.E.E., 112, (1965), 426.
- 2.5 L. Hartshorn, and W.H.Ward, J.I.E.E., 79, (1936), 567.
- 2.6 J.R.Blanco-White, Proc.I.E.E., 120, (1973), 939.
- 2.7 R.N.Blumenthal and M.A.Seitz, (1974) 'Experimental Techniques',  
Electrical Conduction in Ceramics and Glass, Ed. N.M. Tallan,  
Dekker, N.Y.
- 2.8 R. Von Hippel, (1954) 'Dielectric Materials and Applications',  
Wesley, New York.
- 2.9 R.H.Dalton, (1965), 'Electrolysis and Polarisation in Glass',  
Proc. 7th Int.Congress on Glass, Brussels, 55.
- 2.10 C.Kim and M. Tomozawa, J.Am.Ceram.Soc., 59, (1976), 321.
- 2.11 R.A.L.Drew, (1980) 'Nitrogen Glasses', Ph.D.Thesis,  
University of Newcastle.
- 2.12 R.A.L.Drew, S. Hampshire, and K.H.Jack, Special Ceramics 7,  
Proc.Brit.Ceram.Soc., 31, (1981), 119.
- 2.13 B.L.J.Kulesza, J.S.Thorp, A.B.Ahmad, J.Mat.Sci 19 (1984), 915.

## CHAPTER 3

## THE MEASUREMENT OF PERMITTIVITY AND DIELECTRIC LOSS ;

## II MICROWAVE TECHNIQUES

In order to investigate whether the dielectric constant varied with composition at microwave frequencies, and in particular to determine if the trends detected at audio frequencies persisted at microwave frequencies, and therefore might persist over the 8 decades of frequency, techniques to measure the dielectric constant of our specimens at 2.9 GHz and at 9.3 GHz were developed.

### 3.1 CHOICE OF EXPERIMENTAL TECHNIQUE

To meet the objectives, it was obviously essential to find a technique which would detect small differences in the dielectric constants of different specimens. To be practicable experimentally, the technique should accept small specimens without extensive prior machining, and should allow the specimens to be interchanged readily so that a range of materials could be compared quickly with the minimum of change in experimental conditions. These factors considerably narrowed the choice of techniques available.

Whereas at audio frequencies, and up to the lower ranges of radio frequencies, it is satisfactory and convenient to contract a lumped circuit element from the specimen material and measure its electrical characteristics, at higher frequencies the dimensions of lumped circuit components become increasingly comparable with wavelength and accuracy

becomes limited by increasing values of stray impedances. If accuracy is to be maintained, distributed circuits are necessary above about 100 MHz, and waveguide circuits are advisable above 3 GHz. Therefore for the frequencies required here, 2.9 GHz and 9.3 GHz, waveguide techniques are optimum.

In order to measure its dielectric properties, specimen material must be incorporated into a waveguide circuit in a way which produces a measurable and calculable change in electrical behaviour. However, waveguide dimensions limit the wavelengths which can propagate to the extent that waveguide circuits have relatively narrow bandwidths, and because of this, different frequencies may require different sizes of waveguide. For some techniques this would mean different sizes of specimen. As well as the obvious disadvantages of requiring more than one prepared specimen of each material under test, this also *changes* the error between measurements on the same material at different frequencies. A technique which can accept the same specimen at different frequencies is to be preferred.

In general, techniques which use rigorous solutions of the electromagnetic equations are accurate but require specimens of standard shapes fitted with mechanical precision into the waveguide. Some relatively small variations, for example, certain airgaps between specimen and guide wall, can be tolerated if corrections are applied. Techniques which use perturbation theory, however, can in some cases accept small specimens of various shapes without precise positioning, and accuracy is good provided that the limitations of the theory are observed.

Waveguide techniques also tend to fall into two other classes : those which measure the transmission of a section of guide or a component containing specimen material, and those which measure the properties of a resonant cavity containing the material. Rigorous solutions of the wave equations and perturbation treatments are available for both.

The technique chosen for this work was to place a small specimen inside a resonant cavity, and calculate its dielectric constant from perturbation theory. It suited the requirements of the present work in the two most important respects. Firstly, it accepts small specimens without accurate machining and fitting into the cavity and the specimens are easily interchanged. Secondly, it is sensitive to small differences in dielectric constant of the specimen material.

A small change in the material of the wall or dielectric of a resonant cavity changes its electrical properties by an amount which depends on the electrical properties of the material which produced the change. If this change consists of placing a specimen inside the cavity, the dielectric constant of the specimen can be calculated from the change in cavity resonance frequency. Specimens of different dielectric constants produce different resonance frequencies, so that small differences between specimens are easily detected. As the same cavity is used in each case, the effects of cavity imperfections cancel out and do not obscure differences between specimens. Even in cases where absolute values of the dielectric constant cannot be accurately determined, differences between different materials, and trends caused by variations in composition can be detected. However, resonant cavities have the disadvantage of operating effectively at a single

frequency, and although the technique and the specimens were the same in each case, different cavities were required for the 2.9 GHz and 9.3 GHz measurements.

### 3.2 PERTURBATION THEORY OF RESONANT CAVITIES

Bethe and Swinger [ 3.1 ] followed by Kahan [ 3.2 ], derived a perturbation theory which related the change in resonance frequency and Q factor of a resonant cavity to the properties of the disturbance causing the change. A cavity resonator method was used to measure dielectric constants of small samples by Sproull and Linder [ 3.3 ] and a more accurate experimental technique was introduced in 1949 by Barnbaum & Franeau [ 3.4 ] who are widely regarded as the pioneers of the technique. The theory was also discussed by Slater [ 3.5 , 3.6 ], and applied more directly by Casimir [ 3.7 ] to the introduction of a small specimen into a cavity. A derivation by Waldron [ 3.8, 3.9 ] emphasised the inherent assumptions and limitations of perturbation techniques.

Maxwell's equations for a cavity of arbitrary shape filled with a material of dielectric constant  $\epsilon_1$  and permeability,  $\mu_1$ , and resonant at an angular frequency  $\omega_1$  can be written

$$\begin{aligned}\nabla \times \underline{E}_1 &= -j \omega_1 \mu_1 \underline{H}_1 \\ \nabla \times \underline{H}_1 &= j \omega_1 \epsilon_1 \underline{E}_1\end{aligned}\tag{3.1}$$

If the cavity is air filled,  $\epsilon_1 = \epsilon_0$  and  $\mu_1 = \mu_0$ .

If the same cavity is now filled with a material characterised by  $\epsilon_2$  and  $\mu_2$ , the resonance frequency and the amplitudes and configurations of the fields will change and the equations become

$$\begin{aligned}\nabla \times \underline{E}_2 &= -j \omega_2 \mu_2 \underline{H}_2 \\ \nabla \times \underline{H}_2 &= j \omega_2 \epsilon_2 \underline{E}_2\end{aligned}\tag{3.2}$$

If the cavity walls are assumed to be perfectly conducting, the change

in resonance frequency obtained from the above equations is

$$\frac{\omega_2 - \omega_1}{\omega_2} \approx \frac{\int_{V_c} [(\mu_2 - \mu_1) H_1 \cdot H_2 - (\epsilon_2 - \epsilon_1) E_1 \cdot E_2] dV}{\int_{V_c} [\epsilon_1 E_1 \cdot E_2 - \mu_1 H_1 \cdot H_2] dV} \quad (3.3)$$

If the difference between the two conditions is small enough to be regarded as a perturbation, a simpler expression can be obtained in which all the variables are either measurable or known. The necessary condition is that when taken over <sup>the</sup> whole cavity, the distortion in the field configurations must be small. When this condition is met,  $(\omega_2 - \omega_1)$  will be small in comparison to  $\omega_2$ . The field configurations may change by small amounts over a large part of the cavity volume, or by relatively large amounts over a small part of the cavity volume. The former would occur, for example, if different gases were compared by filling the cavity with each in turn, the latter if a small dielectric specimen were placed inside the cavity, or if the cavity were slightly deformed. Field configurations inside such a specimen and in its immediate neighbourhood may differ appreciably from the unperturbed configuration. Specimens of high dielectric constant are acceptable if their volumes are small.

The above condition is equivalent to the condition that the energy stored in the specimen must be a small fraction of the total energy stored in the perturbed cavity [Spencer, LeCraw and Ault, 3.10].

In the case of a cavity containing a small specimen, in the part of the cavity volume outside the specimen volume  $\epsilon_1 = \epsilon_2$  and  $\mu_1 = \mu_2$ , so the numerator of equation (3.3) is zero outside the specimen, and can be integrated over the specimen volume, rather than over the whole cavity.

$$\begin{aligned}
 & \int_{V_c} [(\mu_2 - \mu_1) \underline{H}_1 \cdot \underline{H}_2 - (\epsilon_2 - \epsilon_1) \underline{E}_1 \cdot \underline{E}_2] dV \\
 & = \int_{V_s} [(\mu_2 - \mu_1) \underline{H}_1 \cdot \underline{H}_2 - (\epsilon_2 - \epsilon_1) \underline{E}_1 \cdot \underline{E}_2] dV \quad (3.4)
 \end{aligned}$$

where  $V_s$  is the volume of the specimen.

When the perturbation condition holds, and the difference in the perturbed and unperturbed field configurations is small when considered over the whole cavity, the approximation can be made that :

$$\int_{V_c} (\epsilon_1 \underline{E}_1 \cdot \underline{E}_2 - \mu_1 \underline{H}_1 \cdot \underline{H}_2) dV \approx \int_{V_c} (\epsilon_1 \underline{E}_1 \cdot \underline{E}_1 - \mu_1 \underline{H}_1 \cdot \underline{H}_1) dV \quad (3.5)$$

In a resonant cavity with perfectly conducting walls, the energies stored in the electric field and the magnetic field are equal, and from equation (3.1) are :

$$\int_{V_c} \epsilon \underline{E} \cdot \underline{E} dV = - \int_{V_c} \mu \underline{H} \cdot \underline{H} dV \quad (3.6)$$

Substituting into equation (3.3) :

$$\frac{\delta\omega}{\omega_2} = \frac{(\mu_2 - \mu_1) \int_{V_s} \underline{H}_1 \cdot \underline{H}_2 dV - (\epsilon_2 - \epsilon_1) \int_{V_s} \underline{E}_1 \cdot \underline{E}_2 dV}{2\epsilon_1 \int_{V_c} |\underline{E}_1|^2 dV} \quad (3.7)$$

For an air filled cavity,  $\mu_1 = \mu_0$ ,  $\epsilon_1 = \epsilon_0$  and  $\omega_1 = \omega_0$ . If the

specimen is non-magnetic, or if a magnetic specimen is placed in the cavity at a position of approximately zero magnetic field, then the term in  $\underline{H}$  will be zero and

$$\frac{\delta\omega}{\omega_0} = \frac{(\epsilon_2 - \epsilon_0) \int_{V_s} \underline{E}_1 \cdot \underline{E}_2 \, dV}{2 \epsilon_0 \int_{V_c} |\underline{E}_1|^2 \, dV} \quad (3.8)$$

As the relative dielectric constant of the specimen ( $\epsilon$ ) is equal to  $\epsilon_2/\epsilon_0$ ,

$$\frac{\delta\omega}{\omega_0} = \frac{(\epsilon - 1) \int_{V_s} \underline{E}_1 \cdot \underline{E}_2 \, dV}{2 \int_{V_c} |\underline{E}_1|^2 \, dV} \quad (3.9)$$

A similar expression for relative permeability can be obtained by assuming that the electric field over the specimen is zero. Thus  $\mu$  and  $\epsilon$  for a magnetic specimen can be found separately by placing the specimen in different positions inside the cavity.

The effect of finite dielectric loss in the specimen material is included in equation (3.9). In this case the dielectric constant is regarded as complex,  $\epsilon = \epsilon' - j\epsilon''$ , and the effect on cavity behaviour is included in equation (3.9) by treating the angular frequency  $\omega$  as a complex quantity [Waldron 3.8].

The complex angular frequency of a resonant cavity can be written as

$$\Omega_1 = \omega_1 \left( 1 + \frac{j}{2Q_1} \right) \quad (3.10)$$

In the perturbed cavity,

$$\Omega_2 = \omega_2 \left( 1 + \frac{j}{2Q_2} \right) \quad (3.11)$$

If the dielectric loss is small, and  $\omega \gg (j/2Q)$ , then the change in complex frequency caused by the perturbation is

$$\delta\Omega = \delta\omega + j\omega l \left( \frac{1}{2Q_1} - \frac{1}{2Q_2} \right) \quad (3.12)$$

Substituting in equation (3.9):

$$\frac{\delta\omega}{\omega} - \frac{j}{2} \left( \frac{1}{Q_1} - \frac{1}{Q_2} \right) = \frac{[(\epsilon' - j\epsilon'') - 1] \int_{V_s} \underline{E}_1 \cdot \underline{E}_2 \, dV}{2 \int_{V_c} |\underline{E}_1|^2 \, dV} \quad (3.13)$$

Equating real and imaginary parts :

$$\frac{\delta\omega}{\omega} = \frac{(\epsilon' - 1) \int_{V_s} \underline{E}_1 \cdot \underline{E}_2 \, dV}{2 \int_{V_c} |\underline{E}_1|^2 \, dV} \quad (3.14)$$

$$\frac{1}{Q_1} - \frac{1}{Q_2} = \frac{\epsilon'' \int_{V_s} \underline{E}_1 \cdot \underline{E}_2 \, dV}{\int_{V_c} |\underline{E}_1|^2 \, dV} \quad (3.15)$$

It can be seen that the expression for the real part of the dielectric constant (3.14) has the same form as equation (3.9), and that the dielectric loss can be found from the change in the cavity Q factor.

$\underline{E}_1$ , the field in the cavity, is known for cavities of standard shape. The field inside the specimen,  $\underline{E}_2$ , depends on its dielectric

constant, its dimensions, and the field surrounding it. When the external field is uniform over the specimen volume,  $\underline{E}_2$  is given by

$$\underline{E}_2 = F(\epsilon') \underline{E}_1 \quad (3.16)$$

where  $F(\epsilon')$  is a function of sample dimensions and dielectric constants. Substituting in equation (3.14) and evaluating the integrals for a rectangular cavity oscillating in the  $H_{101}$  mode gives

$$\frac{\delta\omega}{\omega} = \frac{1}{2} \frac{V_S}{V_C} (\epsilon' - 1) F(\epsilon') \quad (3.17)$$

The evaluation of  $\underline{E}_2$  is not always possible, and exact solutions exist for relatively few cases. Solutions are available for ellipsoids and limiting cases of ellipsoids [Stratton 3.11].

The field inside a sample whose surface is everywhere normal to the external field is

$$\underline{E}_2 = \frac{1}{\epsilon'} \underline{E}_1 \quad (3.18)$$

If the field is everywhere tangential to the surface then

$$\underline{E}_2 = \underline{E}_1 \quad (3.19)$$

Intermediate cases have values of  $\underline{E}_2$  which lie between these two limits. Thus for any specimen,

$$\frac{1}{\epsilon'} \leq F(\epsilon') \leq 1 \quad (3.20)$$

The value  $\underline{E}_2 \cong \underline{E}_1/\epsilon'$  is approached by thin discs of large diameter placed normal to the external field. The approximation becomes exact

when the disc is infinitely thin and has an infinitely large diameter : the theoretical "infinite disc". Thin needle-shaped rods or thin rods which terminate on the cavity walls and can be regarded as infinite have the maximum value of internal field,  $E_2 \approx E_1$ . Again the approximation tends towards exactness as the rods become infinitely thin. The error in the approximation for practical rods and discs and therefore the thickness that is acceptable in practice depends on the value of their dielectric constants.

It can be seen from equation (3.17) that the sensitivity of resonance frequency to dielectric constants, that is the magnitude of  $\delta\omega$  produced by a change in  $\epsilon'$ , depends on  $F(\epsilon')$  and is maximum when  $F(\epsilon')$  is maximum. Therefore differences in dielectric constant will be more easily detected if samples are placed tangentially to the electric field.

### 3.3 SPECIMEN PREPARATION

The specimens were cut from bulk samples with a diamond wheel cutting machine. Polishing was not necessary : surface irregularities were small compared to wavelength and to volume, and electrical contact to the surfaces was not required. [An advantage of this technique is that little preparation of the specimens is necessary].

### 3.4 THE RESONANT CAVITIES

A rectangular cavity which oscillated in the  $H_{101}$  mode was constructed for each frequency. Q-factors were made large enough to give sharp resonance curves from which the resonance frequency could be found with good accuracy. The materials under test had low dielectric losses. Insertion of a small sample into the cavities caused only a slight broadening of the resonance curve.

Both cavities were made of copper. Inner surfaces were polished to reduce the resistance of the cavity walls and increase the Q-factor. At

these frequencies current flow is in the surface layers because of the 'skin effect'. Plating the inner surfaces to increase conductivity further was not necessary.

The cavities were driven from a waveguide through an aperture positioned to excite only the  $H_{101}$  mode. Fig.3.1 shows the orientation of the guide and the position of the aperture relative to the cavities. The optimum diameters of the coupling apertures were found experimentally. Undercoupling produced by a small aperture limits the power absorbed in the cavity at resonance and results in a shallow resonance curve, while an overcoupled cavity tends to be influenced by the impedance of the external circuit. Since the measurement of dielectric constant depends on measuring a small perturbation of the cavity, all other influences on the cavity should be minimised, and slight undercoupling is preferable provided that a good resonance curve is also obtained. Theoretical treatments are available for calculating the optimum coupling aperture, but in practice the value depends on imperfections in the system and is best optimised experimentally.

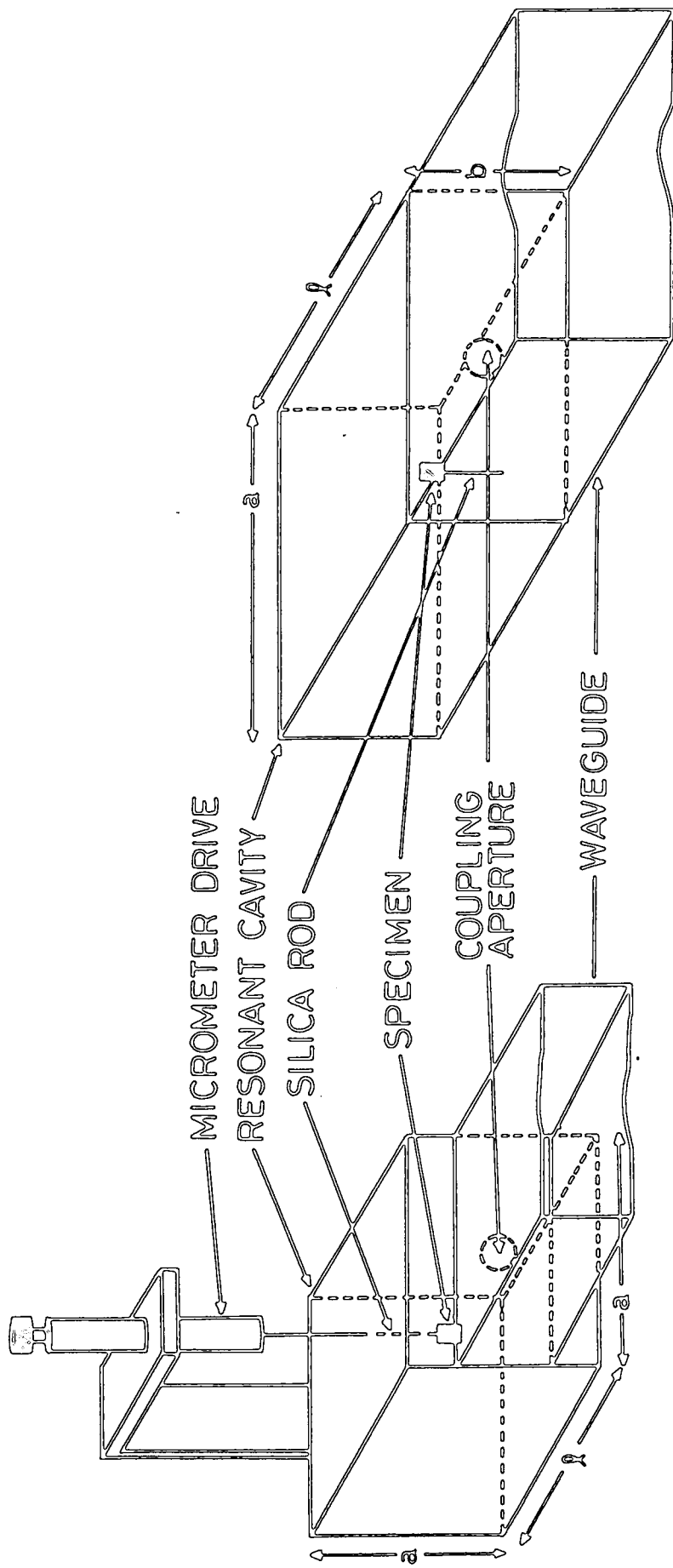
A rectangular cavity oscillates in the  $H_{101}$  mode if the half-wavelength in the guide ( $\frac{\lambda_g}{2}$ ) is equal to the inner dimensions of sides  $a$  and  $l$  (Fig 3.1). The guide wavelength for an  $H_{mn}$  wave in a rectangular guide of dimensions  $a$  and  $b$  is given by

$$\left(\frac{1}{\lambda_g}\right)^2 = \left(\frac{1}{\lambda}\right)^2 - \left(\frac{m}{2a}\right)^2 - \left(\frac{n}{2b}\right)^2 \quad (3.21)$$

where  $\lambda$  is the free space wavelength

and  $m$  and  $n$  are integers

A closed length of this guide will resonate if its length ( $l$ ) is an integral number( $p$ ) of half-wavelength,  $l = p\lambda_g/2$ . Substituting for  $\lambda_g$



9.4 GHz CAVITY

2.9 GHz CAVITY

FIG. 3.1. 9.4 GHz AND 2.9 GHz  $H_{101}$  RESONANT CAVITIES FOR USE WITH IDENTICAL SPECIMENS

in equation (3.21),

$$\left(\frac{1}{\lambda}\right)^2 = \left(\frac{m}{2a}\right)^2 + \left(\frac{n}{2b}\right)^2 + \left(\frac{p}{2l}\right)^2 \quad (3.22)$$

$$\text{Hence } f_o = \frac{c}{2} \sqrt{\left(\frac{m}{a}\right)^2 + \left(\frac{n}{b}\right)^2 + \left(\frac{p}{l}\right)^2} \quad (3.23)$$

where  $f_o$  is the resonance frequency of the cavity

$c$  is the velocity of light.

In the  $H_{101}$  mode,  $m = p = 1$  and  $n = 0$ . If dimensions  $a$  and  $l$  are made equal then the resonance frequency is given by

$$f_o = \frac{c}{a\sqrt{2}} \quad (3.24)$$

If ( $f_o$ ) is in GHz and ( $a$ ) is in cms, then the cavity dimensions for a given resonance frequency are given by the simple equation

$$a = l = \frac{21.213}{f_o} \quad (3.25)$$

It is important to note that the resonance frequency is independent of the dimension ( $l$ ).

When the cavity is air-filled, the resonance frequency of the cavity with the specimen in place ( $f_o$ ) is always higher than that of the

cavity without a specimen ( $f$ ). The specimen has a larger dielectric constant than the air which it displaces, so the wavelength is shorter in the specimen than in the displaced air. The cavity is returned to resonance by increasing the wavelength of the incident microwave signal, that is, by decreasing its frequency to ( $f$ ). By choosing ( $f_0$ ) to lie at the higher end of the microwave generator range, the maximum usable frequency range is obtained.

It was noted above that resonance frequency is independent of cavity height ( $b$ ) in the  $H_{101}$  mode. Cavity volume therefore is also independent of resonance frequency, and can be optimised to the requirements of the perturbation technique, provided that an adequate Q-factor is maintained. From equation (3.17), the frequency shift  $(f_0 - f)/f_0$  or  $\delta f/f_0$  depends on cavity volume, together with dielectric constant and sample volume. The ratio  $\delta f/f_0$  should be small enough to render the perturbation approach valid, but large enough to keep measurement errors acceptably small and the cavity volume can be chosen accordingly.

This fact was used to permit the measurement of the same specimen in both cavities, rather than measuring a larger specimen in the larger cavity. The error in measuring specimen volume is therefore the same at the two frequencies. More importantly, the error due to approximations in the function  $F(\epsilon')$  is the same at each frequency ; this error can be relatively large and is difficult to estimate. In order to obtain practical values of  $\delta f$  with the same specimen in the different cavities, the volume of the 2.9 GHz cavity was made smaller with respect to its resonance frequency than was the case for the 9.4 GHz cavity. The cavities were designed to different proportions : the 9.4 GHz cavity was cubical, so that  $a = b = \lambda$ , while the 2.9 GHz cavity was rectangular with  $b < a = \lambda$ .

The dimensions of the cavities and their resonant frequencies are given in Table 3.1.

An alternative method of using the same specimen size in cavities of different resonance frequencies is to resonate the high frequency cavity in a higher mode, so that a relatively large cavity can be used. The specimen should be placed at a point of maximum electric field, which may or may not occur at the cavity centre, depending on the mode. This technique can be useful in increasing the Q-factors of high frequency cavities by increasing the volume, and in keeping  $\delta f/f$  within the limits of perturbation theory.

### 3.5 POSITIONING THE SPECIMENS

The specimens were suspended at the centre of the cavities from fine silica rods, as shown in Fig 3.1.

In order to place the specimen accurately at the cavity centre, where the electric field is maximum and approximately uniform over the specimen volume, the rod in the 9.4 GHz cavity was controlled by a micrometer head. The rod entered the cavity through a hole drilled in the centre of the top face where, in the  $H_{101}$  mode, wall currents are not interrupted and the effect on cavity behaviour is negligible. The longer wavelength of the 2.9 GHz cavity allowed the specimen to be positioned with sufficient accuracy without a micrometer drive. A silica rod was fixed directly to the inner wall of the cavity.

The cavities were constructed so that one wall could be easily removed to insert the specimen. It was necessary to replace the wall as accurately as possible, to avoid causing small changes which could produce additional perturbations. Metal rods were used to align the detachable wall of the larger cavity.

TABLE 3.1 : Cavity Parameters

Parameter	2.9 Gz Cavity	9.4 GHz Cavity
a cm	7.21	2.23
b cm	3.40	2.23
l cm	7.21	2.23
D cm		0.6
Vol cm <sup>3</sup>	176.746	11.0896
f <sub>o</sub> GHz	2.92	9.40

### 3.6 MEASUREMENT OF RESONANCE FREQUENCY

The resonance absorption curve of the test cavity was displayed on an oscilloscope by driving the cavity with a periodic frequency swept input signal, and the resonance frequency was compared to that of a calibrated cavity wavemeter. Displayed resonance curves are accurate provided that the frequency sweep is slow in comparison to the response time of the resonant cavity,  $Q/\omega_0$ . This condition is easily satisfied at microwave frequencies. Dynamic methods do not require the extreme frequency stability and fine tuning of the static methods and are generally faster.

The microwave system used for the 9.4 GHz measurements is described in detail in the following section. The 2.9 Gz system was similar and is described more briefly.

### 3.7 THE 9.4 GHz SYSTEM

The 9.4 GHz waveguide bench is illustrated in Fig 3.2. All components were standard except the cavity and its tuning unit, and the sawtooth waveform generator.

#### 3.7.1 The Waveguide Circuit

Microwave power was generated in a klystron selected for good frequency stability. A frequency swept output was obtained applying a 150V variable sawtooth waveform to the klystron reflector. The power supply was selected for good stability and low noise. A finite isolator I.1 provided a matched load for the klystron, and isolated it from reflections and changing impedances in the following circuit. Attenuator R.1 increased the isolation and allowed adjustment of the total power fed to the following circuit. The 10 dB directional coupler DC.1 fed 10% of the incident power to the wavemeter via attenuator R.2, and the remaining 90% towards the test cavity. The wavemeter consisted

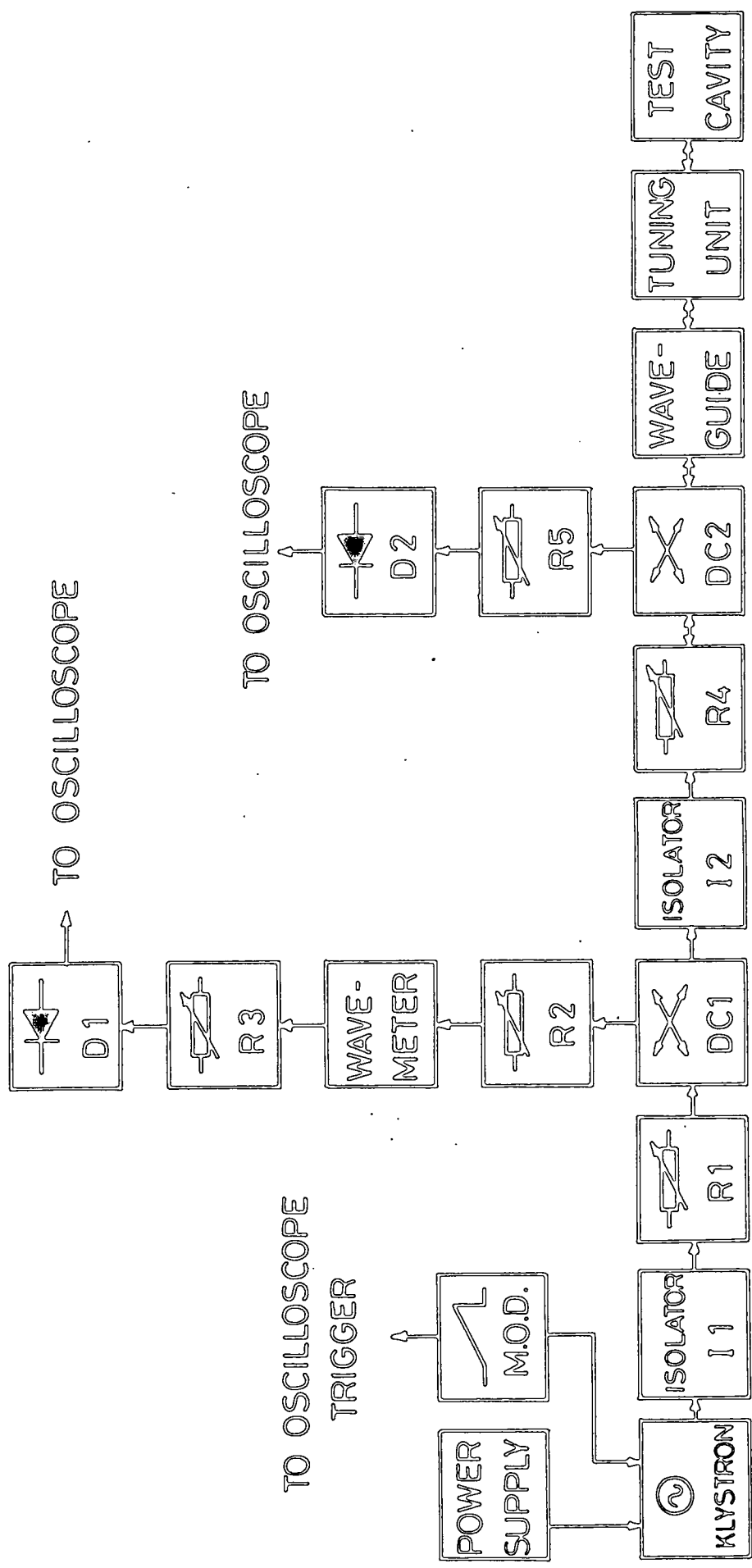


FIG. 3.2. MEASUREMENT OF DIELECTRIC CONSTANT AT 9.4 GHz.

of a frequency calibrated resonant cavity which could be tuned by varying its length with a piston driven by a micrometer head. It was connected in the absorption mode, in which power is not transmitted through the cavity ; instead the cavity is coupled to its transmitting waveguide section by apertures in the guide wall. Off resonance, power is transmitted with little attenuation. At resonance, power is absorbed to sustain oscillation within the cavity. A high Q-factor gives a sharp resonance curve. The degree of coupling determines the 'depth' of the resonance curve, that is the quantity of power absorbed. Attenuator R.2 matched the wavemeter input and isolated the rest of the circuit from resonance effects.

Attenuator R.3 matched the crystal detector D.1. R.2 and R.3 were adjusted to produce a satisfactory absorption curve in the sensitive range of D.1. The crystal detector D.1 applied a d-c signal proportional to the amplitude of the microwave input to one beam of a dual-beam oscilloscope, whose timebase was synchronised to the klystron output, so that a display of amplitude against frequency was produced. When the wavemeter is tuned to resonate at a frequency within the klystron output sweep, its absorption curve is displayed. Most of the power from the directional coupler DC.1 passes through an isolator I.2 and an attenuator R.4, which again provided matching and isolation. A second 10 dB directional coupler DC.2 was connected to transmit power from R.4 through to the cavity circuit, which consisted of a length of waveguide, a tuning unit and the test cavity itself. The tuning unit consisted of a short section of waveguide fixed to the cavity, fitted with conducting screws which could be lowered into the guide. Imperfections in the cavity and at the cavity/waveguide interface cause unwanted disturbances in the fields within the guide. If the tuning screws are adjusted to cause equal and opposite disturbances, matching is achieved.

Power incident on the cavity is reflected back through the circuit at all frequencies except the cavity resonance frequency, when power is absorbed to sustain the oscillations. Directional coupler DC.2 transmits 90% of the reflected power to R.4 and I.2, where it is absorbed, and 10% to attenuator R.5 and the crystal detector D.2. The rectified signal from D2 is applied to the second beam of the oscilloscope which therefore displayed the resonance curve of the test cavity.

The length of waveguide was necessary to isolate the cavity from mismatch in the directional coupler DC.2. The two crystal detectors were selected for similar responses over the frequency and power ranges used.

### 3.7.2 Initial Adjustments

The klystron voltages were set to give maximum output over the widest frequency range, which occurs when the power envelope displayed on the oscilloscope consists of a single smooth curve of maximum amplitude over the duration of the sawtooth waveform. The output frequency sweep was centred on the cavity resonance frequency by adjusting the mechanical tuning control. During adjustment the power envelope should be monitored from detector D.1, and the position of the cavity resonance from D.2. The envelope displayed from the D.2 output is not reliable at this stage.

When the klystron output is optimum the cavity tuning unit can be adjusted. It was found experimentally that the best matching was obtained by adjusting the tuning screws until the envelope of the reflected power, from D.2, was most similar in shape to the envelope of incident power from D.1. The actions of the tuning screws are interdependent. By starting with all screws fully withdrawn, and

monitoring the effect of lowering each while the other two are not in use, the individual effects can be assessed and the final positions of all three screws determined without difficulty. The tuning should hold over the frequency range and power range expected to occur over a set of specimen measurements, and should not change when the cavity is opened and closed for specimen insertion. If this does occur, mechanical couplings and alignments should be improved. Obviously, tuning cannot be adjusted during a measurement. The cavity should be tuned with the silica suspension rod in place.

Attenuators R.2, R.3, and R.5 were set to equalise the powers incident on detectors D.1 and D.2. In order to do this, the cavity and tuning unit were replaced by a short circuit at the cavity input position, consisting of a closed length of waveguide. The baselines of the oscilloscope traces were set to coincide. The attenuators were adjusted until the power envelopes also coincided. Attenuator R.1 was used to check that the coincidence held over a range of input powers, and then set at a level which gave good detector sensitivity. The cavity was replaced, and retuned if necessary.

### 3.7.3 Measurement of $\epsilon'$ and $\epsilon''$ at 9.4 GHz

With the silica rod in position, the klystron was tuned to place the cavity resonance curve in the centre of the frequency sweep. The wavemeter was tuned until its resonance frequency coincided with the test cavity resonance frequency, that is until both resonance curves were centred on the same frequency. The reading of the wavemeter micrometer was noted, and the frequency found from the calibration chart. This was frequency ( $f_0$ ). The specimen was placed inside the cavity, and the new resonance frequency, ( $f$ ), was found in the same way. The dielectric constant was then calculated from equation (3.17). The

reading of the micrometer which supported the silica rod was noted when measuring ( $f_0$ ) and reset to the same position when measuring ( $f$ ) ; any change in the length of the silica rod within the cavity would produce an additional spurious perturbation.

### 3.8 THE 2.9 GHz SYSTEM

The test cavity was compared with a calibrated wavemeter as before, but here a simpler system was used and both resonance curves were superimposed on the same oscilloscope trace. The circuit is shown in Fig 3.3

#### 3.8.1 The Waveguide Circuit

A Flann S-Band Generator Type PCLS provided a swept frequency signal from an internal klystron. A 16 dB attenuator R.1 provided isolation and matching, and a variable attenuator R.2 controlled the power level. The 20 dB directional coupler DC.1 transmitted the power from R.1 to the waveguide circuit and split the reflected power from the cavity directing 99% to R.2 and R.1 where it was attenuated to a level which did not influence the signal generator, and 1% to attenuator R.3. The wavemeter was a calibrated tuned cavity used in the absorption mode, as in the 9.4 GHz circuit. The signal was rectified by a crystal detector D.1 and displayed as amplitude against frequency on the oscilloscope.

#### 3.8.2 Initial Adjustments

The wavemeter was tuned to a frequency far from the test cavity resonance, so that its absorption curve was not displayed on the oscilloscope. The signal generator was set for optimum output at the test cavity resonance frequency. The cavity had been fitted with its silica suspension rod. Its resonance curve was now displayed on the oscilloscope. Attenuators R.2 and R.3 were varied to check detector sensitivity, and set to give a good display. The wavemeter was tuned

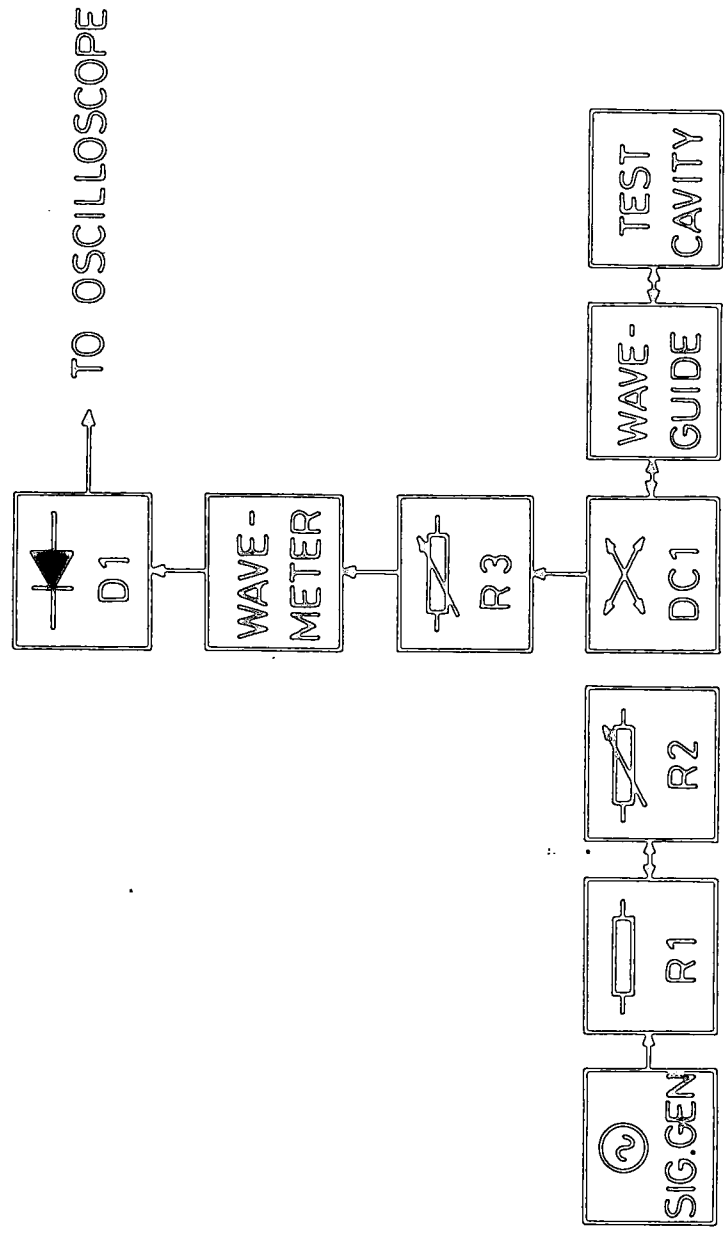


FIG. 3.3. MEASUREMENT OF DIELECTRIC CONSTANT AT 2.9 GHz.

until its resonance curve was also seen, and R.2 and R.3 were readjusted if necessary.

### 3.8.3 Measurement of $\epsilon'$ and $\epsilon''$

The resonance generator was tuned to display the resonance curve of the test cavity containing the silica rod but without a specimen in place. The wavemeter was tuned until its resonance curve was superimposed on the cavity resonance curve, and  $f_0$  was found from the calibrated micrometer. Greater accuracy was obtained by also measuring frequencies equal distances above and below the cavity resonance frequency, and averaging. The result should agree with the initial measurement. The resonance frequency ( $f$ ) with the specimen in the cavity was found in the same way, and  $\epsilon'$  calculated from equation (3.17).

### 3.9 CONCLUSIONS

The two waveguide systems described were built and used successfully to measure the dielectric constants of the oxynitride glasses. The 9.4 GHz system was also used to measure both dielectric constants and dielectric losses of pure MgO and MgO systematically doped with iron or chromium [Thorp, Kulesza, Rad and Kenmuir, 3.12], [Rad, 3.13].

## CHAPTER 3

### REFERENCES

- 3.1 Bethe, H.A. & Schwinger, J. (1943), 'Perturbation Theory for Cavities', N.R.D.C. Report D1-177, Cornell University.
- 3.2 Kahan, T. (1945) 'Methode de Perturbation Appliquee a l' étude des Cavities E'lectromagnétique'. *Comptes Rendus*. 221, 536.
- 3.3 Sproull, R.L., Linder, E.G. (1946), Proc.I.R.E. 34, 305.
- 3.4 Birnbaum, G & Frangau, J. (1949), 'Measurement of the Dielectric Constant and Loss of Solids and Liquids by a Cavity Perturbation Method', J.App.Phys., 20, 817.
- 3.5 Slater, J.C. (1946), Rev.Mod.Phys. 18, 480.
- 3.6 Slater, J.C. (1950), 'Microwave Electronics', page 80, Van Nostrand
- 3.7 Casimir, H.B.G., (1951), 'On the Theory of Electromagnetic Waves in Resonant Cavities', Philips Research Reports 6, 162.
- 3.8 Waldron, R.A. (1960), 'Perturbation Theory of Resonant Cavities', I.E.E.Monograph No.373E, 272.

- 3.9 Waldron, R.A. (1961), 'Perturbation Theory and its Applications'  
Electronic Technology, 38, 178.
- 3.10 Spencer, E.G., Le Craw, R.c. and Ault, L.A. (1957), 'Note on Cavity  
Perturbation Theory', J.App.Phys. 28, 130.
- 3.11 Stratton, J.A. (1941), 'Electromagnetic Theory', McCraw Hill, N.Y.
- 3.12 J.S.Thorp, B.L.J.Kulesza, N.E.Rad, S.V.J.Kenmuir, J.Mat.Sci.19  
(1984), 3211.
- 3.13 N.E.Rad, Ph.D Thesis, University of Durham 1979.

## CHAPTER 4.

THE DIELECTRIC BEHAVIOUR OF OXY-NITRIDE GLASSES IN THE  
A.F. AND R.F. RANGES4.1 INTRODUCTION

The dielectric properties of glasses of the Mg, Ca, Y and Nd oxynitride systems were initially measured at room temperature over the frequency range 500 Hz to 10 KHz using the bridge techniques described in Chapter 2.

Later, in collaboration with A.B.Ahmad, the work was extended using co-axial line techniques to cover the frequency range from 500 MHz to 5 GHz.

The specific objectives of the study were firstly to establish the order of magnitude of the permittivity and, in particular, the dielectric loss so as to enable these glass systems to be placed on a comparative scale with the more widely studied oxide glasses. In the second place the effect of changing the cation, (e.g. from Mg to Ca or Y etc), was to be investigated. Thirdly, and perhaps most importantly, the effect of nitrogen substitution for oxygen in a glass system with a given cation was to be examined and here, although the range of nitrogen substitution is curtailed by chemical and structural factors to less than about 14%, it was hoped to establish the trend of the variations of both  $\epsilon'$  and  $\epsilon''$  with nitrogen concentration. In addition to the foregoing, all of which relate to the chemical compositions of the glass

systems, an attempt was made to elucidate the conductivity mechanism in the glasses by observing the variation of the dielectric properties with frequency over as wide a frequency range as the techniques allowed.

## 4.2 RESULTS IN THE A.F. RANGE

### 4.2.1 Glass Compositions

The compositions of the glasses examined, all of which were prepared at the Crystallography Laboratory, University of Newcastle-upon-Tyne, [Jack et al, 4.1, Drew 4.2, Drew et al 4.3], are given in Table 4.1. It can be seen from this that the compositions were varied systematically. Each of the four cation systems [Mg, Ca, Y and Nd] included an oxide glass without nitrogen. The oxynitrides of the system were formed by substituting chemical equivalents of nitrogen for proportions of the oxygen of the oxide glass. The percentage of oxygen replaced in this way is given in Table 4.1 for each oxynitride composition. Proportions of other elements were held constant, although the decrease in the total number of atoms caused by the substitution of two nitrogen atoms for three oxygen atoms naturally increased the numerical values of their concentrations when expressed in atomic percent. The same system was followed between the different cation series, which therefore contained equal chemical equivalents of either Mg, Ca, Y or Nd. The ratio of (total positive valences)/(total negative valences) did not vary with either nitrogen concentration or cation type, and was equal to one for all the materials investigated.

### 4.2.2 Experimental Data at A.F.

The variations of  $\log(\epsilon' - \epsilon_\infty)$  with  $\log(f)$  for the different compositions are given in Fig.4.1. The values of  $\epsilon_\infty$  were calculated from the optical refractive index measurements of Drew [Jack et al 4.1],

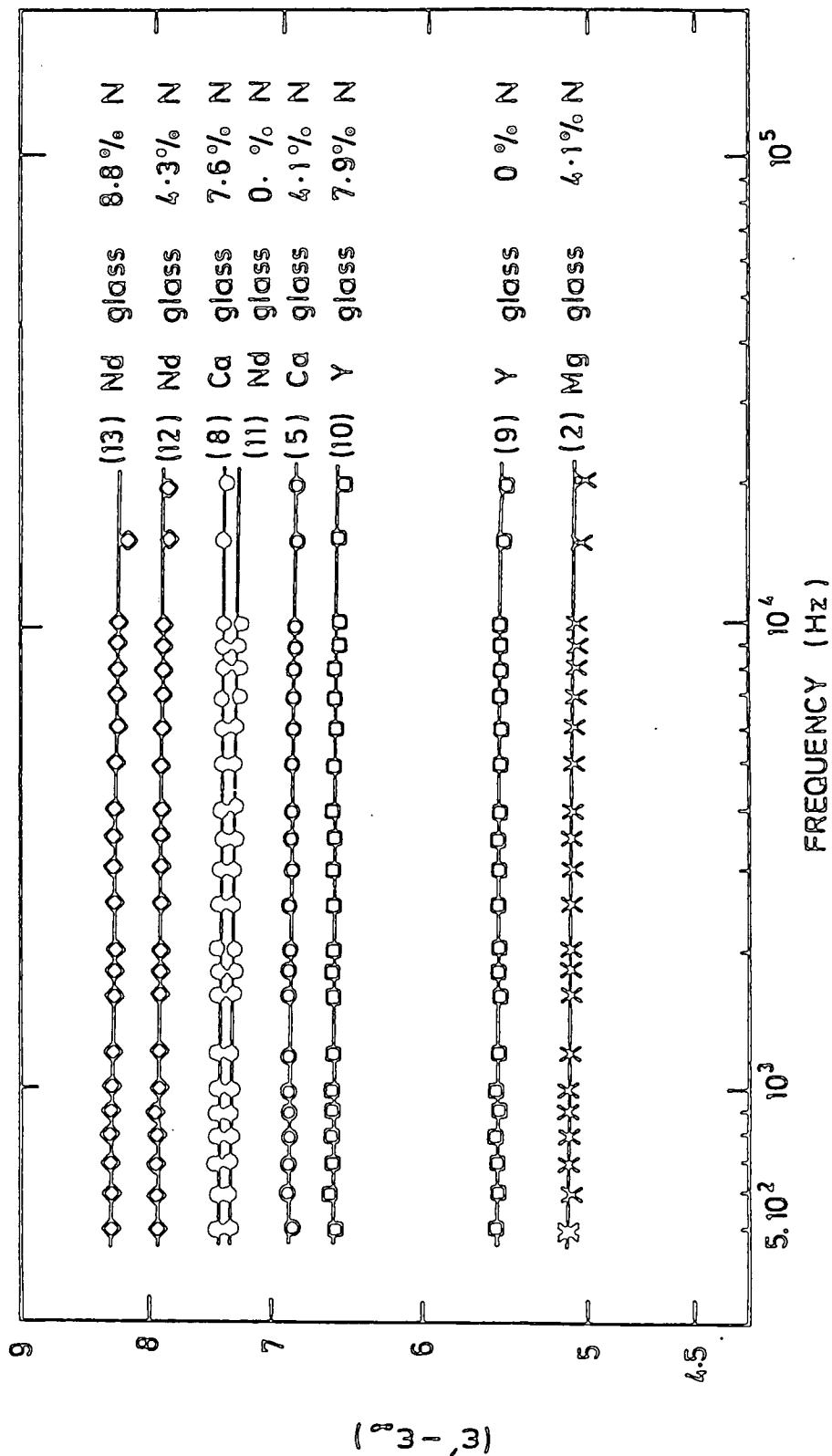


FIG. 4.1 Dependence of ( $\epsilon' - \epsilon_\infty$ ) on frequency and composition.

and are included in Table 4.1. It may be noted, however, that, since other dielectric dispersions are likely to occur between this frequency range and the optical range, the value of  $\epsilon_{\infty}$  relevant to these frequencies may be rather higher than that corresponding to the optical refractive index. Each composition showed a linear variation. The slopes of the plots were independent of composition and had the value  $0.99 \pm 0.02$  for all specimens. At any given frequency the value of  $\epsilon'$  depended markedly on composition, increasing as nitrogen concentration increased and varying with cation type. It is useful to refer to the loss behaviour in two alternative ways. In the first place, in order to facilitate comparison with previously published data on oxy-nitride glasses [Loehman 4.4, Leedecke and Loehman 4.5, Thorp and Kenmuir, 4.6] it is convenient to use conductivities, ( $\sigma$ ).

The plots of  $\log(\sigma)$  against  $\log(f)$  shown in Fig 4.2 are also linear with the same slope for all compositions, in this case  $1.0 \pm 0.1$ . Again, the value of  $\sigma$  at any frequency in the range depended on both nitrogen concentration and cation type, although the variation of  $\sigma$  with composition was different from that of  $\epsilon'$ . The observed power law dependence of  $\epsilon'$  and  $\sigma$  on frequency is in good agreement with the Universal law of dielectric response in solids [Jonscher 4.7, 4.8, 4.9] in that

$$(\epsilon' - \epsilon_{\infty}) \propto \omega^{n-1}$$

and

$$\sigma(\omega) \propto \omega^n$$

For each composition the values of  $n$  found from Figs 4.1 and 4.2 agree within experimental error. The fact that the same value of  $n$  was found

Sample	Composition in atomic percent										% oxygen replaced by nitrogen	$\epsilon_{\infty}$	$\sigma \cdot 10^{-12} \text{ ohms}^{-1} \text{ cms}^{-1}$ (1600 Hz)
	Mg	Ca	Y	Nd	Si	Al	O	N					
(1)	17.0	-	-	-	17.0	6.0	60.0	-	-	-	-	2.46	12
(2)	17.2	-	-	-	17.2	6.4	55.1	4.1	8.1	2.62	2.71	22.7	
(3)	17.4	-	-	-	17.4	6.6	51.0	7.6	14.8	2.59	2.73	12.8	
(4)	-	17.0	-	-	17.0	6.0	60.0	-	-	2.77	2.80	15.8	
(5)	-	17.2	-	-	17.2	6.4	55.1	4.1	8.1	2.84	2.84	15.6	
(6)	-	17.2	-	-	17.2	6.5	54.2	4.9	9.8	2.76	3.05	16.9	
(7)	-	17.3	-	-	17.3	6.5	53.1	5.8	11.5	11.4	11.0	16.6	
(8)	-	17.4	-	-	17.4	6.6	51.0	7.6	14.8	2.90	3.14	14.5	
(9)	-	-	11.8	-	17.8	6.8	63.6	-	-	2.76	3.05	11.4	
(10)	-	-	12.3	-	18.5	7.1	54.2	7.9	14.8	2.76	3.05	11.0	
(11)	-	-	-	11.8	17.8	6.8	63.6	-	-	2.90	3.14	14.5	
(12)	-	-	-	12.1	18.2	7.0	58.4	4.3	8.1	3.14	3.29	14.5	
(13)	-	-	-	12.4	18.6	7.1	53.1	8.8	16.5	3.29	3.29	14.5	

TABLE 4.1 : Compositions of the Mg-Al-Si, Ca-Al-Si, Y-Al-Si and Nd-Al-Si oxynitride glasses examined.

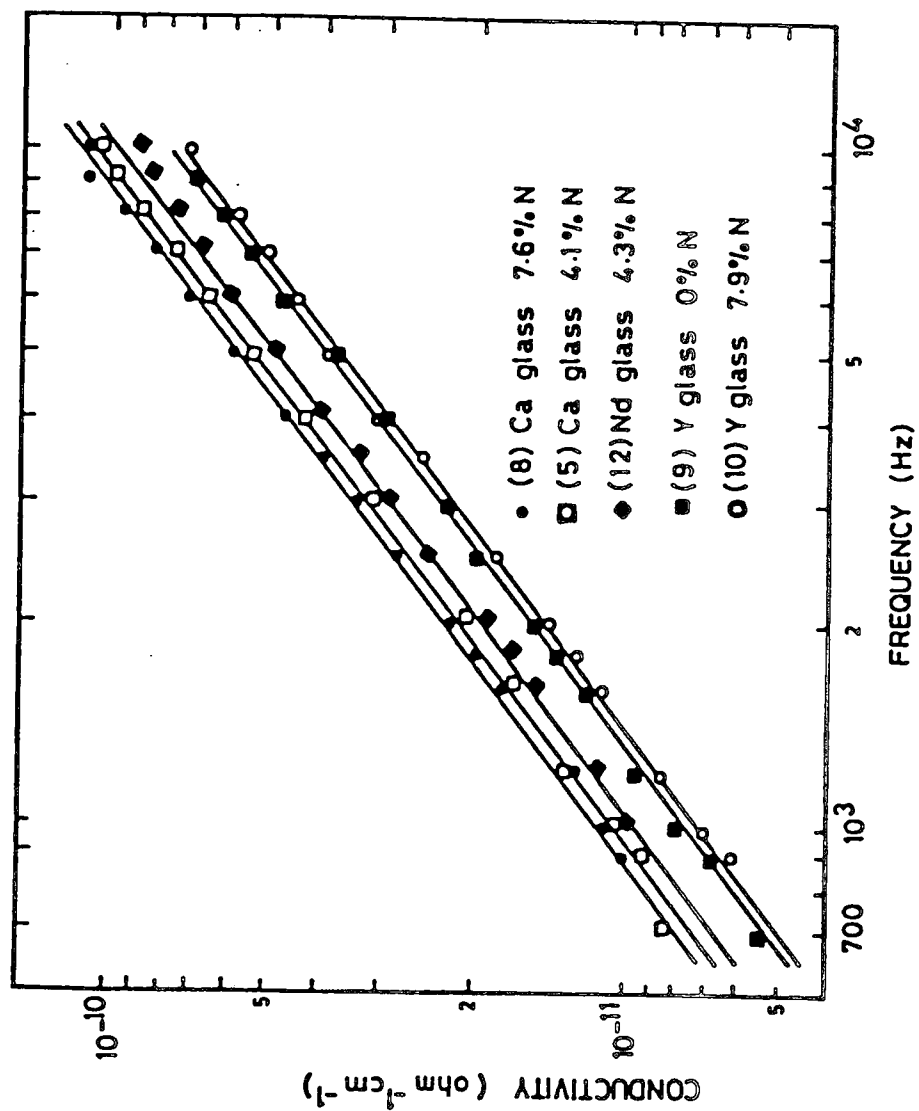


FIG.4.2 Dependence of conductivity on frequency and composition.

for all the specimens suggests that, at room temperature in this frequency range, dielectric polarisation and a-c conductivity in all the compositions examined result from the same hopping mechanism, and that this mechanism is not changed by the substitution of nitrogen. On the other hand a more direct appreciation of the nature of the dependence of loss on frequency is obtained by plotting  $\log \epsilon''$  and  $\log f$ . This plot is given in Fig 4.3 and shows that over the frequency range covered, the loss for each particular composition is almost independent of frequency.

The nature of the dependence of dielectric behaviour on nitrogen becomes more apparent when dielectric constant and dielectric loss ( $\tan \delta$ ) are plotted against nitrogen concentration at a single frequency for all the compositions examined. Fig 4.4 shows the variation of dielectric constant with nitrogen concentration at a frequency of 1600 Hz ( $\omega \approx 10$  KHz). Fig 4.5 shows the variation of dielectric loss ( $\tan \delta$ ) with nitrogen concentration at 1600 Hz. Values of conductivity at this frequency are given in Table 4.1. In order to provide a more consistent comparison of the nitrogen dependence of different cation systems, nitrogen concentration has been expressed as the percentage of the oxygen of the appropriate oxide glass for which nitrogen has been substituted.

#### 4.2.3 Discussion of A.F. Data

Values of dielectric constant ranged from 6.8 for the Mg oxide glass to 11.6 for a Nd oxynitride containing 8.8 atomic percent nitrogen. The dielectric constant increased with increasing nitrogen concentration for each glass system, and substitution of the same proportion of nitrogen produced increases ( $\Delta \epsilon'$ ) of similar magnitude. A comparison of  $\Delta \epsilon'$  for 14.8% substitution is given in Table 4.2. At each

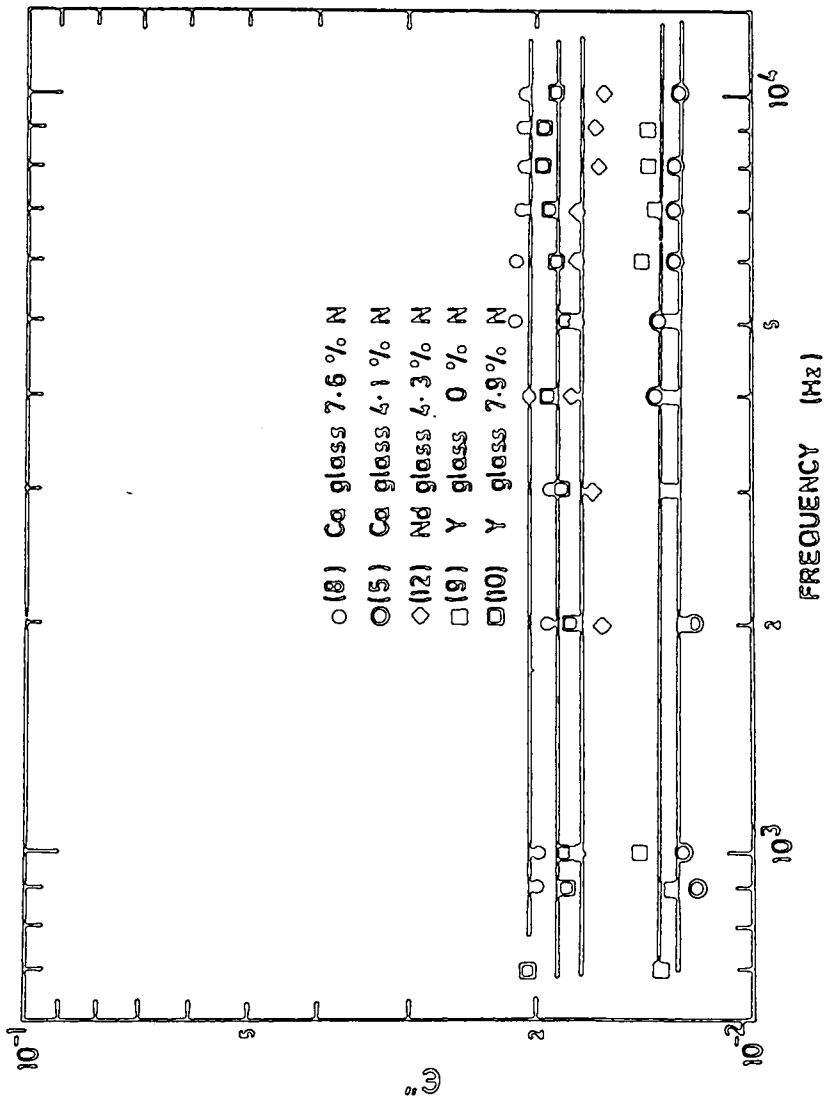


FIG.4.3 Variation of  $\epsilon''$  with frequency.

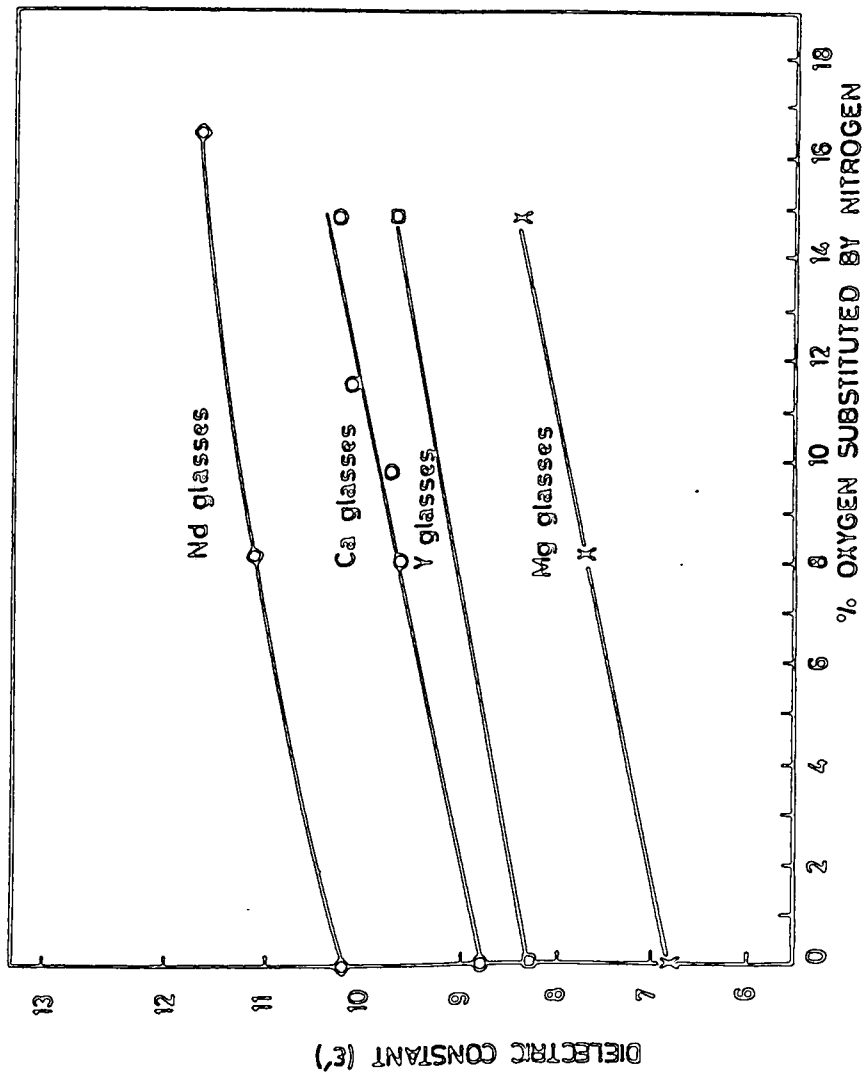


FIG. 4.4 The variation of dielectric constant ( $\epsilon'$ ) with nitrogen concentration for magnesium, calcium, yttrium and neodymium glasses (1600 Hz).

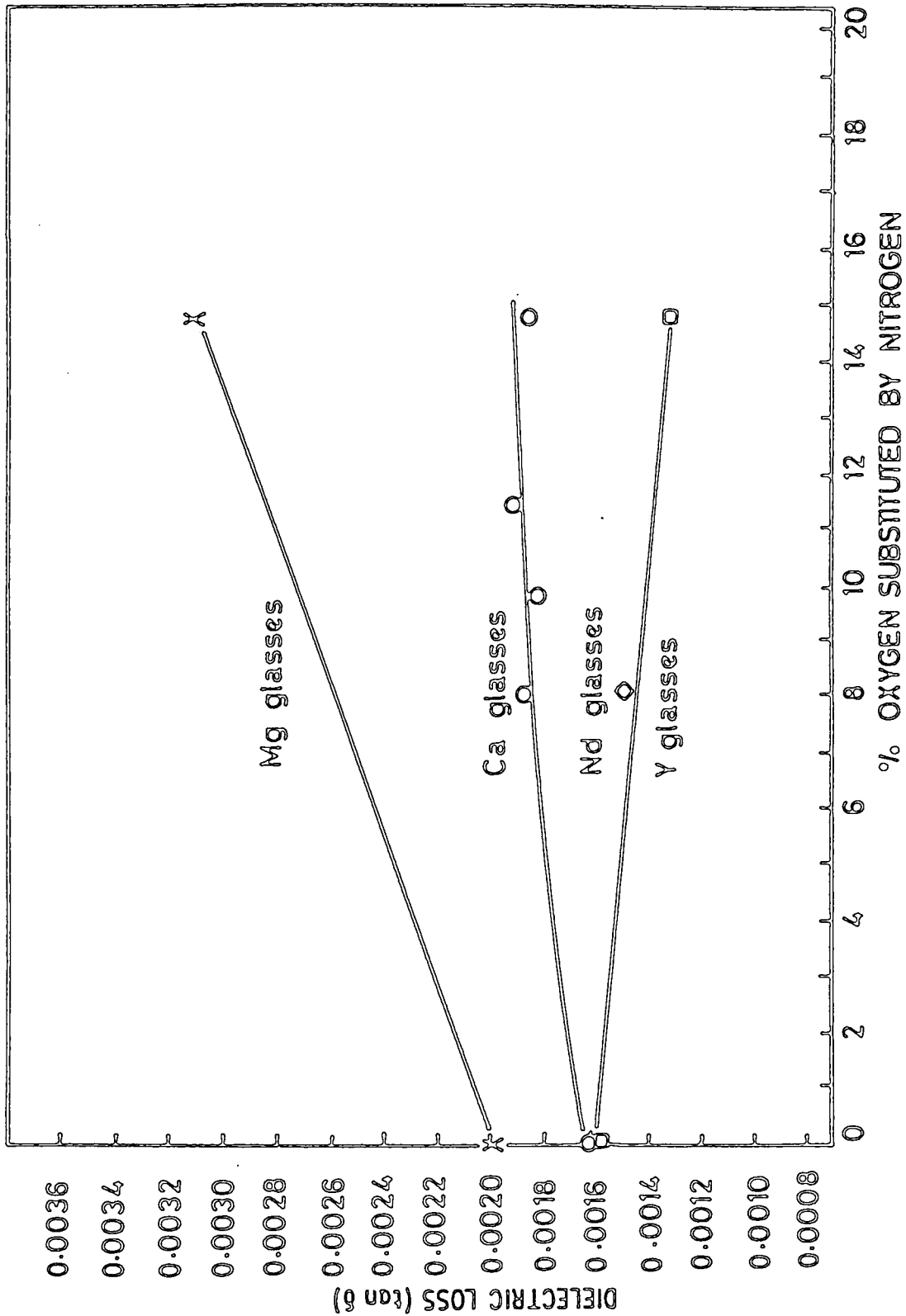


FIG. 4-5 The variation of dielectric loss (tan δ) with nitrogen concentration for magnesium, calcium, yttrium and neodymium glasses (1600 Hz).

Glass System	$\Delta\epsilon'$	Percentage increase relative to oxide
Mg-Al-Si	+ 1.5	21
Y-Al-Si	+ 1.3	17
Ca-Al-Si	+ 1.5	15
Nd-Al-Si	+ 1.3	12

Table 4.2 : The increases in dielectric constants caused by substitution of 14.8% of oxygen by nitrogen.

concentration of nitrogen, and for the oxide glasses, the dielectric constant increased with cation type in the order Mg, Y, Ca, Nd.

As regards the dielectric loss behaviour several features emerge. One of the most significant is that for this whole group of glasses the exponent  $n$  has a value very near to unity and that this corresponds, as shown by Fig 4.3 to frequency independent loss. This is the limiting form of dielectric behaviour, referred to as "lattice loss" by Jonscher [4.10] in which most dipolar processes have been eliminated. The other features refer mainly to changes in composition. Unlike the behaviour of the dielectric constant, the dependence of the dielectric loss on nitrogen concentration varied from system to system : an increase in nitrogen concentration produced a relatively large increase in  $\tan \delta$  in the magnesium glasses, a smaller increase in the calcium glasses, and a decrease in the yttrium glasses. Substitution of 14.8% of oxygen by nitrogen increased  $\tan \delta$  by 55% for magnesium, by 13% for calcium and decreased  $\tan \delta$  by 20% for yttrium glass. A Nd oxynitride glass with 8.1% substitution had a value of  $\tan \delta$  similar to that of the yttrium glasses. Comparing the oxide glasses, the Ca and Y glasses had approximately equal values of  $\tan \delta = .0016$ , while the Mg glass was higher at .002.

The magnesium, calcium and yttrium oxide glasses, at 1600 Hz, had similar values of conductivity [Table 4.1]. Nitrogen substitution increased the conductivities of the magnesium and calcium glasses, magnesium more than calcium, and slightly decreased the conductivity of the yttrium glass. A neodymium oxynitride had a conductivity higher than the yttrium glasses but lower than the corresponding calcium and magnesium glasses.

The dielectric behaviour of some yttrium-aluminium-silicon-oxynitride glasses was reported by Loehman [4.4] and Leedecke and Loehman [4.5]. Two samples similar in composition to sample (10) of Table 4.1 had room temperature dielectric constants of 10, in good agreement with the value of 9.6 reported here. Substitution of 1.5 atomic % of nitrogen for 1.5 atomic % of the oxygen of a yttrium-aluminium-silicon-oxide glass of composition different to the yttrium-aluminium-silicon-oxide glass investigated here, sample (9), increased the room temperature dielectric constant. Room temperature a-c conductivity and dielectric loss decreased with nitrogen by an extent greater than reported here for samples (9) and (10). However, the variation of conductivity with nitrogen concentration has been shown here to depend on the composition of the glass system ; for example substitution of one alkaline earth for the same concentration of another produced a significant change in behaviour. It may be the case that the conductivity variation is also dependent on specific compositions within a glass system, changing with changing concentrations of its elements, and it may be sensitive to different ratios of (total positive valences)/(total negative valences).

It is clear from this work that the substitution of nitrogen into oxide glasses does influence dielectric behaviour, but in a manner which depends on the other constituents of the oxide glass, so that systematic variations of composition are necessary if the effects of the nitrogen are to be distinguished. Oxynitride glass systems can be prepared in which increasing dielectric constant is coupled with either increasing, decreasing or approximately constant dielectric loss. This may be of value in optimising dielectric characteristics for specific

applications, particularly as incorporating nitrogen tends to enhance other physical properties : the mobility of alkali ions in the material is reduced, increasing d-c resistivity and reducing devitrification near electrodes due to electrolysis [Elmer and Nordberg, 4.11], and oxynitride glasses are harder and more refractory [Elmer and Nordberg 4.11, Harding and Ryder 4.12, Shillito et al 4.13]. It is interesting to note that in the system containing neodymium (one of the Period 6 elements of the periodic table included in glass in order to increase the dielectric constant) the oxynitrides have higher dielectric constants than the oxide glass.

Systematic studies of the dielectric behaviour of other oxynitride glasses would be of interest. Systems in which nitrogen substitution has already been achieved include high silica glasses [Elmer and Nordberg 4.11], soda-lime-silica, sodium borate and boric acid [Mullfanger and Meyer 4.16, Mullfanger 4.17].

### 4.3 RESULTS IN THE R.F. RANGE

#### 4.3.1 Measurement Methods

Measurements on the same group of glasses were extended to the 500 MHz to 5 GHz range in order to establish whether the trends of behaviour found at the lower frequencies were maintained in the higher frequency regions. These measurements were facilitated by the developments of precision coaxial line techniques which were themselves initiated by the need encountered in earlier work on doped magnesium oxide for greater precision in the dielectric constant measurements with low loss materials.

The measurements were made using coaxial line methods in which a disc-shaped sample is fitted in a coaxial holder terminated by either a short-circuit, a matched termination or a resonance circuit ; the

details of these techniques have been described recently by Kulesza et al [2.13]. For these measurements circular samples of about 6.5 mm diameter and 0.5 mm thick were cut from the bulk oxynitride glasses using conventional diamond cutting methods and polished with diamond paste to 0.25  $\mu\text{m}$  finishes. The coaxial line with short-circuit termination proved most suitable for the determination of  $\epsilon'$  in the frequency range 500 MHz to 5 GHz while the coaxial line resonance method was found to be preferable for  $\epsilon''$  determination. The matched termination method gave reliable answers only below about 1 GHz and was more suitable for the lower dielectric constant compositions. Above 5 GHz the voltage standing wave ratio (VSWR) measured by the coaxial line resonance method becomes very high, thus effectively setting an upper frequency limit of about 5 GHz for the loss measurements on these glasses. All the data were obtained at room temperature.

#### 4.3.2 Glass Compositions

The compositions of the glasses examined, all of which were prepared by the Crystallography Laboratory, University of Newcastle upon Tyne, are given in Table 4.3. The compositions were varied systematically and each of the three cation systems (magnesium, calcium and yttrium) included an oxide glass without nitrogen. The oxynitrides of the system were formed by substituting chemical equivalents of nitrogen for proportions of the oxygen of the oxide glass. The percentage of oxygen replaced in this way (R) is given in Table 4.3 for each of the oxynitride compositions. The proportions of other elements were held constant, and the same system was followed between the different cation series, which therefore contained equal chemical equivalents of either magnesium, calcium or yttrium. The ratio of (total

Sample	Composition (at %)							% oxygen replaced by nitrogen (R)	$\epsilon_{\infty}$
	Mg	Ca	Y	Si	Al	O	N		
1	17.0	-	-	17.0	6.0	60.0	0	0	2.46
2	17.0	-	-	17.2	6.4	55.1	4.1	8.1	2.62
3	17.4	-	-	17.4	6.6	51.0	7.6	14.8	2.71
4	-	17.0	-	17.0	6.0	60.0	0	0	2.59
5	-	17.2	-	17.2	6.4	55.1	4.1	8.1	2.73
6	-	17.2	-	17.2	6.5	54.2	4.9	9.8	2.77
7	-	17.3	-	17.3	6.5	53.1	5.8	11.5	2.80
8	-	17.4	-	17.4	6.6	51.0	7.6	14.8	2.84
9	-	-	11.8	17.8	6.8	63.6	0	0	2.76
10	-	-	12.3	18.5	7.1	54.2	7.9	14.8	3.05

TABLE 4.3 : Compositions of the Mg-Al-Si, Ca-Al-Si and Y-Al-Si oxynitride glasses examined at R.F.

positive valence)/(total negative valences) did not vary with either nitrogen concentration or cation type, and was equal to one for all the materials investigated. Table 4.3 also includes the limiting high-frequency dielectric constant,  $\epsilon_{\infty}$ , deduced from optical refractive index measurements [Drew 4.2].

#### 4.3.3 Experimental Data at R.F.

The variations of  $\log (\epsilon' - \epsilon_{\infty})$  with  $\log (f)$  for the different compositions are given in Fig 4.6. The values of  $\epsilon_{\infty}$  were calculated from the optical refractive index data given by Drew and are included for reference purposes in Table 4.3. Each composition showed a linear variation. The slopes of the plots were independent of composition and have the value  $1.0 \pm 0.1$  for all specimens. (It may be noted here that, since there are likely to be some other loss processes between the microwave and optical regions, the optical refractive index may not be the relevant value for the purpose of the present investigation.) At any given frequency the value of  $\epsilon'$  depended markedly on composition, increasing as nitrogen concentration increased and varying with cation type. The corresponding loss ( $\epsilon''$ ) behaviour is shown in Fig 4.7 and this shows that over the extended frequency range from 0.5 to 9 GHz the loss for each particular composition is almost independent of frequency. The observed power law dependences of both  $\epsilon'$  and  $\epsilon''$  on frequency are consistent with the universal dielectric response law in solids [Jonscher 4.8, 4.9, 4.10] in that  $(\epsilon' - \epsilon_{\infty}) \propto \omega^{n-1}$  and  $\epsilon'' \propto \omega^{n-1}$ . For each composition the values of  $n$  found from Figs 4.6 and 4.7 agree within experimental error and the observation of the same value of  $n$  for all the specimens suggests that, at room temperature in this extended frequency range, the dielectric polarization and loss in all the

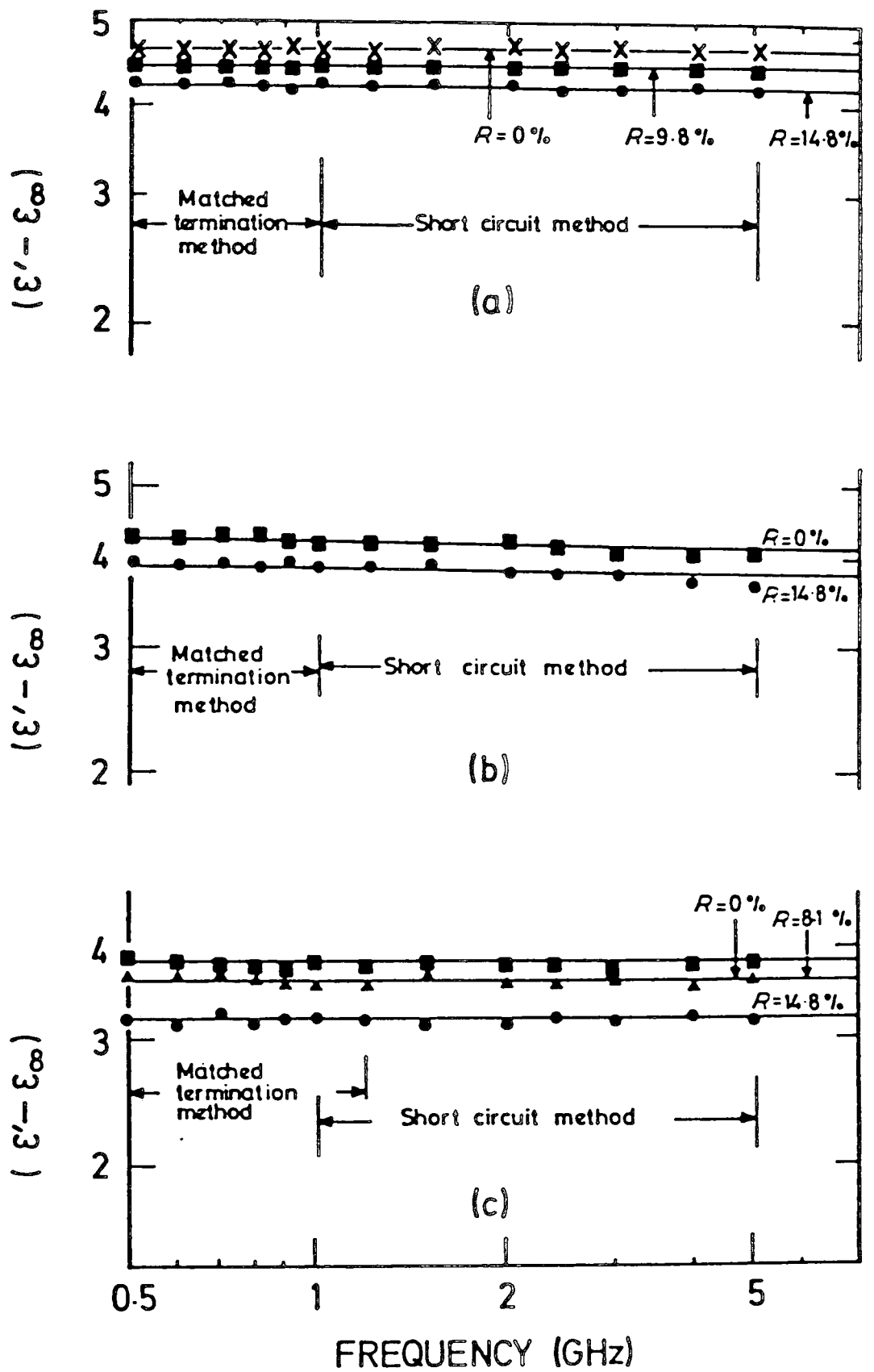


FIG.4-6 Variation of reduced dielectric constant ( $\epsilon' - \epsilon_{\infty}$ ) with frequency;  
 (a) calcium glasses, (b) yttrium glasses, (c) magnesium glasses.

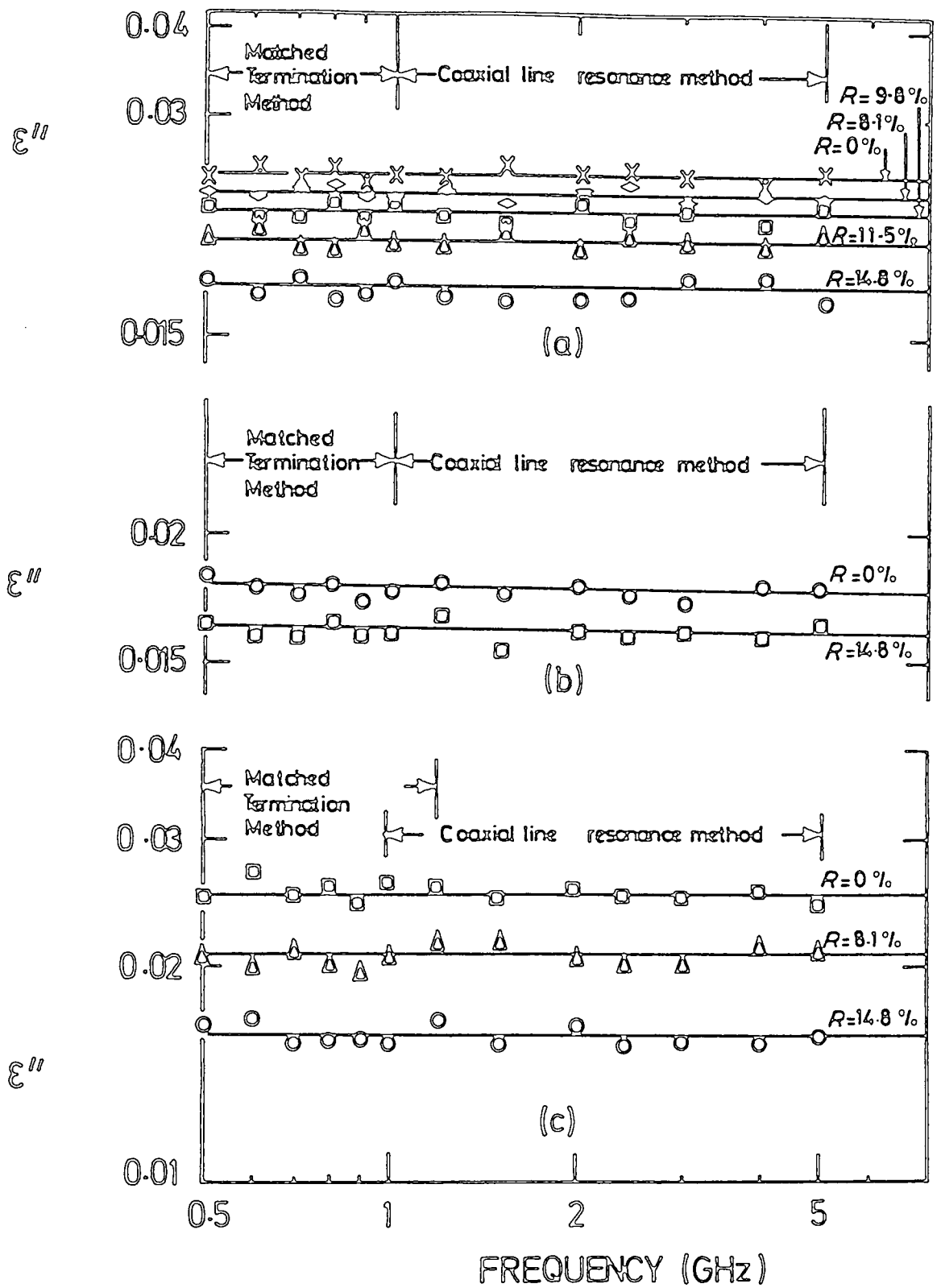


FIG. 4.7 Variation of loss  $\epsilon''$  with frequency;

(a) calcium glasses, (b) yttrium glasses, (c) magnesium glasses.

compositions examined results from the same mechanism, and that this mechanism has not been changed by the substitution of nitrogen for oxygen.

The nature of the changes in dielectric behaviour caused by the substitution of nitrogen for oxygen becomes more apparent when the dielectric constant ( $\epsilon'$ ) and  $\tan \delta$  values are plotted against the nitrogen concentration at a single frequency for all the compositions examined. In order to provide a more consistent comparison of the nitrogen dependence of different cation systems, the nitrogen concentration has been expressed as a percentage of the oxygen of the appropriate oxide glass for which nitrogen has been substituted (R%). Fig 4.8 shows the variation of dielectric constant ( $\epsilon'$ ) with nitrogen concentration at a frequency of 1 GHz ( $\omega \approx 6.3 \times 10^9$ ). Fig 4.9 shows the corresponding variation of  $\tan \delta$  with nitrogen concentration at 1 GHz and the results obtained for  $\epsilon'$ ,  $\epsilon''$  and  $\tan \delta$  are summarised in Table 4.4.

#### 4.3.4 Discussion of R.F.Data

Since the present measurements, made over the frequency range 500 MHz to 5 GHz, and the previous observations over the lower frequency region from 500 Hz to 20 kHz, were all taken with the same series of oxynitride glass samples, a unique opportunity exists for assessing the dielectric behaviour over this very extensive frequency range. A number of important features are revealed.

For each individual glass composition the frequency dependencies of both the dielectric constant  $\epsilon'$  and loss  $\epsilon''$  are consistent with the universal law of dielectric response. Taking the results for all the individual compositions collectively reveals that this whole group of

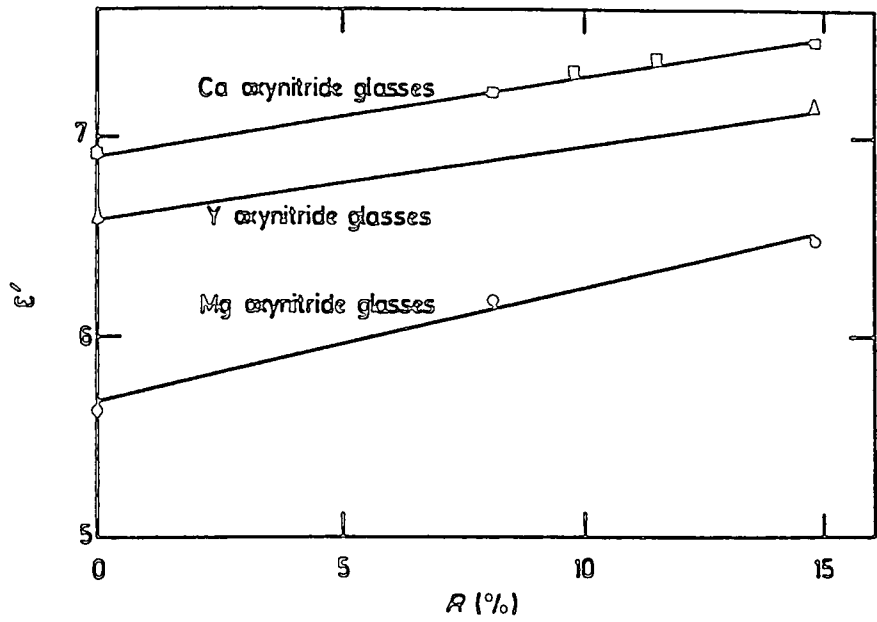


FIG.4.8 Variation of dielectric constant  $\epsilon'$  with % oxygen replaced by nitrogen in oxy-nitride glasses; 1 GHz data.

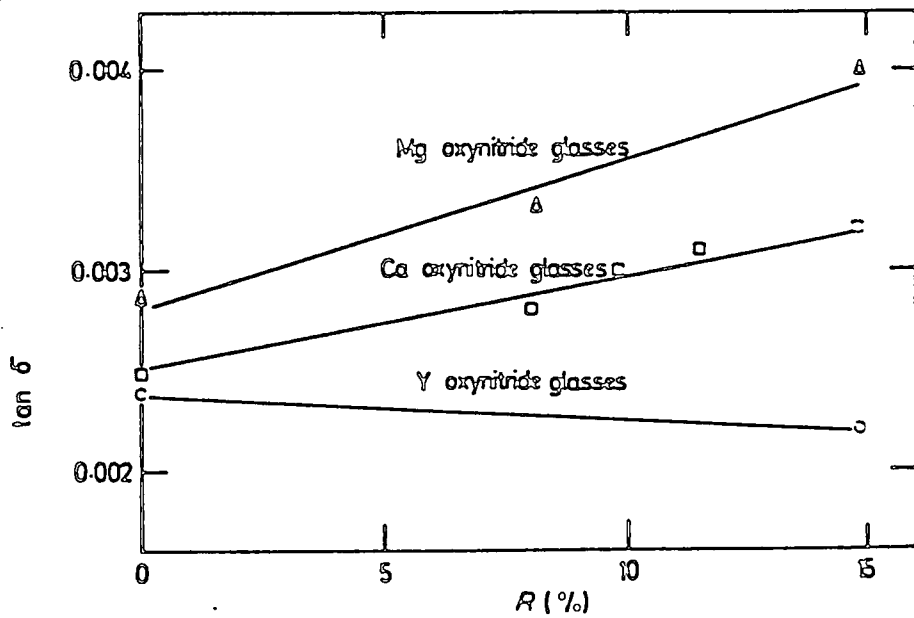


FIG.4.9 Variation of loss tangent with % oxygen replaced by nitrogen in oxynitride glasses; 1 GHz data.

rigid ceramics gives dielectric behaviour corresponding to the limiting form of "lattice loss" [Jonscher 4.10] in which most dipolar processes have been eliminated and frequency independent loss is expected. This is not common though it is interesting to note that similar properties have been reported both for doped magnesium oxide [Thorp, Kulesza, Rad and Kenmuir, 4.14], a rigid refractory oxide ceramic and for several sialon materials [Thorp and Sharif, 4.15], high frequency refractory ceramics containing oxygen and nitrogen.

A second point of interest is to note the range of values of  $\epsilon'$  which can be obtained by compositional changes in the glass system. At the lowest extreme one finds  $\epsilon' \approx 5.6$  at 1 GHz for magnesium oxide glass and at the highest  $\epsilon' = 11.6$  at 1 kHz for a neodymium oxynitride glass containing 8.8 at % nitrogen. This wide range suggests potential for the choice of special glasses where dielectric matching is important, e.g. in substrate materials for devices. In the oxide glasses  $\epsilon'$  is dependent on the cation type and increase in the order magnesium, yttrium, calcium, neodymium while in all the systems the addition of nitrogen increased  $\epsilon'$ . It should be noted, however, that there are limits to the latter method for increasing  $\epsilon'$  since, depending on the particular system, the maximum nitrogen solubility lies in the range 10 to 15 at %, the highest nitrogen-containing glasses so far produced being in the Y-Si-Al-O-N system. It would be of interest to compare simpler oxide and nitride systems (e.g.  $\text{Al}_2\text{O}_3$  and  $\text{AlN}$ ;  $\text{SiO}_2$  and  $\text{Si}_3\text{N}_4$ ) to find whether there are generalized behaviour rules for nitrogen substitution or whether the effects described above are specific to the oxynitride glasses examined here. A similar increase in  $\epsilon'$  when 1.5 at % nitrogen was substituted for the same amount of oxygen in an yttrium

oxynitride glass has been reported by Loehman [ 4.4 ] and by Leedecke and Loehman [ 4.5 ].

A third feature revealed by a comparison of the measurements in the different frequency ranges relates to the cation order found to give increasing values of the dielectric constant  $\epsilon'$ . This feature may most easily be demonstrated by reference to the oxide glasses. At low frequencies it can be stated quite definitely that  $\epsilon'$  increases with change in the cation in the order Mg<Y<Ca<Nd; here the differences in  $\epsilon'$  between compositions are very much greater than any possible experimental errors so that the trend is firmly established. A similar result has now been found at the higher frequencies (between 500 MHz and 5 GHz) and these coaxial line measurements confirm that  $\epsilon'$  increases in the order Mg<Y<Ca.

Some remarks may be made in conclusion regarding the influence of nitrogen substitution on the dielectric loss  $\epsilon''$ . Unlike the behaviour of the dielectric constant  $\epsilon'$  the dependence of dielectric loss on nitrogen concentration varied from system to system. The measurements in the lower frequency range showed that an increase in nitrogen concentration produced a relatively large increase in  $\tan \delta$  in the magnesium glasses and a smaller though definite increase in the calcium glasses ; by contrast a small decrease was observed in the yttrium glasses. The difference in behaviour has been confirmed by the new measurements in the higher frequency range. Substitution of 14.8% oxygen by nitrogen increased  $\tan \delta$  by 39% for magnesium glasses, by 22% for calcium glasses and decreased  $\tan \delta$  by 16% for yttrium glasses [Fig 4.9]. These figures may be compared with the low frequency data where increases of 55% and 13% for magnesium and calcium glasses, and a

decrease of 20% yttrium glasses were observed between 500 Hz and 10 kHz for the same increase in nitrogen concentration. It is interesting to note the close similarity between the values obtained in the two frequency ranges and further that the contrast in behaviour between the yttrium glasses and the others has been confirmed. If the changes in dielectric loss are to be attributed to changes in the chemical bonding there seems no obvious reason why the yttrium ion should differ so markedly from both calcium and magnesium. It must be borne in mind, however, that, at the present stage of development of the preparative techniques for making the oxynitride glasses, there may be other impurities present at low levels and that the measured dielectric loss may be determined by these rather than being a direct monitor of the changes in cation-oxygen or cation-nitrogen bonding schemes.

## CHAPTER 4

### REFERENCES

- 4.1 K.H.Jack, D.Thompson, S. Hampshire, R.A.L.Drew (University of Newcastle upon Tyne), (1980), private communications.
- 4.2 R.A.L.Drew, Ph.D.Thesis, University of Newcastle upon Tyne, (1980).
- 4.3 R.A.L.Drew, S.Hampshire, K.H.Jack, International Symposium on Ceramic Components for Engines, Hakone (Japan) 1983.
- 4.4 R.E.Loehman, J.Amer.Ceram.Soc. 62 (1978), 491.
- 4.5 C.J.Leedecke and R.E.Loehman, J.Amer.Ceram.Soc.63, (1980), 190.
- 4.6 J.S.Thorp and S.V.J.Kenmuir, J.Mat.Sci. (1981).
- 4.7 A.K.Jonscher, J.Phys.C. 6 (1973), L 235.
- 4.8 A.K.Jonscher, Nature 267, (1977), 719.
- 4.9 A.K.Jonscher, Thin Solid Films 36, (1978), 1.
- 4.10 A.K.Jonscher, J.Mat.Sci 16 (1981), 2037.
- 4.11 T.H.Elmer and M.E.Nordberg, J.Amer.Ceram.Soc.50 (1967), 275.
- 4.12 F.L.Harding and R.J.Ryder, Glass Tech 11 (1970), 54.
- 4.13 K.R.Shillito, R.R.Wills, R.B.Bennett, J.Amer.Ceram.Soc. 61, (1978), 537.
- 4.14 J.S.Thorp, B.L.J.Kulesza, N.E.Rad and S.V.J.Kenmuir, J.Mater.Sci.16, (1981), 1052.
- 4.15 J.S.Thorp, R.I.Sharif, J.Mater.Sci.12 (1980), 2274.
- 4.16 H.O.Mulfinger and H.Meyer, Glastechn.Ber.38 (1965), 235.
- 4.17 H.O.Mulfinger, J.Amer.Ceram.Soc.49 (1966), 462.

## CHAPTER 5

## THE DIELECTRIC BEHAVIOUR OF OXYNITRIDE GLASSES

## IN THE MICROWAVE FREQUENCY RANGE

5.1 INTRODUCTION

Three glass systems, magnesium, calcium and yttrium, were studied at microwave frequencies. The oxide glass and an oxynitride glass of the magnesium and calcium systems were measured at 2.9 GHz and 9.3 GHz ; the oxide and an oxynitride of the yttrium systems were measured at 9.3 GHz.

The main objective was to investigate whether nitrogen concentration and cation type had any effect on dielectric constant, and if so whether it was similar or different to the effects at lower frequencies. The absence of, or a different type of dependence would imply that the dielectric properties were now controlled by a different mechanism, with a changeover in the intervening frequency range.

5.2 GLASS COMPOSITIONS

The specimens were supplied from the same bulk samples of material as those measured at audio frequencies. Their compositions are given in Table 3.1 in Chapter 3 and correspond to sample numbers (1), (3), (4), (6), (9) and (10).

5.3 SPECIMEN DIMENSIONS AND ASSOCIATED ERRORS

Specimen sizes of about (5mm x 3mm x 0.5mm) were used. Dimensions varied slightly from specimen to specimen giving a range of volumes from  $6 \text{ mm}^3$  to  $12 \text{ mm}^3$ . The dimensions and volumes are given in Table 5.1.

TABLE 5.1: The dimensions and volumes of the specimens measured at  
2.9 GHz and 9.3 GHz

Sample	Dimensions (mm)	Volume (mm <sup>3</sup> )
(1)	5.322 x 2.954 x 0.663	10.423
(3)	5.982 x 2.880 x 0.656	11.302
(4)	5.338 x 2.940 x 0.460	7.219
(6)	5.318 x 2.950 x 0.501	7.860
(9)	5.642 x 3.194 x 0.381	6.886
(10)	5.266 x 3.239 x 0.714	12.178

Polishing was unnecessary as the cut faces were smooth enough to have no irregularities large enough to introduce significant errors into the calculation of volume.

Where possible the two specimens of each glass system were cut to similar dimensions, so that the only variable when specimens in the cavity were interchanged was that of composition. As can be seen from Table 5.1, this was achieved for the magnesium and calcium glasses, but was not possible for the yttrium glasses.

The cavities and the perturbation method described in Chapter 4 were used and the specimens placed in the cavity with the maximum surface area tangential to the electric field in order to achieve maximum sensitivity. Values of  $\epsilon'$  were calculated from equation 3.17 using the approximation that  $F(\epsilon') = 1$ , when the expression simplifies to

$$\frac{\partial \omega}{\omega} = \frac{1}{2} \frac{v_s}{v_c} (\epsilon' - 1)$$

While this approximation introduces a systematic error which causes the values of  $\epsilon'$  to be lower than the true values, it does not introduce errors into the nature of the dependence of  $\epsilon'$  on composition if specimens of similar dimensions are used. The errors due to this were estimated to be between + 12% and + 20%.

The use of very thin samples would have reduced this error considerably, but at the expense of increasing two other errors which would have been random rather than systematic and which would therefore have tended to obscure systematic variations of dielectric constant with

composition. For very small cross-sections, irregularities in cross-section would have an appreciable effect on specimen volume ; errors in measuring the cross-sections and therefore volume would also be larger. Unless longer specimens were used, and these were not available in the materials investigated here, reducing the cross-sections would reduce the specimen volume. The difference in resonant frequency caused by inserting a specimen into the cavity would therefore be smaller (and the differences between different specimens smaller still), hence the error in measuring  $\delta\omega$  would be increased.

#### 5.4 EXPERIMENTAL MICROWAVE DATA

The values of  $\epsilon'$  measured at 2.9 GHz and 9.3 GHz, with the corresponding values of  $(\epsilon' - \epsilon'_{0s})$  calculated using Drew's values of refractive index [Drew and Jack 5.1, Drew 5.2] are given in Table 5.2.

For each composition, the difference in  $\epsilon'$  between 2.9 GHz and 9.3 GHz was within experimental error, showing that any change with frequency over this narrow range is small, and therefore that the response in this microwave region forms part of a region of flat response and is therefore distant from a dielectric dispersion. Also, as resonant dispersions occur at microwave frequencies, the first resonance can be assumed to be above 10 GHz. The values of permittivity  $\epsilon'$  ranged from 5.6 to 7.8, large enough for possible industrial dielectric applications in the S and X bands. It was found that  $\epsilon'$  shows a strong dependence on both the concentration of nitrogen for a given cation, and on the type of cation for a given concentration of nitrogen. Fig 5.1 and Fig 5.2 show the values of  $\epsilon'$  and  $(\epsilon' - \epsilon'_{0s})$  plotted against nitrogen concentration for all the glasses measured, at 2.9 GHz and 9.3 GHz respectively. As the variation with frequency is

TABLE 5.2 : Values of Dielectric Constant  $\epsilon''$  measured at 2.9 GHz and 9.3 GHz, with the corresponding calculated values of  $(\epsilon'' - \epsilon''_{\text{Ca}})$

Sample	Cation	% oxygen replaced by nitrogen	$\epsilon''$ 2.9 GHz	$\epsilon''$ 9.3 GHz	$(\epsilon'' - \epsilon''_{\text{Ca}})$ 2.9 GHz	$(\epsilon'' - \epsilon''_{\text{Ca}})$ 9.3 GHz
(1)	Mg	0	5.63	5.70	3.17	3.24
(3)	Mg	14.8	6.92	6.53	4.21	3.82
(4)	Ca	0	7.13	7.04	4.54	4.45
(6)	Ca	9.8	7.83	7.75	5.06	4.98
(9)	Y	0		6.87		4.11
(10)	Y	14.8		7.38		4.33

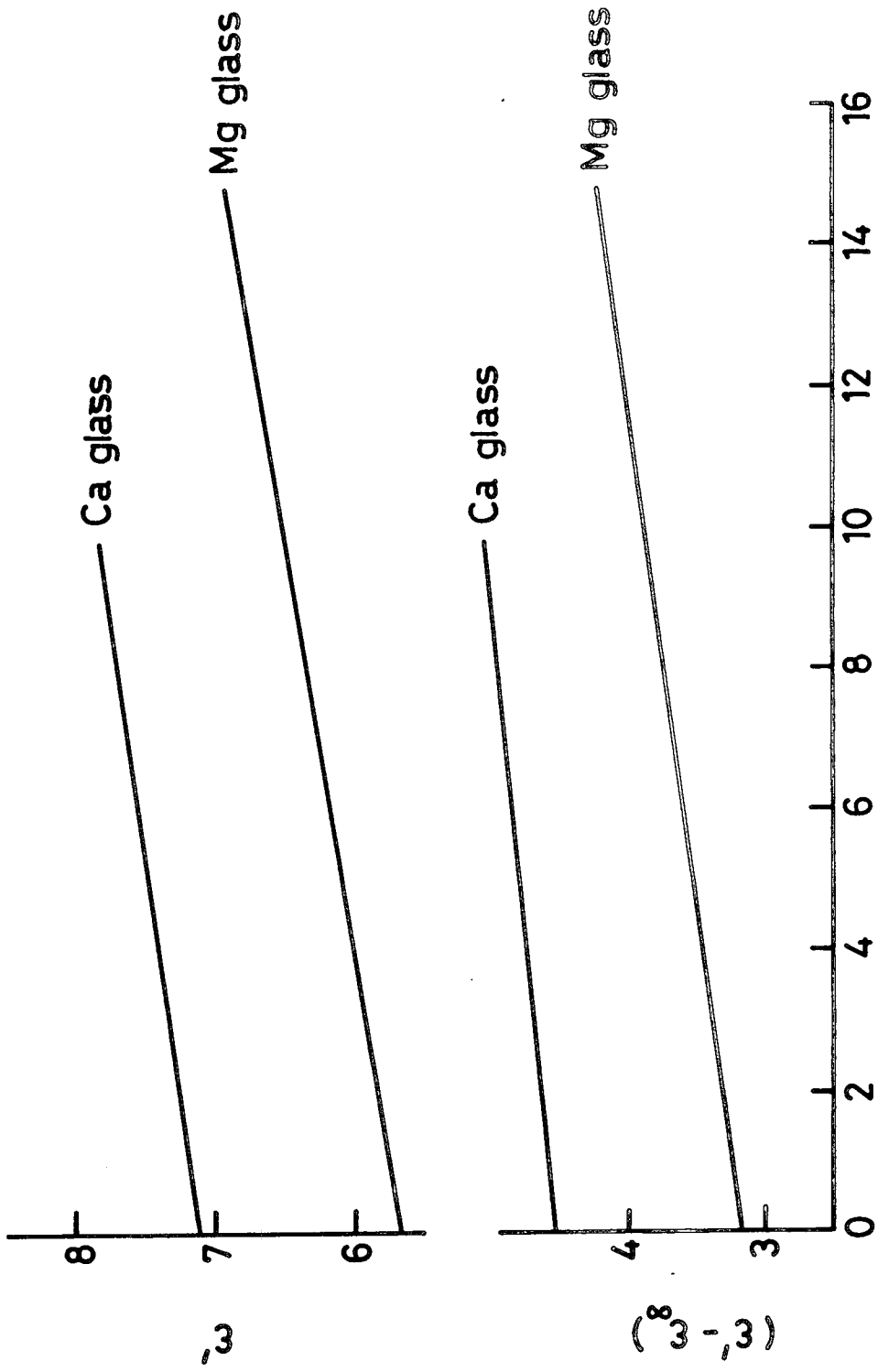


FIG. 5.1. EFFECT OF NITROGEN ADDITION ; 2.9 GHZ DATA.

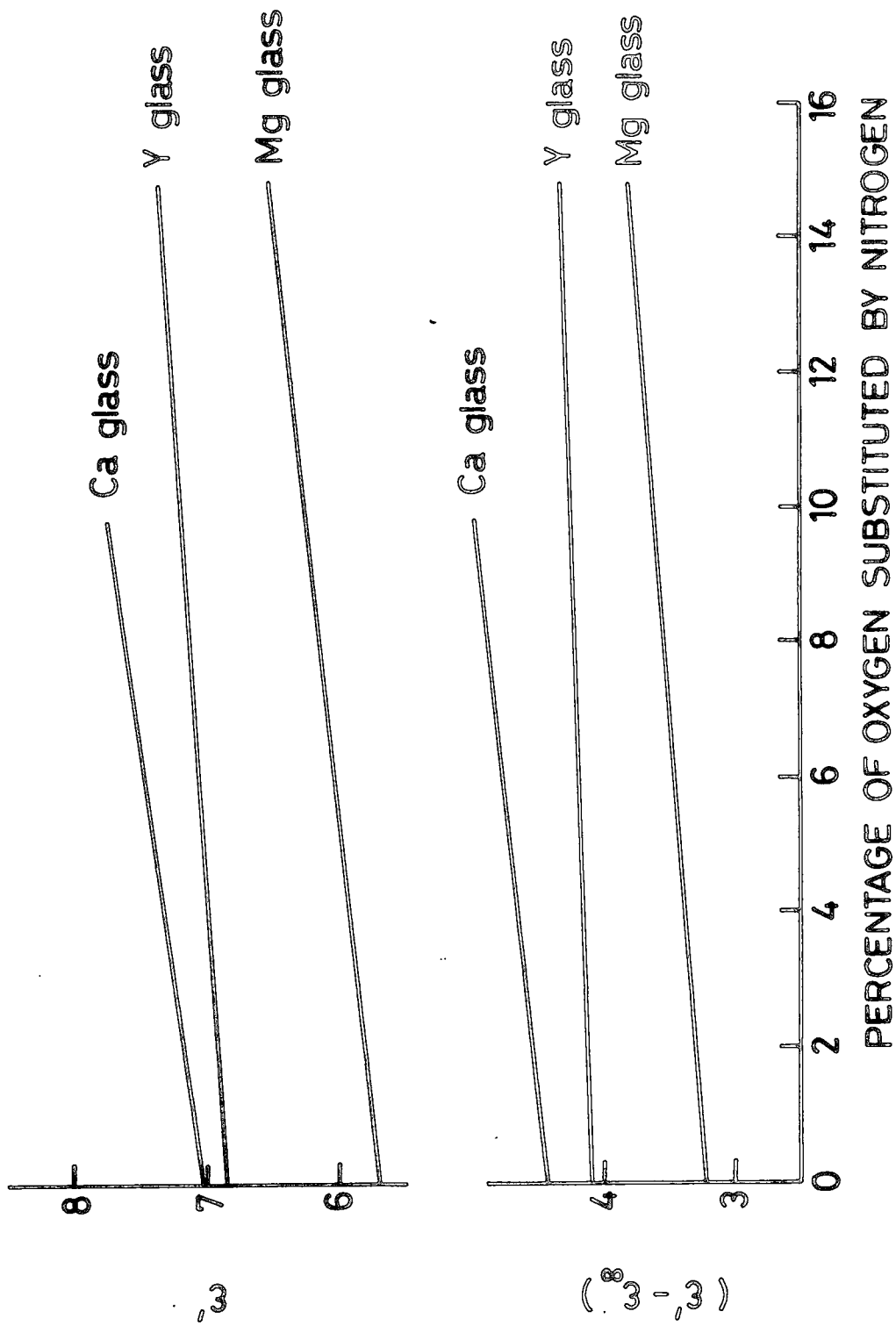


FIG. 5-2. EFFECT OF NITROGEN ADDITION ; 9.3 GHz DATA.

small, the two plots are similar. Nitrogen concentration has again been expressed as the percentage of oxygen of the appropriate oxide glass for which nitrogen has been substituted. For each glass system increasing the nitrogen concentration increased the dielectric constant, and as the cation type changed, the dielectric constant increased in the order magnesium, yttrium, calcium.

Considering the results at 9.3 GHz, which were measured for three systems, substituting nitrogen for 14.8% of the oxygen of the oxide glass increased  $\epsilon'$  by 15% in the magnesium system and by 7% in the yttrium system. The maximum nitrogen concentration measured in the calcium system was 9.8%, but extrapolating to 14.8% assuming a linear relationship similar to that found at audio frequencies gave an increase in  $\epsilon'$  of 16%. The increase in  $\epsilon'$  at both 2.9 GHz and 9.3 GHz are given in Table 5.3.

#### 5.5 COMPARISON WITH LOWER FREQUENCY RESULTS

Comparing these microwave results with the audio frequency results, all the trends of  $\epsilon'$  with composition are the same;  $\epsilon'$  increases with cation type in the order magnesium, yttrium, <sup>calcium</sup> and with increasing nitrogen concentration. At audio frequencies substitution of 14.8% of nitrogen increased  $\epsilon'$  by 21% for magnesium, 15% for calcium and 17% for yttrium. The increases in the two frequency ranges are in good agreement for the magnesium and calcium glasses, but not for the yttrium glasses. This difference may be partly caused by the different dimensions of the yttrium oxide and oxynitride specimens and cannot be considered significant unless confirmed by measurements on samples of more similar dimensions. The oxynitride has almost twice the cross-sectional area, which would give a larger error in  $\epsilon'$ , producing a smaller measured value and hence decreasing of  $\epsilon'$ .

TABLE 5.3 : The increases in dielectric constant caused by substitution of 14.8% of oxygen by nitrogen (The values for calcium are extrapolated from 9.8%)

Glass  System	2.9 GHz		9.3 GHz	
	$\Delta\epsilon'$	% increase relative to oxide glass	$\Delta\epsilon$	% increase relative to oxide glass
Mg-Al-Si	1.3	23	0.83	15
Ca-Al-Si	1.1	15	1.1	16
Y-Al-Si			0.51	7

For each composition, the value of  $\epsilon'$  at 9.3 GHz is about 20% lower than the audio frequency value. The maximum difference, 23%, is found in the yttrium oxynitride glass.

When compared with the radio frequency results, there is also good agreement. The microwave results at 2.9 GHz and 9.4 GHz fall with experimental error on the plots of  $\log (\epsilon' - \epsilon'_\infty)$  against  $\log \frac{f}{\nu}$ , which in the radio frequency case range from 500 MHz to 5 GHz.

#### 5.6 DISCUSSION OF MICROWAVE DATA

The flat responses at both audio and microwave frequencies, with a 20% decrease in the value of  $\epsilon'$  between the two regions is compatible with two types of behaviour. A dispersion (or dispersions) may have occurred in the intervening frequency range, 20 KHz to ~~2.0 GHz~~<sup>500 MHz</sup>. If so, their centre frequencies must be distant from 20 KHz at the low frequency side and from 500 MHz at the high frequency side, as at these frequencies the response is again flat with no indication of the changing 'n' values of @ dispersion. As resonant dispersions normally occur at microwave frequencies and above, any such dispersion is highly likely to be a dielectric relaxation, which suggests that in all these glasses, the first dielectric resonance occurs at a frequency higher than 10 GHz. If a relaxation is present between 20 KHz and 500 MHz, the observations that the value of  $\epsilon'$  falls by just 20% of its 20 KHz value, between 1 KHz and 10 GHz and that all the trends with composition are unchanged in the frequency ranges, above and below the dispersion suggest that the mechanism which produces this relaxation is not the dominant dielectric mechanism of these materials.

The other possible type of behaviour is that the response for each glass composition is flat over the intervening frequency range, and that

the power law found at audio frequencies extends without interruption over the seven decades of frequency to the microwave region. For this to be possible, the value of  $n$  found at audio frequencies must be compatible with a 20% decrease in  $\epsilon'$  over the complete range. The maximum decrease in  $\epsilon'$  was the 23% change of the yttrium oxynitride glass. This requires a value of  $n$  not less than 0.985. The value of  $n$  given by the audio frequency measurements was  $0.99 \pm 0.02$ . A flat response with  $n$  between 0.985 and 1.0 is therefore consistent with both sets of data. The results also show that taking all the glass compositions measured, the order in which  $\epsilon'$  increases with composition is exactly the same in both frequency ranges. This is compatible with either type of response, and also with the suggestion that any relaxation which may occur is not due to the dominant dielectric mechanism.

The type of response has implications for the possible applications of these glasses. The fact that the response over the microwave frequency range is flat with a usefully high value of  $\epsilon'$  suggests that these glasses may have applications as dielectrics at S-band and X-band. It also suggests that none of these glass compositions, if found in the glassy phase in  $\text{Si}_3\text{N}_4$  ceramics, will cause the ceramic to have a dielectric dispersion in this region. This microwave behaviour also suggests that extending the dielectric study to both lower and higher frequencies would be worthwhile. Measurements in the 20 KHz to 500 MHz range would determine the type of response. If the response were flat, then these glasses could have applications as very broad band dielectrics whose response could be adjusted by changes in composition. If a relaxation were found, its behaviour and dependence on composition

would be important because of its effect on the behaviour of  $\text{Si}_3\text{N}_4$  ceramics. A response which was found to give a flat response at frequencies above 10 GHz could lead to applications in millimetre wavelength radome materials, and in millimetre wave electronic devices.

## 5.7 COMPARISON OF CAVITY PERTURBATION AND CO-AXIAL LINE

### MEASUREMENT TECHNIQUES

As mentioned earlier coaxial line techniques were developed independently for use in the frequency range 500 MHz to 5 GHz. At the upper end of this range the frequency approaches those characteristic of the microwave region and it is consequently of interest and importance to compare the techniques - and the results obtained with them - in more detail, especially in the region where coaxial line and cavity perturbation measurements can be made at the same frequency.

In parallel with the development of the techniques to measure small differences in dielectric behaviour between physically small specimens at audio frequencies (bridge methods), radio frequencies (a meter) and microwave frequencies (perturbed cavities) described here, two coaxial techniques for high frequencies were developed by Ahmad [5.3] and by Kulesza, Thorp and Ahmad [5.4] working in the same group. A coaxial matched termination method gave good accuracy in the measurement of dielectric constant  $\epsilon'$ , and a resonant line method proved capable of measuring the dielectric loss,  $\epsilon''$ , in low loss materials. The apparatus was designed so that both methods used the same coaxial line (a General Radio slotted line system) and the same sample holder, and differed only in the termination: a matched load was used in one case and a variable short circuit stub in the other.

~~Ahmad used these techniques to measure the dielectric properties of~~

A comparison of the different sets of data shows the following points :-

- (a) Where  $\epsilon'$  has been measured again for the oxynitrides reported here, there is very good agreement between the two sets of data.
- (b) The data for 9.3 GHz for all the specimens measured when plotted on the  $\log \epsilon'$  against  $\log f$  graphs lie on the same straight lines, showing that in all cases the power law response extends to 9.3 GHz. The 2.9 GHz are also in good agreement, again lying on the corresponding straight lines.

It is interesting that the cavity data and the coaxial data fall on the same straight lines when plotted. Measurements at audio frequencies and at coaxial line frequencies are carried out on the same disc specimens, so that errors between the different regions originate from the techniques themselves with no contribution from the use of different specimens. Also, data taken with a single technique will have smaller errors between the data at different frequencies, as systematic errors between techniques are absent. The cavity data were obtained with a different size of specimen from the coaxial data, and with different cavities. The overlap in frequency at 2.9 GHz is important in that it confirms the continuity of the data taken with the different techniques. This continuity, and this fact that all the data formed a linear plot shows that the experimental errors between the coaxial technique and the cavity technique, and between the different cavities, are small enough to show the nature of the frequency dependence of the dielectric constant over the complete frequency range, and either detect dielectric dispersions or measure the exponent 'n' of a power law. The agreement

between the results for the different cavities confirms that a range of cavities, each at a different frequency, will give consistent data within the limitations of the perturbation technique, and can be used to study the frequency dependence at higher frequencies. However, as frequency increases and cavity size decreases, certain experimental errors become significant. A modification of the cavity technique which reduced these errors was developed, and is described in Section 8.

#### 5.8 THE PERTURBATION METHOD AT HIGHER FREQUENCIES

The smaller cavities required for higher frequencies have increased experimental errors which become more significant as size decreases. The major one is caused by the removal of one side of the cavity after measuring the resonant frequency of the empty cavity in order to insert the specimen. Any difference in repositioning the removable wall, or in the contact which it makes to the fixed walls of the cavity introduce additional perturbations which cannot be distinguished from that due to the specimen. The smaller cavities need greater precision in handling, and their smaller value of  $Q$  make errors more significant. A second major source of increased error is the necessity for smaller specimens, in order to prevent the distortion of the cavity fields becoming large enough to invalidate the perturbation theory. Error in measuring specimen volume increases with decreasing specimen size. Associated with this is the problem that as cavity volume and specimen volume decreases, the effect of the silica suspension rod begins to become significant. The presence of a silica rod in a cavity of relatively small volume distorts the fields in the cavity, from the normal  $H_{101}$  mode assumed in deriving equation

$$\frac{\delta\omega}{\omega} = \frac{1}{2} \frac{v_s}{v_c} (\epsilon' - 1) F(\epsilon')$$

from the general equations of Chapter 3. Tests with the 9.3 GHz cavity using a silica rod relatively thick in comparison to the specimen indicated that the measured values of the specimen permitted, would be increased by the presence of the rod.

A different method of introducing specimen material into the cavity eliminated the errors due to removal of the cavity wall and the silica rod, and reduced the error in sample volume. Instead of suspending a small specimen at the centre of the cavity, a rod shaped specimen was lowered gradually into the cavity as shown in Fig 5.3. The specimen was again fixed to a silica rod, but this rod did not enter the cavity. This method requires a rod shaped sample of uniform cross-section which can be a disadvantage in some materials, but no other disadvantages were noted. The specimen is lowered into the cavity by adjusting the micrometer head. When the edge of the specimen is level with the cavity wall the cavity resonance frequency is noted. The specimen is then lowered further in steps of 0.25 mm, and the resonance frequency is noted at each position. Each increment introduces an additional equal volume of specimen material into the cavity, as the specimen has uniform cross-section, and hence caused equal increments in the resonance frequency as

$$\Delta f \propto \Delta v$$

(from eqn.3.17). The plot of frequency against length is linear, after an initial non-linear region when the end of the specimen just enters the electric field. Permittivity is calculated from the change in resonance frequency and the corresponding length of sample. Here the

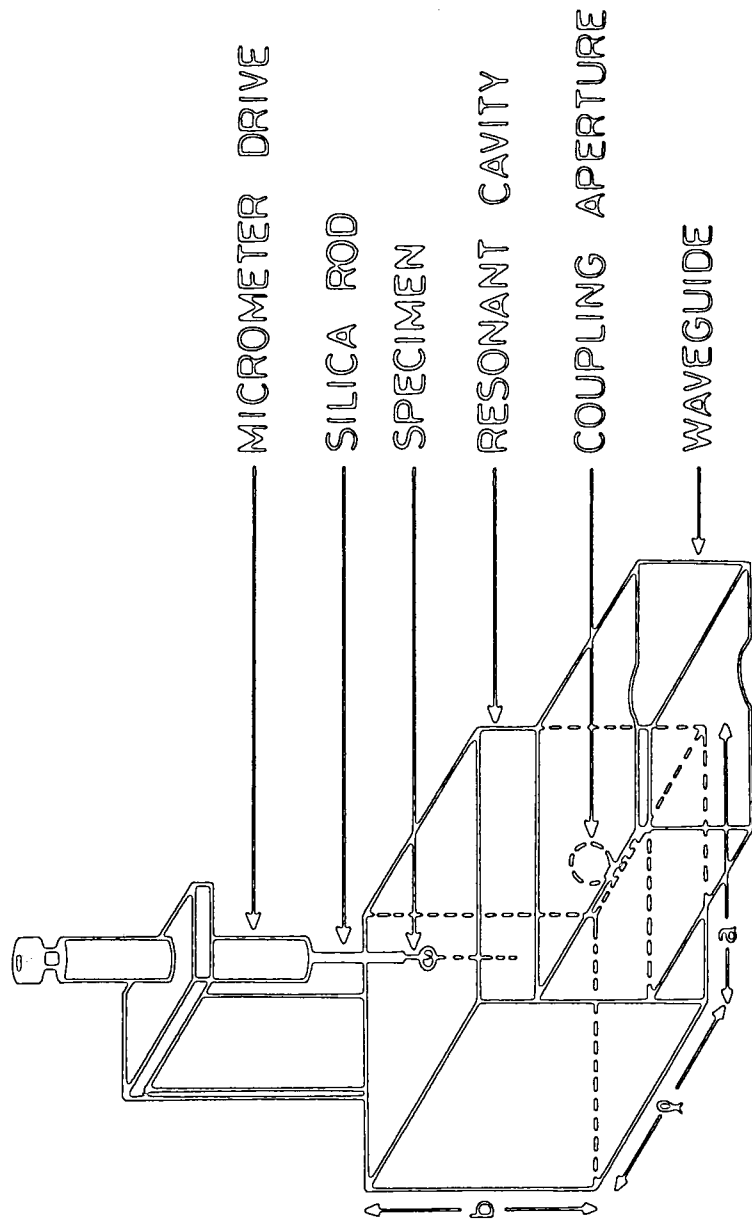


FIG. 5-3. IMPROVED CAVITY PERTURBATION METHOD FOR ROD SHAPED SPECIMENS

specimen length, and therefore volume, is found more accurately than in the previous method, as it is now the difference between two micrometer readings, and irregularities in the end-faces or non-perpendicular end faces have no effect. Errors in the other two dimensions may be slightly reduced as irregularities in cross-section appear as non-linearities in the plot, and are averaged out, as the value of  $\epsilon'$  calculated from the plot is effectively the average over several very small specimens.

This method has further advantages when the same material is to be measured at different frequencies. As the change in cavity resonance frequency is continuously monitored while the specimen is being lowered, the final position, that is, the specimen volume, is chosen to give the optimum change in resonance frequency. Further, the same specimen can be used in cavities of different sizes by introducing smaller lengths of specimen into smaller cavities as perturbation theory requires. The linearity of the plot as more specimen material is introduced automatically provides a check that the conditions of the perturbation technique have not been exceeded. Material of known dielectric constant was used to check the accuracy of the method. The plot of Fig 5.4 is for a cylindrical silica rod. It gives a value of  $\epsilon' = 3.84$ , which agrees with the published value for silica.

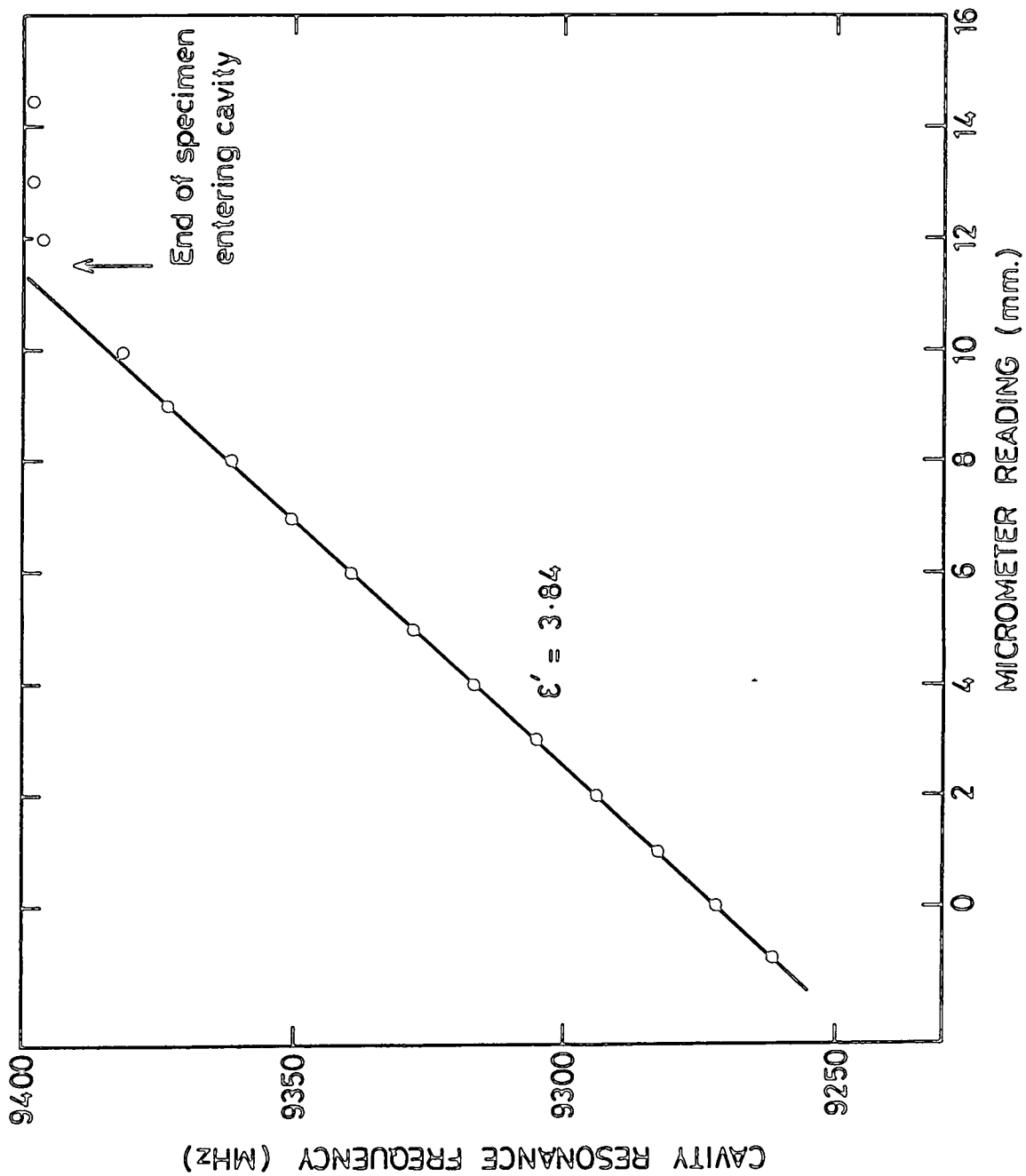


FIG. 5.4. EFFECT OF SPECIMEN LENGTH ON RESONANT FREQUENCY

## CHAPTER 5

### REFERENCES

- 5.1 R.A.L.Drew, S.Hampshire, K.H.Jack  
Special Ceramics 7, Proc.Brit.Ceram.Soc. 31 (1981), 119.
- 5.2 R.A.L.Drew, Ph.D.Thesis, University of Newcastle-upon-Tyne, (1980).
- 5.3 A.B.Ahmad, Ph.D.Thesis, University of Durham (1983).
- 5.4 B.L.J.Kulesza, J.S.Thorp, A.B.Ahmad, J.Mat.Sci.19, (1984), 915.

CHAPTER 6THE TEMPERATURE VARIATIONS OF PERMITTIVITYAND DIELECTRIC LOSS6.1 INTRODUCTION

Some preliminary measurements were made of the temperature variations of both permittivity and dielectric loss using the high temperature bridge techniques outlined in Chapter 2. These measurements proved to be quite difficult to make and consequently it was only possible to examine one sample, the oxy-nitride glass of composition Ca(28) Si(56) Al(16) O(88) N(12) in any detail. However, as will be seen from the sections below, the results which were obtained, establish certain trends of behaviour which are of considerable interest.

6.2 TEMPERATURE DEPENDENCE OF PERMITTIVITY; EXPERIMENTAL DATA

Some of the results illustrating the permittivity behaviour are given in Fig.6.1 which shows the changes in the frequency dependence of permittivity induced by successively increasing temperatures. They refer to measurements made by the low frequency bridge and Q-meter techniques at frequencies up to 50 KHz. The trend of the data is shown by the lines drawn on the Figure which are not intended to define the functional dependence of  $\epsilon'$  on frequency. Examination of Fig.6.1 shows that the general effect is that, at any particular frequency,  $\epsilon'$  is increased by increasing the temperature ; this effect is noticeable as soon as the temperature is raised above room temperature but becomes markedly more pronounced at the higher temperatures approaching 500°C.

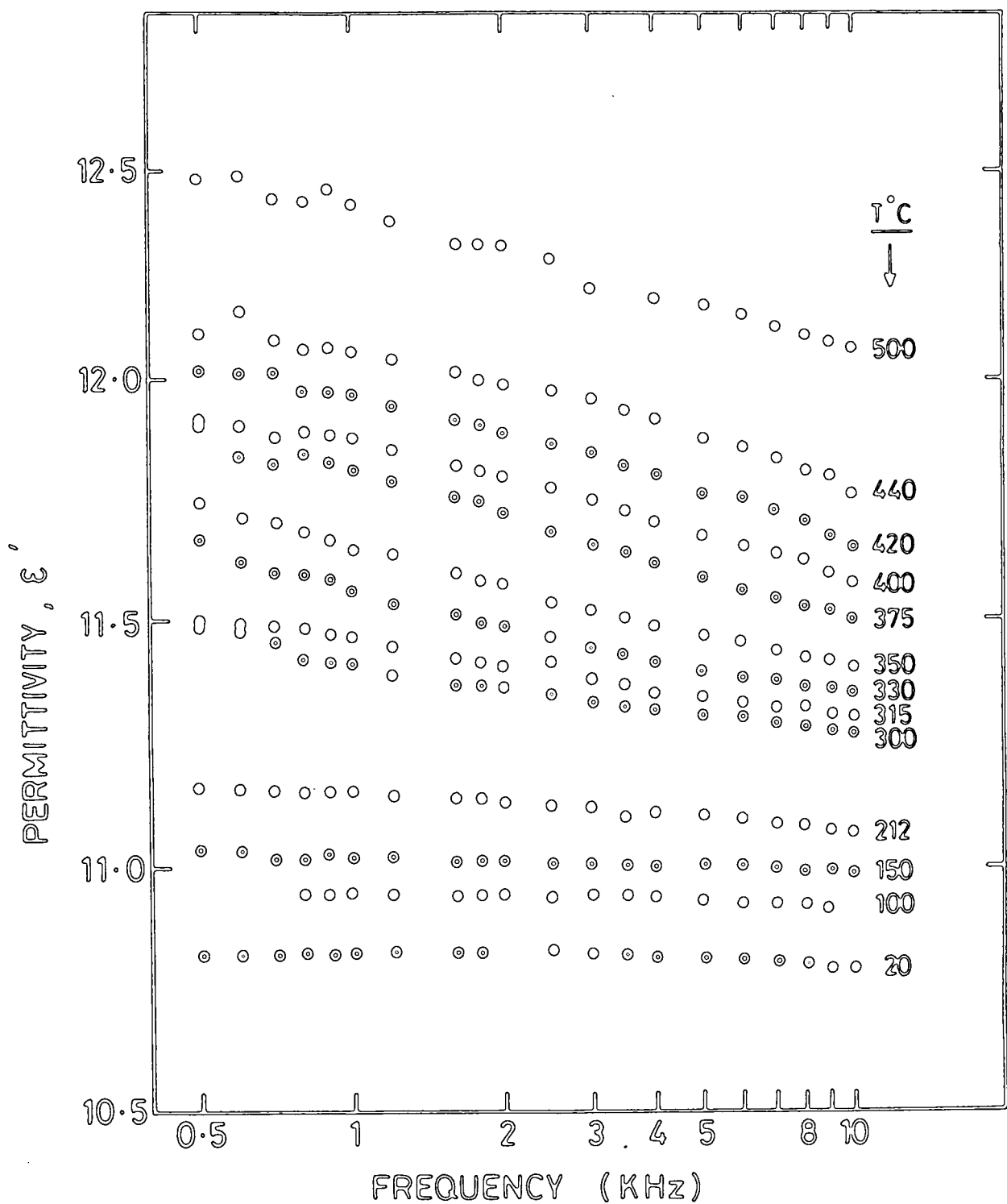


FIG.6.1. VARIATION OF PERMITTIVITY  $\epsilon'$  WITH FREQUENCY AT DIFFERENT TEMPERATURES ;  
 [ Ca (28) Si(56) Al (16) O (88) N(11) ]

Comparison of the results of room temperature and 100°C shows that both exhibit virtually frequency independent behaviour. However, as the temperature is increased, the plots show successively stronger frequency dependence. It may also be noted that, at any given frequency, the increase in  $\epsilon'$  caused by a given temperature increment is greater the higher the temperature. Furthermore, the results show that the difference between corresponding high temperature and low temperature values of  $\epsilon'$  is greater at a low frequency than at a higher frequency.

### 6.3 TEMPERATURE DEPENDENCE OF DIELECTRIC LOSS ;

#### EXPERIMENTAL DATA

The variation of dielectric loss with frequency at different temperatures is shown (for the same sample) in Fig 6.2. These differ from the room temperature behaviour discussed in previous Chapters. It will be recalled that, at room temperature the observed loss ( $\epsilon''$ ) is virtually frequency independent over the range of frequency (i.e. up to at least 10 KHz) examined here. The first difference to be emphasised is that, at higher temperatures, the dielectric loss decreases with frequency. This is particularly clearly shown by the lowest and highest curves for 212°C and 500°C respectively. The second point to note is that, as expected, the loss at any particular frequency does increase quite rapidly with increasing temperature. The third feature revealed (on examining the region between the 330°C and 420°C data) is the occurrence of a relaxation peak which moves towards higher frequencies as the temperature is increased ; this relaxation peak is shown more clearly in Fig 6.3 which displays the 300°C to 440°C data on a larger scale. Analysis of the form of the relaxation peak (most clearly shown in the 375°C plot of Fig 6.4) shows that the low frequency and high

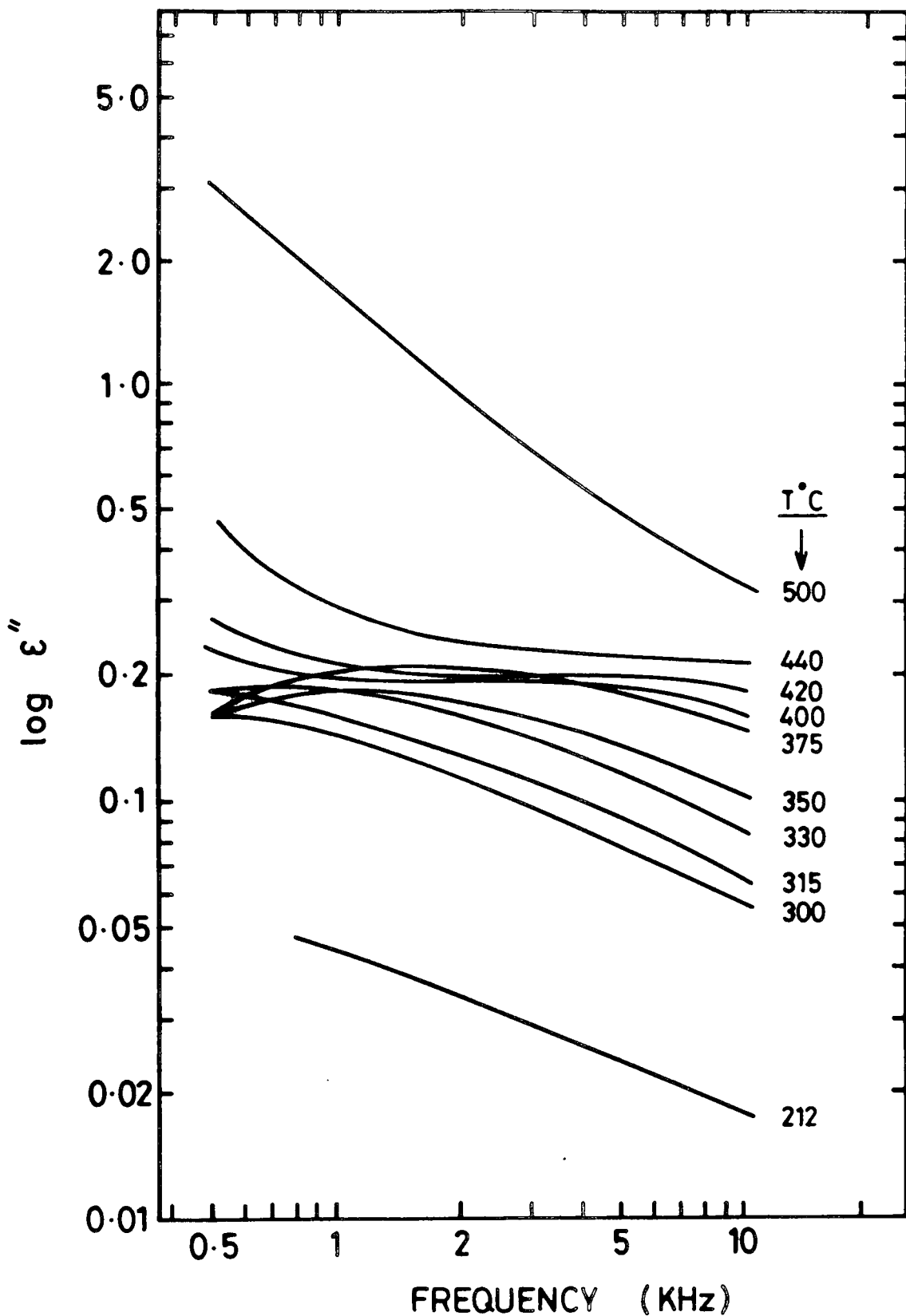


FIG.6.2. VARIATION OF DIELECTRIC LOSS,  $\epsilon''$ , WITH FREQUENCY AT DIFFERENT TEMPERATURES ; [Ca(28) Si(56) Al(16) O(88) N(12)]

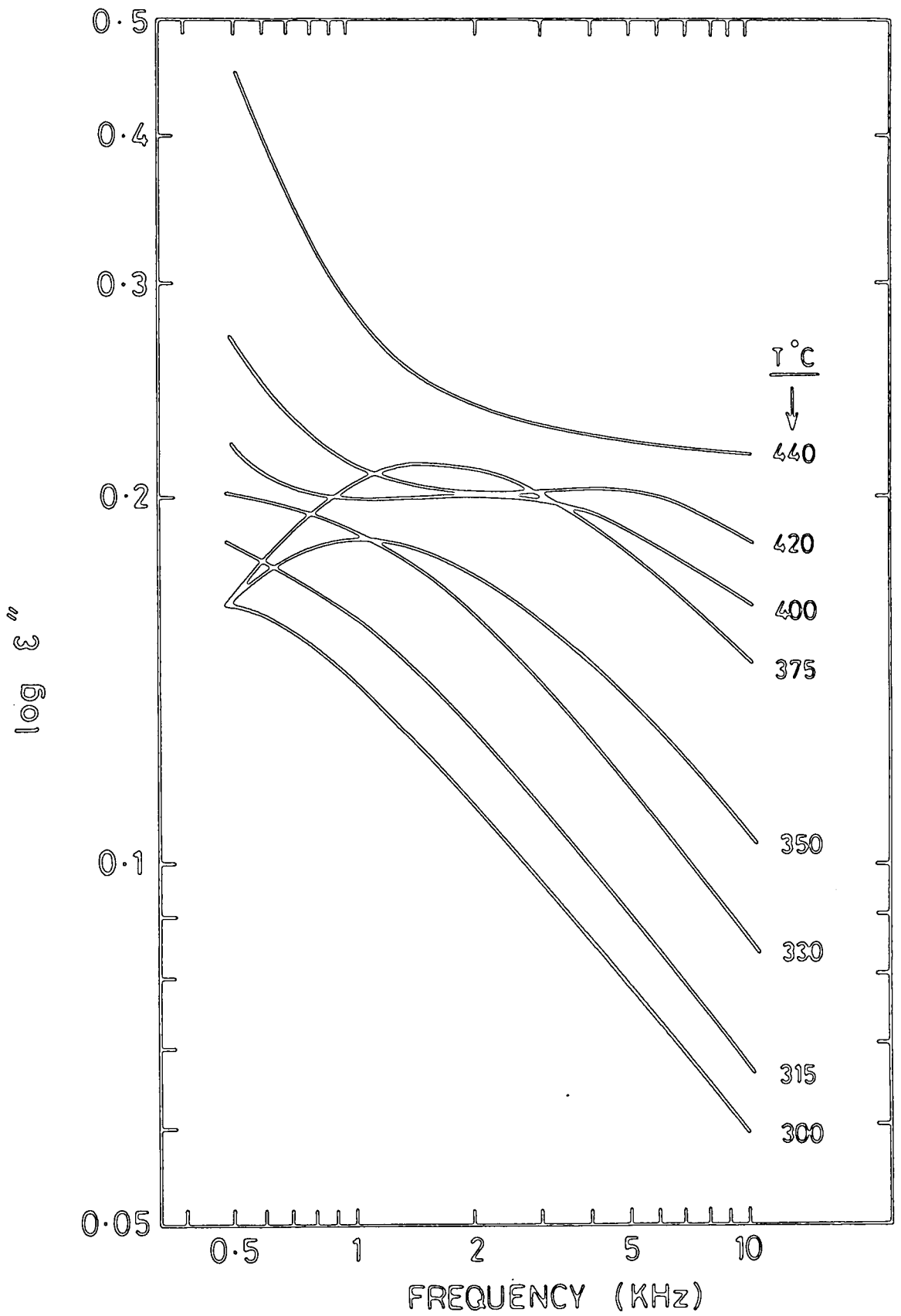


FIG. 6.3. FORMATION OF LOSS PEAKS IN THE HIGHER TEMPERATURE REGIME

frequency slopes, labelled m and n respectively on Fig 6.4, are not equal and this suggests that the relaxation is not of purely Debye form. An examination of the temperature dependence of the frequency  $f_p$  corresponding to the centre of the loss peak was attempted, although the individual estimates of  $f_p$  for particular temperatures are subject to considerable error. The variation of  $f_p$  with reciprocal temperature is given in Fig 6.5. The linearity of this plot implies that a thermally activated process is involved ; the activation energy derived from the slope of the line appears to be of a reasonable order of magnitude.

#### 6.4 DISCUSSION

The temperature dependencies of both permittivity and dielectric loss are not well defined in general terms for any class of materials either experimentally or theoretically. Most textbooks [e.g. Harrop 6.1] refer rather loosely to an exponential rise, basing this prediction on arguments based on the Clausius-Mosotti equation. Over limited temperature ranges below and near room temperature the more precise relations developed by Havinga and subsequently by Bosman and Havinga [6.2,6.3] have been found to be satisfactory for a number of cubic crystalline dielectrics. These relations apply to the temperature variation of permittivity and, according to Bosman and Havinga, it can be expressed as

$$\frac{1}{(\epsilon' - 1)(\epsilon' + 2)} \cdot \frac{\partial \epsilon'}{\partial T} = A + B + C$$

where the parameter A arises from volume expansion ; expansion reduces the number of polarisable particles per unit volume and, since the

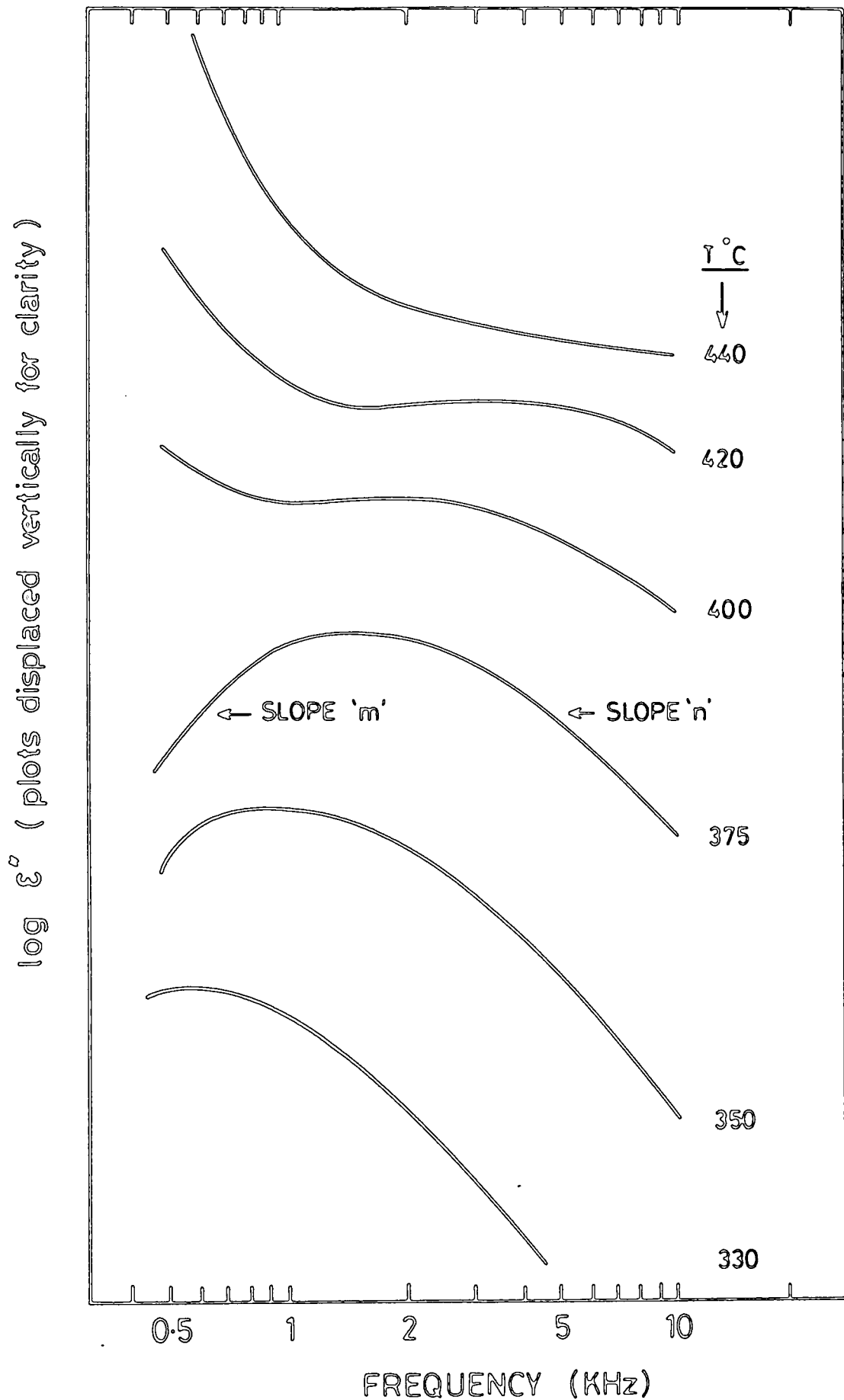


FIG.6.4. DETAILED SHAPES OF LOSS PEAKS

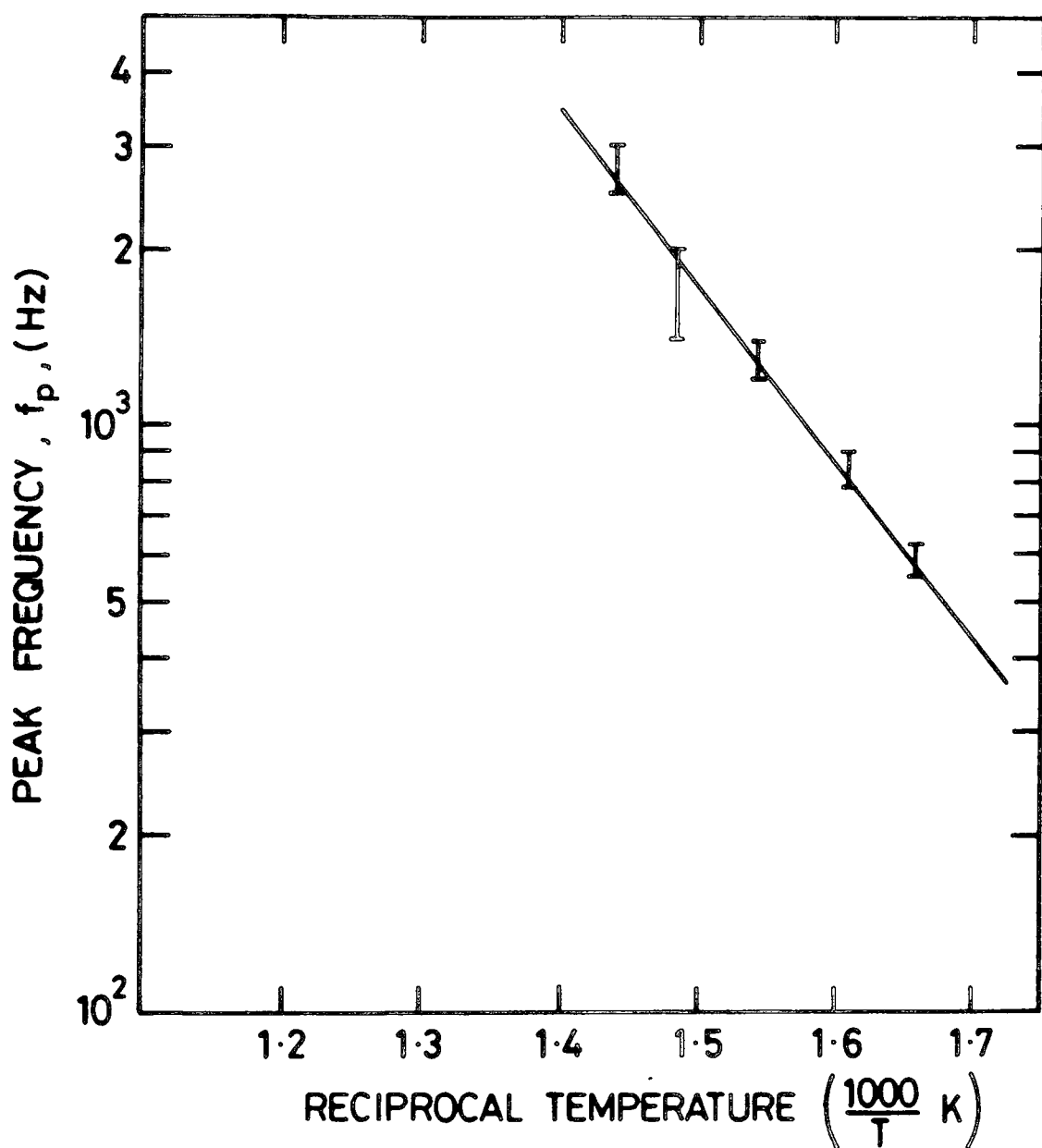


FIG. 6.5. THE TEMPERATURE DEPENDENCE OF  $f_p$

number of particles is constant,  $\epsilon'$  decreases with increasing temperature. The quantity B relates to the increase of polarisability of the particles when expansion occurs and the parameter C arises from the dependence, in a constant volume, of the polarisability of the particles on temperature. Good agreement with this relation has been reported for magnesium oxide by several authors [Barbers and Smith 6.4, Wintersgill and Fontenella 6.5] for temperatures below about 200°C, and Bosman and Havinga's postulate that the temperature dependence should be positive for materials having  $\epsilon' < 20$  has also been verified. Departures from this type of behaviour have however previously been noted in two senses, namely at low frequencies and at higher temperatures. The strong temperature dependence of  $\epsilon'$  at low frequencies has been discussed by Rao and Smakula [6.6]. These authors reported that in cobalt oxide and in nickel oxide the permittivity increased exponentially with temperature above 120°C and 150°C respectively with corresponding exponential variations of dielectric loss  $\epsilon''$  and they explained these variations in terms of space charge polarisation caused by impurities or defects. More recently, in a more extended study of the frequency variation of the permittivity and dielectric loss of magnesium oxide at high temperatures. Thorp, Rad, Evans and Williams [6.7] pointed out that above 200°C the permittivity changes much more rapidly than the Havinga formula predicts ; they also reported that the frequency dependence of  $\epsilon'$  is temperature dependent such that below 200°C  $\epsilon'$  follows

$$\left| \epsilon'(\omega) - \epsilon'_{\infty} \right| \propto \omega^{n-1}$$

with  $n = 0.98 \pm 0.02$  whereas above 200°C the value of  $\epsilon'$  falls more

rapidly with frequency than would be expected from this law. It is interesting to note the form of the temperature dependent frequency variations found and these are reproduced in Fig 6.6.

The results obtained in the present work on oxy-nitride glasses bear some striking similarities with the pattern of behaviour these authors found for magnesium oxide. One feature is of particular importance, bearing in mind the potential applications of the oxy-nitride glasses as R.F. windows or radome material at microwave frequencies. As indicated by the dotted extrapolations in Figure 6.6  $\epsilon'$  falls progressively faster with frequency from a higher starting value as the temperature is increased ; consequently at some frequency greater than the upper value used in that experiment, perhaps in the region 10 MHz, the temperature variation will become very small if the trend continues. A similar effect has now been observed, Fig 6.1, in the oxy-nitride glasses' behaviour. Approximate extrapolation of the individual plots of Fig 6.1 suggests convergence near a frequency of around 5 MHz - 10 MHz. If this is correct the temperature variations in the microwave regions, i.e. near 3 GHz, 9 GHz or 35 GHz would be expected to be very small indeed. Furthermore, the similarity of behaviour between the crystalline magnesium oxide and the non-crystalline oxy-nitride glass suggests that similar mechanisms form the temperature dependent processes hold for both types of material. This is an area where further work would be fruitful both as regards clarification of the detailed processes involved and in determining the magnitudes of the residual temperature variations at the particular frequency bands envisaged for oxy-nitride glass applications.

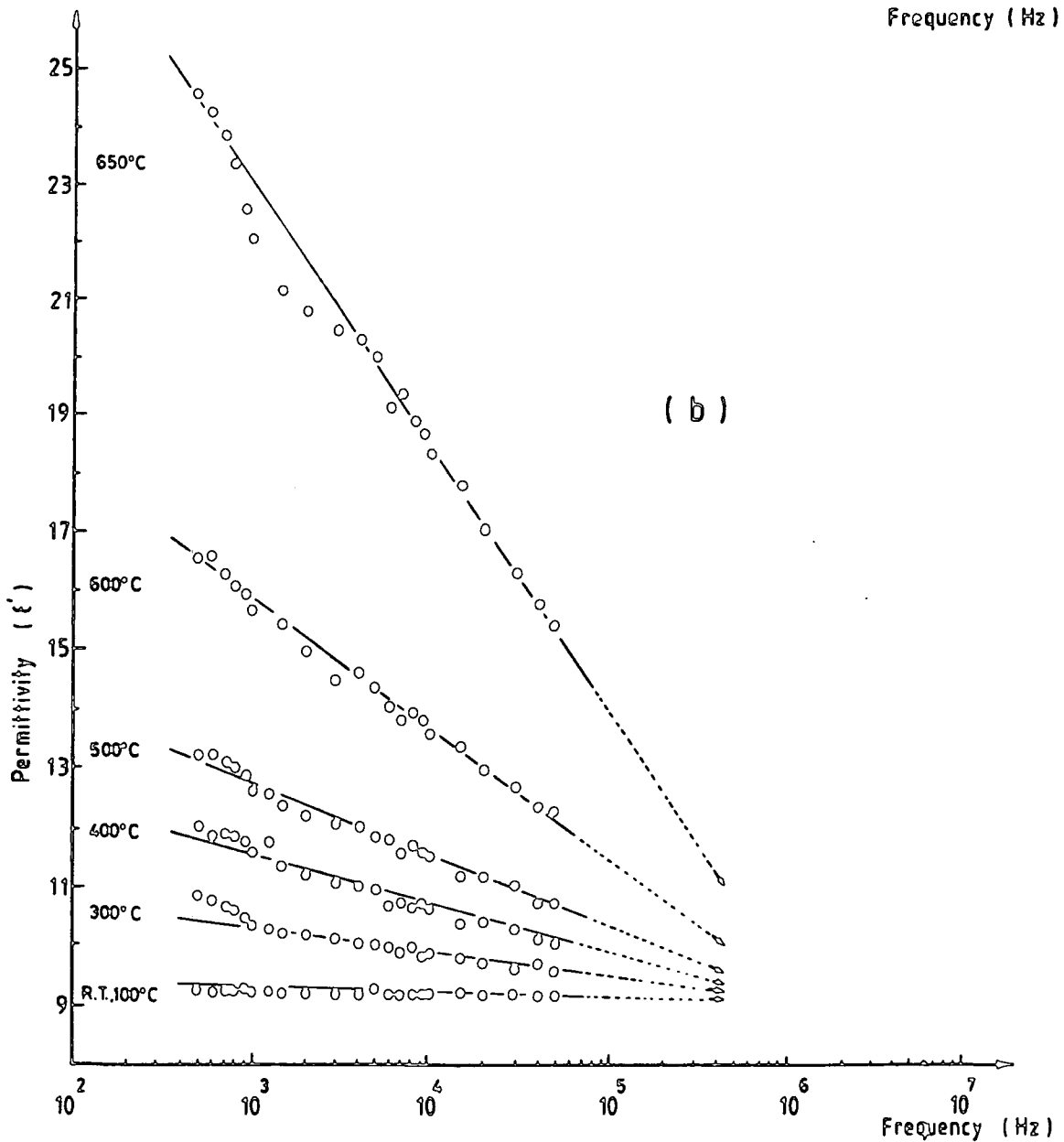
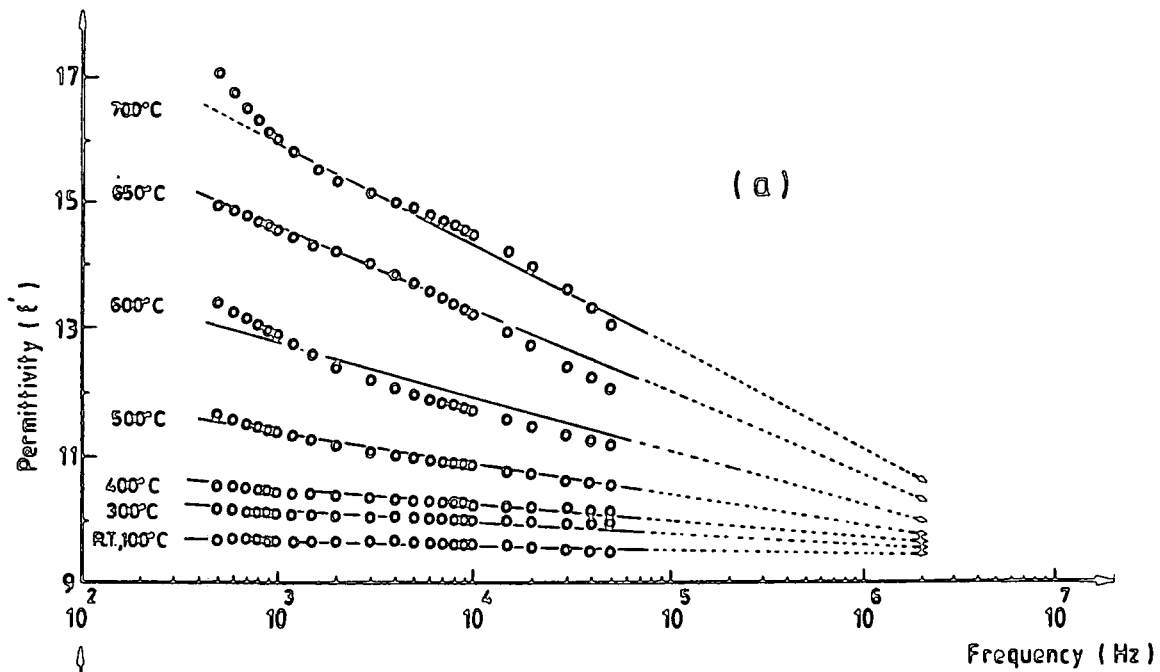


FIG. 6-6. Variation of permittivity versus frequency at different temperatures; (a): MgO (pure) and (b): MgO + 12,800 ppm Fe. (Lines show data trend not a function)

## CHAPTER 6

### REFERENCES

- 6.1 P.J.Harrop, Dielectrics  
Butterworths (London) 1972.
- 6.2 E.E.Havinga,  
J.Phys.Chem.Solids 18, (1961) 253.
- 6.3 A.J.Bosman, E.E.Havinga,  
Phys.Rev.129, (1983), 1593.
- 6.4 R.A.Bartels, P.A.Smith  
Phys.Rev.B 7, (1973), 3885.
- 6.5 M.Wintersgill, J. Fontamella  
J.Appl.Phys.50 (12), (1979) 8259.
- 6.6 K.V.Rao, A.Smakula  
J.Appl.Phys. 36 (1965), 2031.
- 6.7 J.S.Thorp, N.E.Rad, D.Evans, C.D.H.Williams  
J.Mater.Sci - to be published.

CHAPTER 7SOME OPTICAL PROPERTIES OF OXY-NITRIDE GLASSES7.1 INTRODUCTION

The optical properties of oxy-nitride glasses are important for several reasons. In the first place it is important when assessing a new material for potential applications to have as complete a characterisation - for example of dielectric, optical, thermal and mechanical properties - as possible because it is very rare to find situations in real applications where only one property is important. For the oxy-nitride glasses one potential application is for radio-frequency and microwave windows and here, whilst a low dielectric loss at the r.f. frequency concerned is of paramount importance, the thermal properties (i.e. the thermal conductivity, thermal expansion and thermal shock resistance) have to be considered in view of the environmental conditions under which radomes may have to operate. There may also be a need for simultaneous low absorption both at microwave and at infra-red frequencies and there is also the over-riding general requirement for the material to be able to be formed (or machined) into the shape and size required. In the second place the optical properties can provide a further insight into the composition and structural relationships in the glass ; a major point here is that any independent method of monitoring the nitrogen content of the glasses would be welcome and, in principle, optical methods offer two possibilities, namely the possible effect of nitrogen addition on the visible absorption edge and the infra-red spectrum respectively.

Thirdly, some specific optical measurements are necessary in order to complete analysis and interpretation of the frequency dependence of the permittivity ; in particular (as has been mentioned in the previous Chapters dealing with dielectric measurements) it is necessary to know the value of  $\epsilon_{\infty}$ , the relative permittivity at infinite frequency, in order to clarify the conduction mechanisms involved. This quantity is usually deduced from optical measurements of the refractive index (n) since, at frequencies which are very high relative to those to which the main ionic polarisation processes can respond, it is valid to use the result

$$n = \sqrt{\epsilon_{\infty}}$$

obtained from electromagnetic theory.

In this Chapter some preliminary studies on the visible and infra-red spectra of a series of oxy-nitride glasses are described ; for the glass compositions studied refractive index data had already been obtained by Drew.

## 7.2 VISIBLE/UV ABSORPTION SPECTRA

All the visible/uv spectra were recorded with a conventional spectrophotometer concentrating on the wavelength range from about 400 nm to 200 nm since initial studies showed that, for all the glasses, the major increases in absorption occurred in this region. A comparison of the behaviour of the different oxide glasses is shown in Figure 7.1. It can be seen that the variations of absorption with wavelength for the calcium and magnesium oxide glasses are very similar in that at wavelengths greater than about 350 nm nearly 95% transmission is

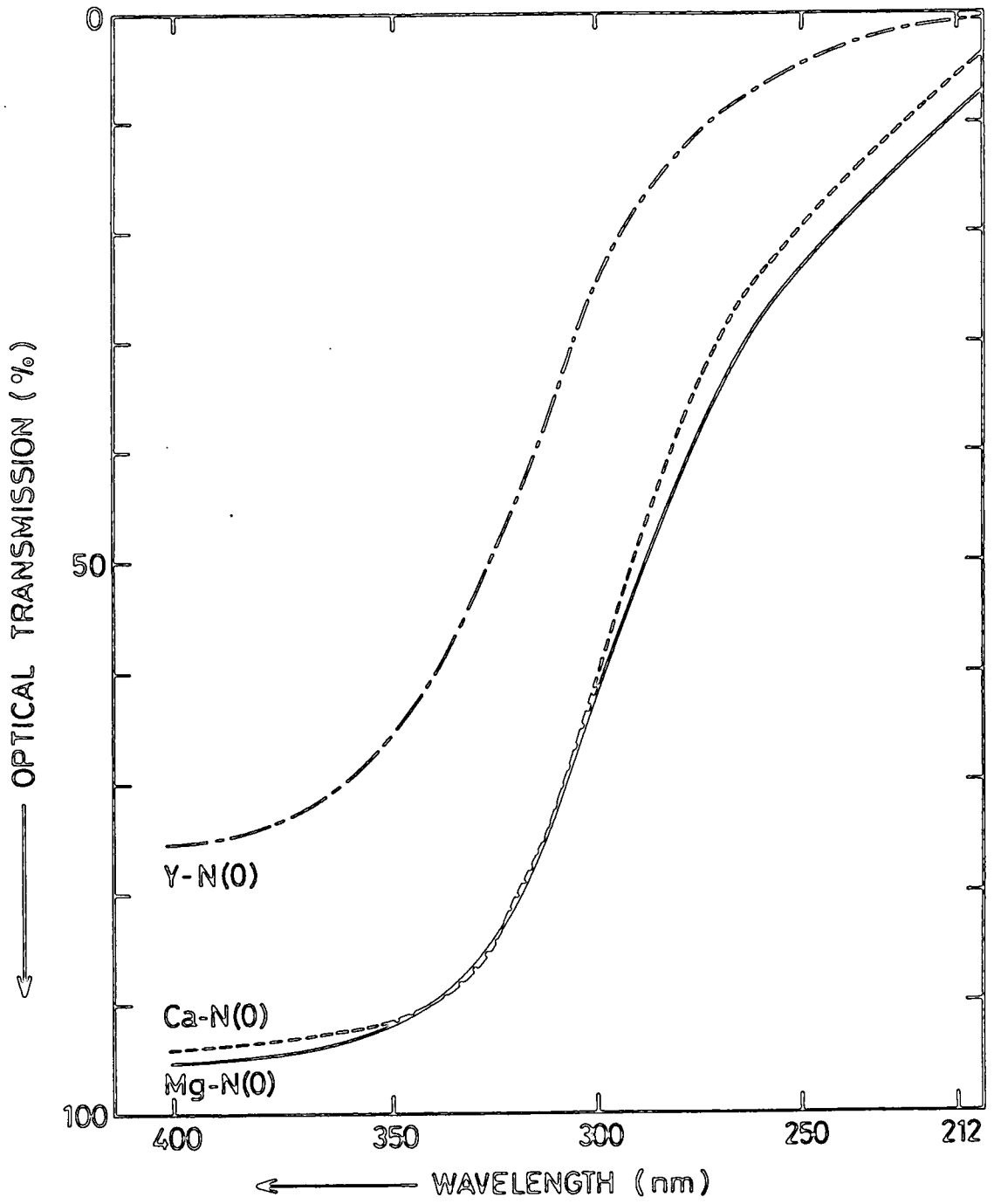


FIG. 7-1. U.V. ABSORPTION FOR THE DIFFERENT OXIDE GLASSES.

obtained and that the increase in absorption occurs over a range from 350 nm to 200 nm beyond which the samples are virtually opaque. With the yttrium glass on the other hand the absorption for  $\lambda > 350$  nm is distinctly higher (the transmission at 400 nm being only 75%) although the main increase again occurs as a steady rise between about 350 nm and 200 nm.

The effects of nitrogen addition were next investigated. Again, similarities were found between the calcium and magnesium oxy-nitride glasses but a different effect was observed in the yttrium glass. Figure 7.2 shows the effect of nitrogen addition on the visible/uv absorption of a series of magnesium oxy-nitride glasses ; the main results are that (i) addition of nitrogen slightly increases the absorption for  $\lambda > 350$  nm, and (ii) addition of nitrogen causes a small shift of the main absorption to shorter wavelengths. The first of these results also applies to the calcium oxynitride glasses, Fig.7.3, where for example at  $\lambda = 400$  nm the transmission for the Ca-N(18) glass is only 82% compared with 95% for the pure oxide Ca-N(o) glass ; however here the main rise in absorption occurs at about the same wavelength. A major difference becomes apparent when examining the visible/uv spectrum of the yttrium oxynitride glasses. These are shown in Figure 7.4. Here, in complete contrast to the behaviour of both the calcium and magnesium glasses, the addition of nitrogen decreases the absorption ; thus at 400 nm the transmission of the oxide glass Y-N(o) is only 76% but that of the oxy-nitride Y-N(18) has increased to 92%. [It should be noted that only one sample of each glass composition was examined so that the possibility of having a non-typical sample must be considered ; it is noteworthy however that the yttrium glasses displayed different

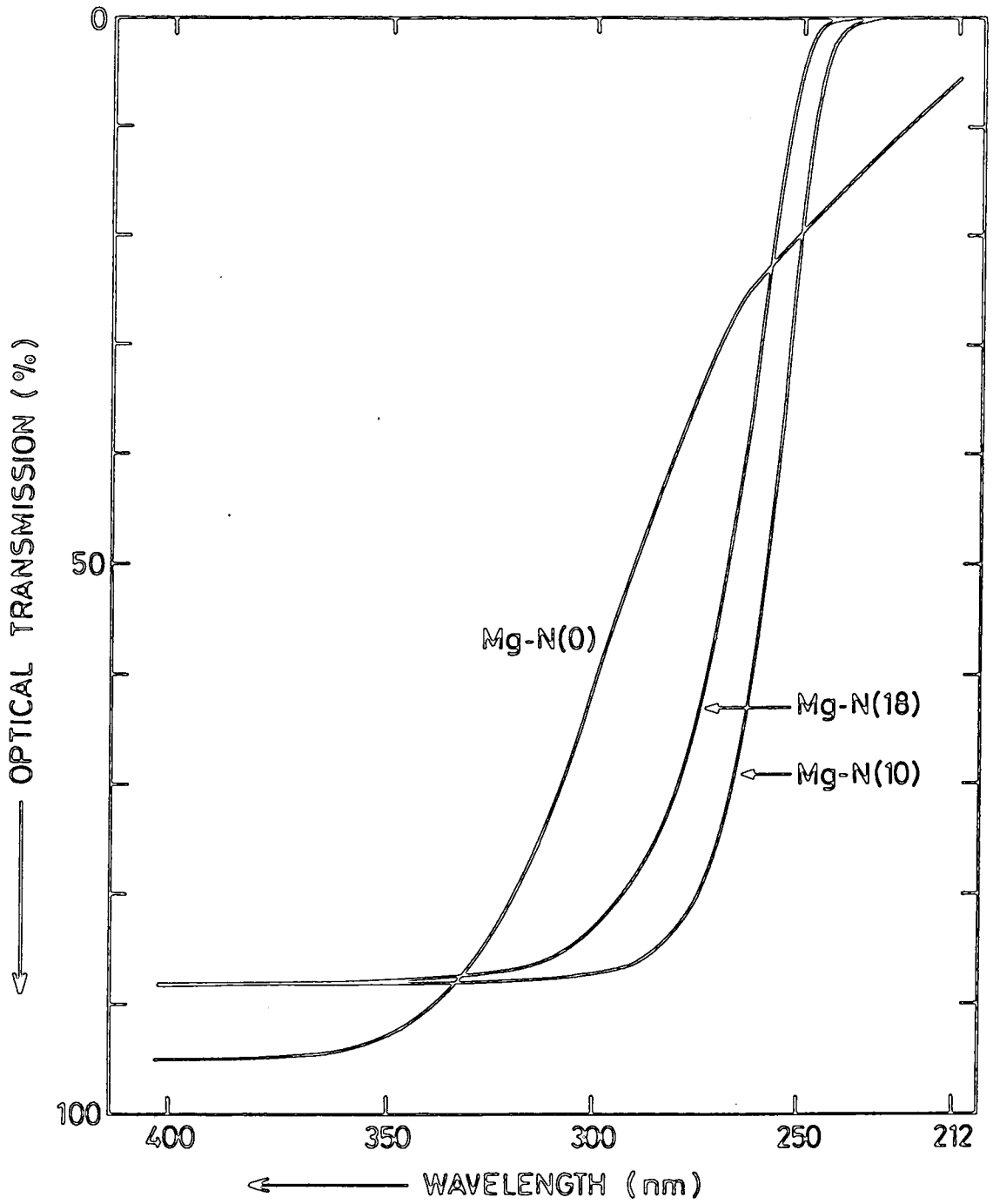


FIG. 7-2. EFFECTS OF NITROGEN ADDITION ; MAGNESIUM OXYNITRIDE GLASSES.

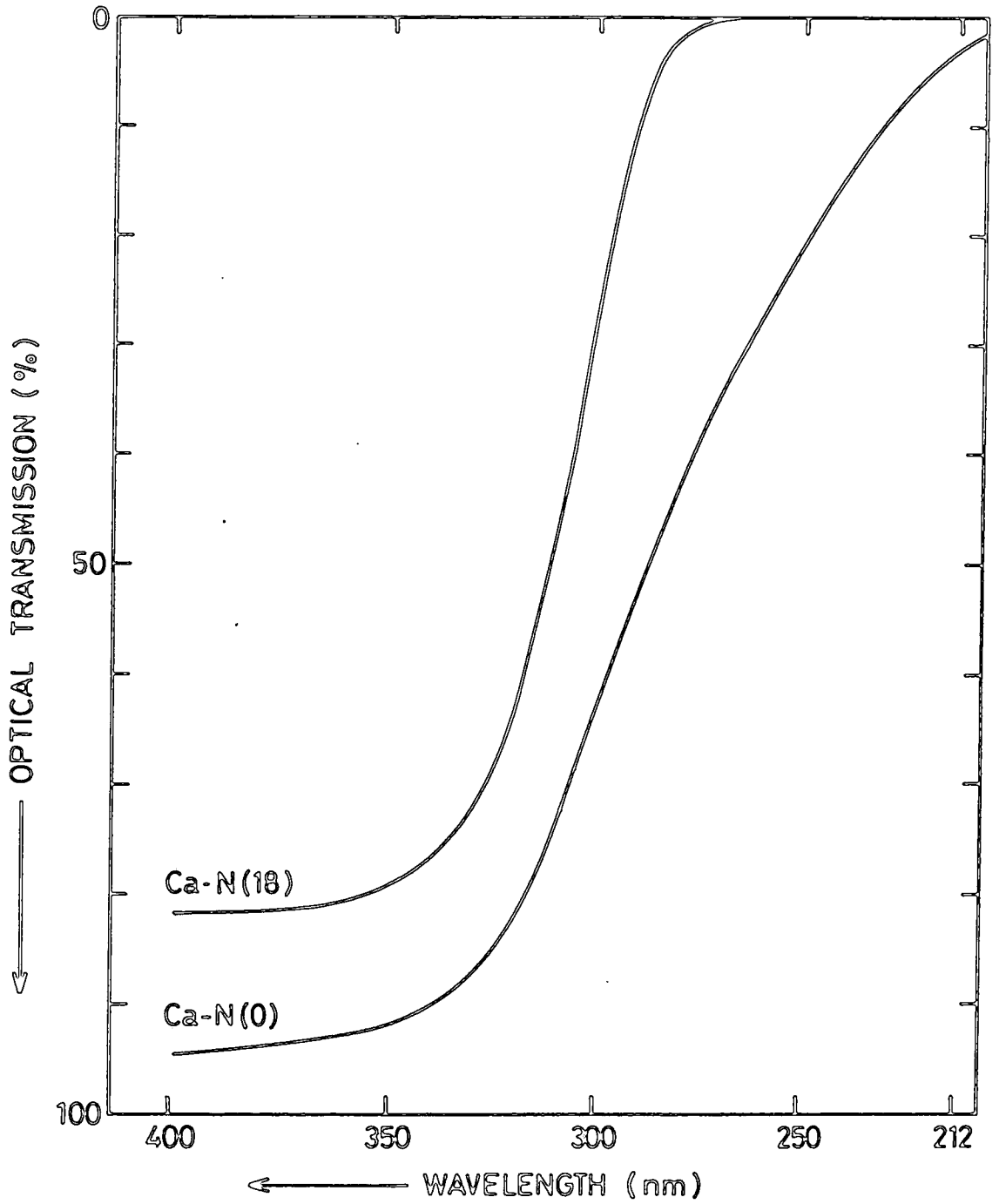


FIG. 7-3. EFFECTS OF NITROGEN ADDITION ; CALCIUM OXYNITRIDE GLASSES.

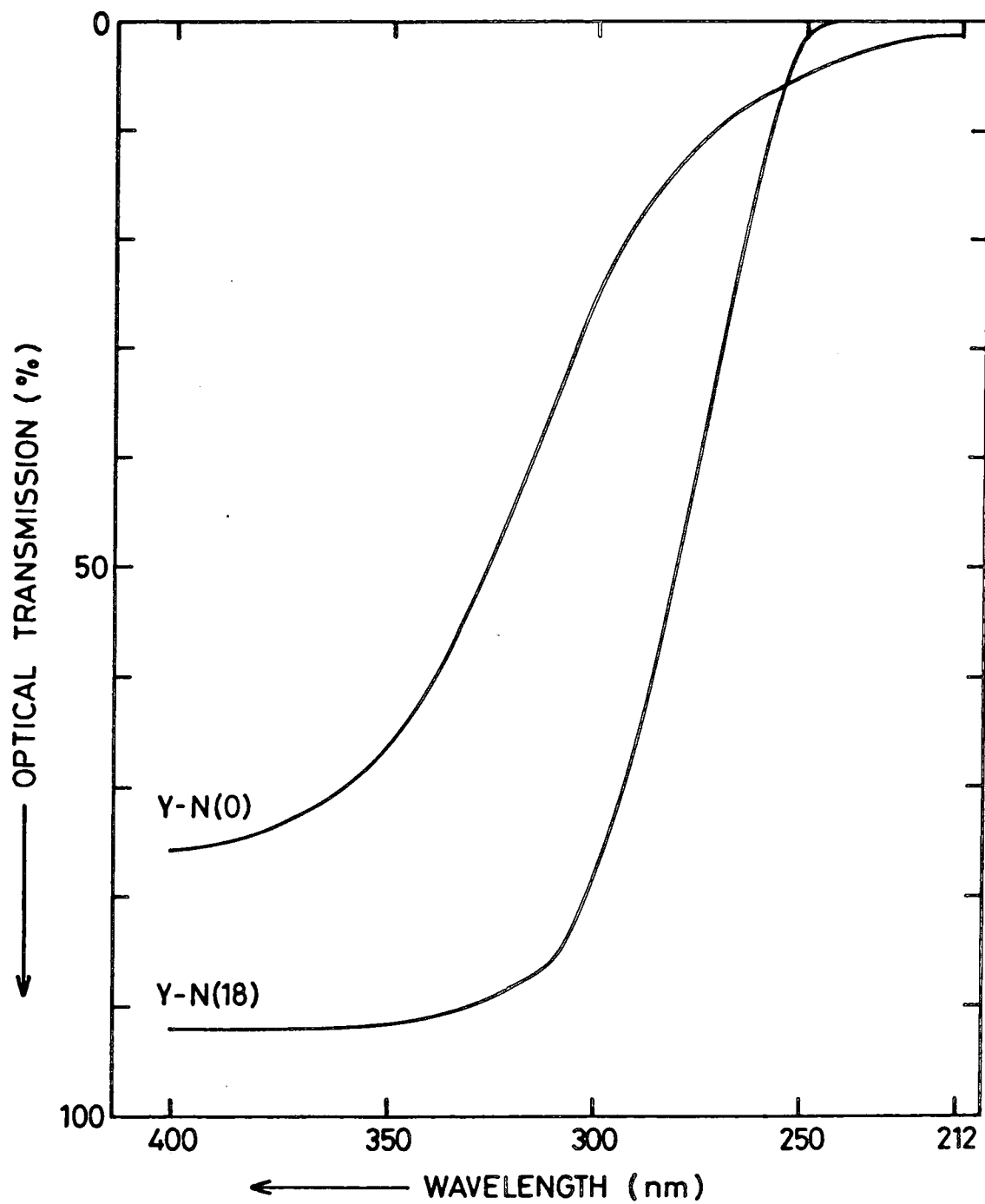


FIG. 7-4. EFFECT OF NITROGEN ADDITION ; YTTRIUM OXYNITRIDE GLASSES.

dielectric loss variations from both magnesium and calcium glasses and this lends support to the view that this rather surprising result is genuine]. A comparison of the visible/uv spectra of the three oxynitride glasses containing the same (maximum) amount of nitrogen - i.e. Ca-N(18), Mg-N(18) and Y-N(18) - is made in Figure 7.5 which again shows that for wavelengths greater than about 350 nm the yttrium oxynitride glass gives the greatest transmission.

### 7.3 INFRA-RED SPECTRA

The infra-red spectra were also obtained using standard spectroscopic techniques for which the specimens were prepared from powdered glass mixed with KBr and pressed into disc-shaped pellets. In this section of the work the aim was to try to identify the wavelengths at which significant IR absorptions occurred since, mainly because of limitations of sample availability, it was not possible to attempt to measure the actual infra-red absorption coefficients.

Comparative spectra of the corresponding oxide and oxynitride and oxynitride glasses are given in Figures 7.6, 7.7 and 7.8 for the magnesium, calcium and yttrium glasses respectively. Taken as a whole these spectra show quite a high degree of similarity, with the main fairly broad absorption features occurring near  $3500\text{ cm}^{-1}$ ,  $950\text{ cm}^{-1}$  and  $500\text{ cm}^{-1}$  and evidence for fine structure (particularly evident with Ca-N(10), Fig. 7.7) near  $650\text{ cm}^{-1}$  and  $760\text{ cm}^{-1}$ ; in addition there is evidence for an extra absorption line near  $250\text{ cm}^{-1}$  which appears for two of the nitrogen containing glasses (i.e. Ca-N(10), Fig 7.7 and Y-N(18), Fig 7.8) but is not observable in any of the oxide glass spectra.

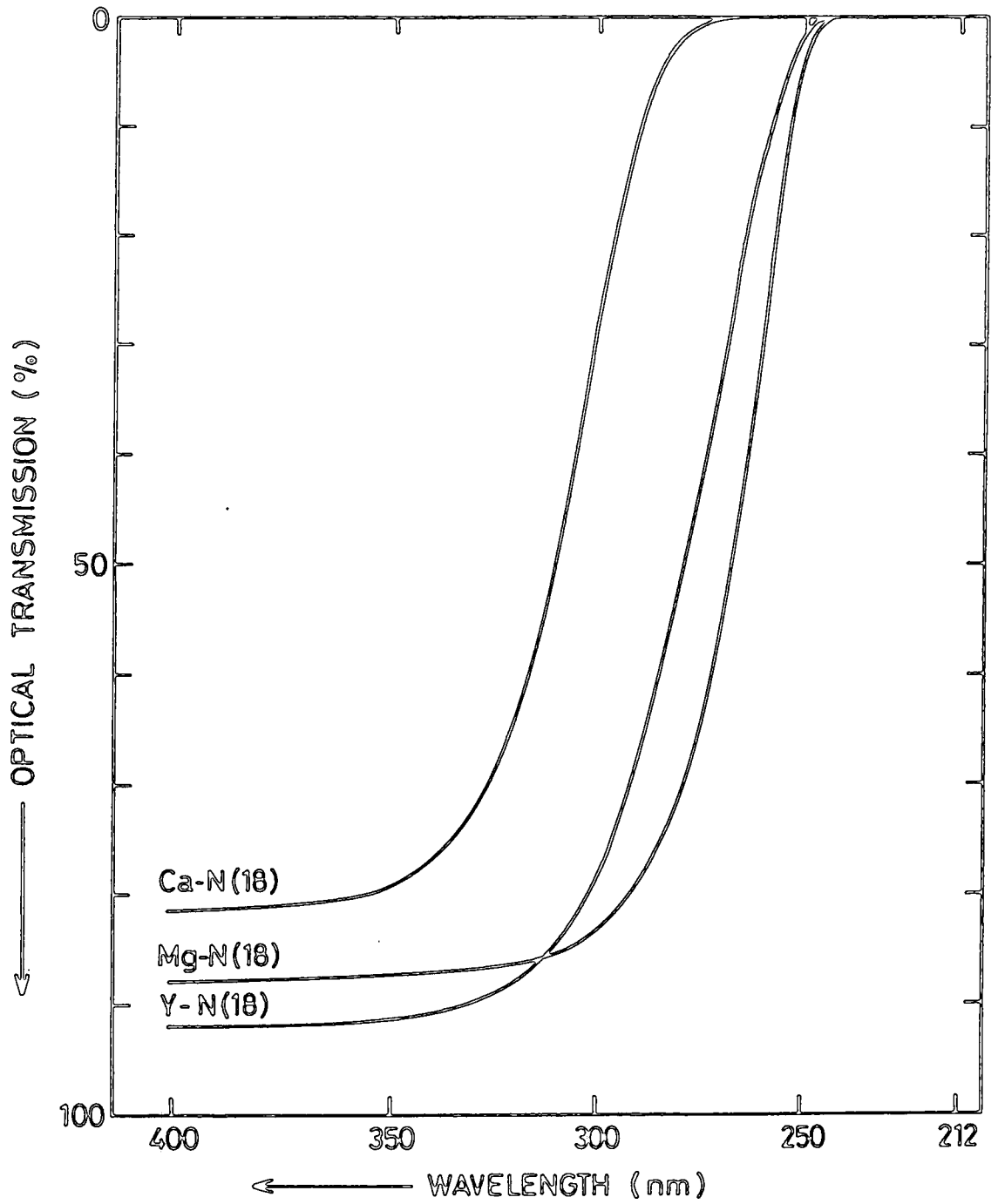


FIG. 7-5. COMPARATIVE VISIBLE /  $\mu$ V SPECTRA OF Ca, Mg AND Y OXYNITRIDE GLASSES CONTAINING 18% NITROGEN.

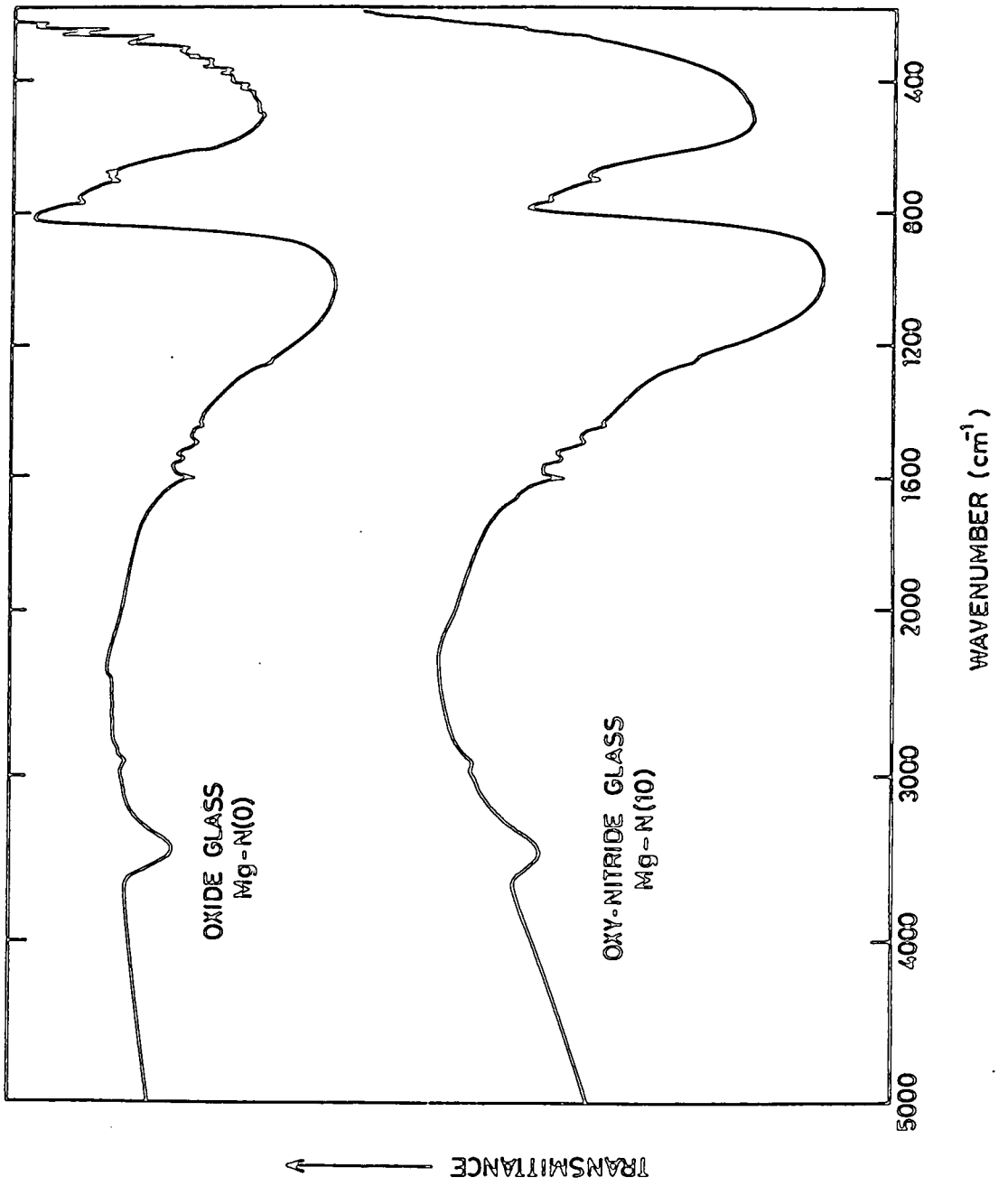


FIG. 7-6. INFRARED SPECTRA OF Mg GLASSES

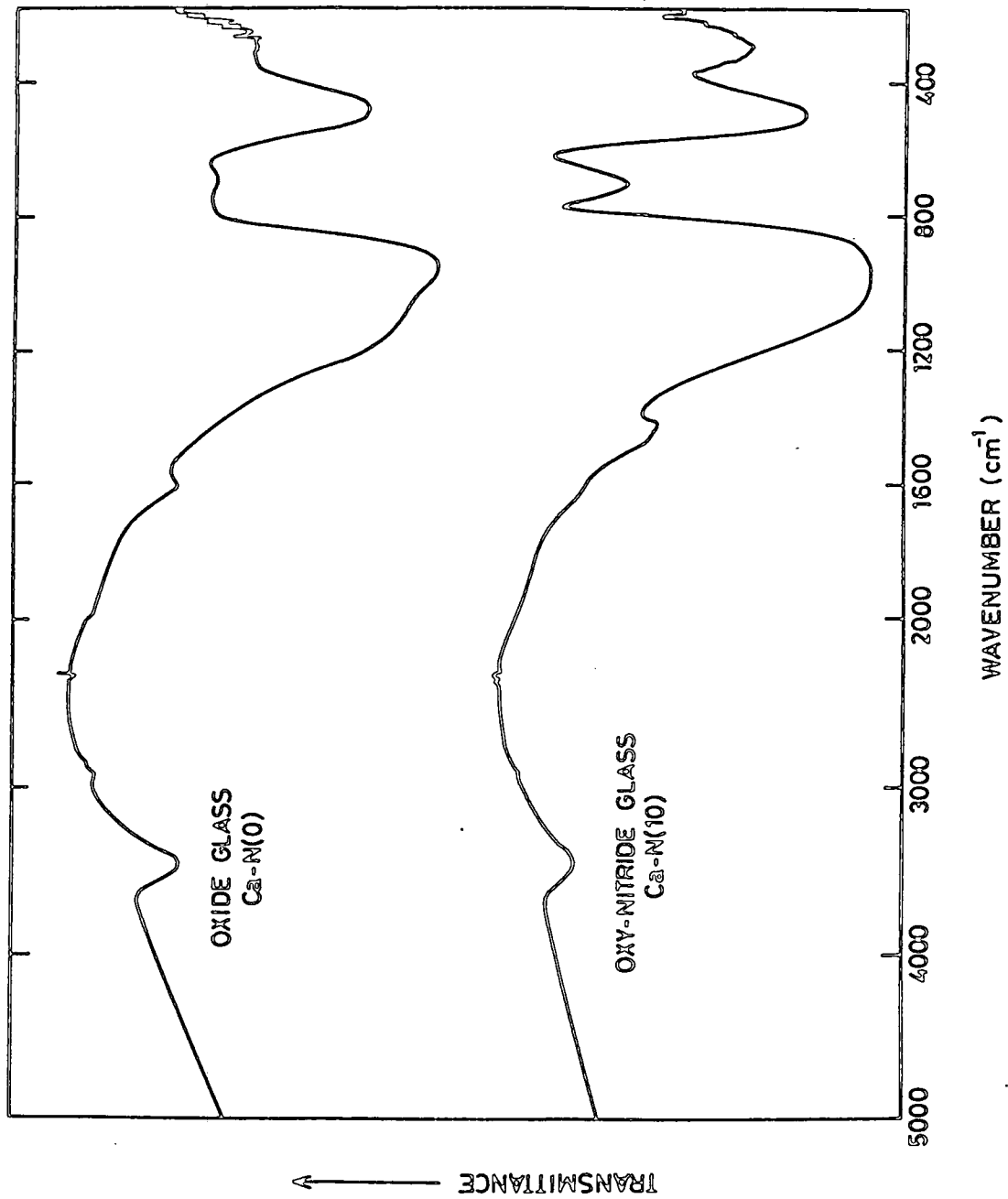


FIG. 7.7. INFRARED SPECTRA OF Ca GLASSES

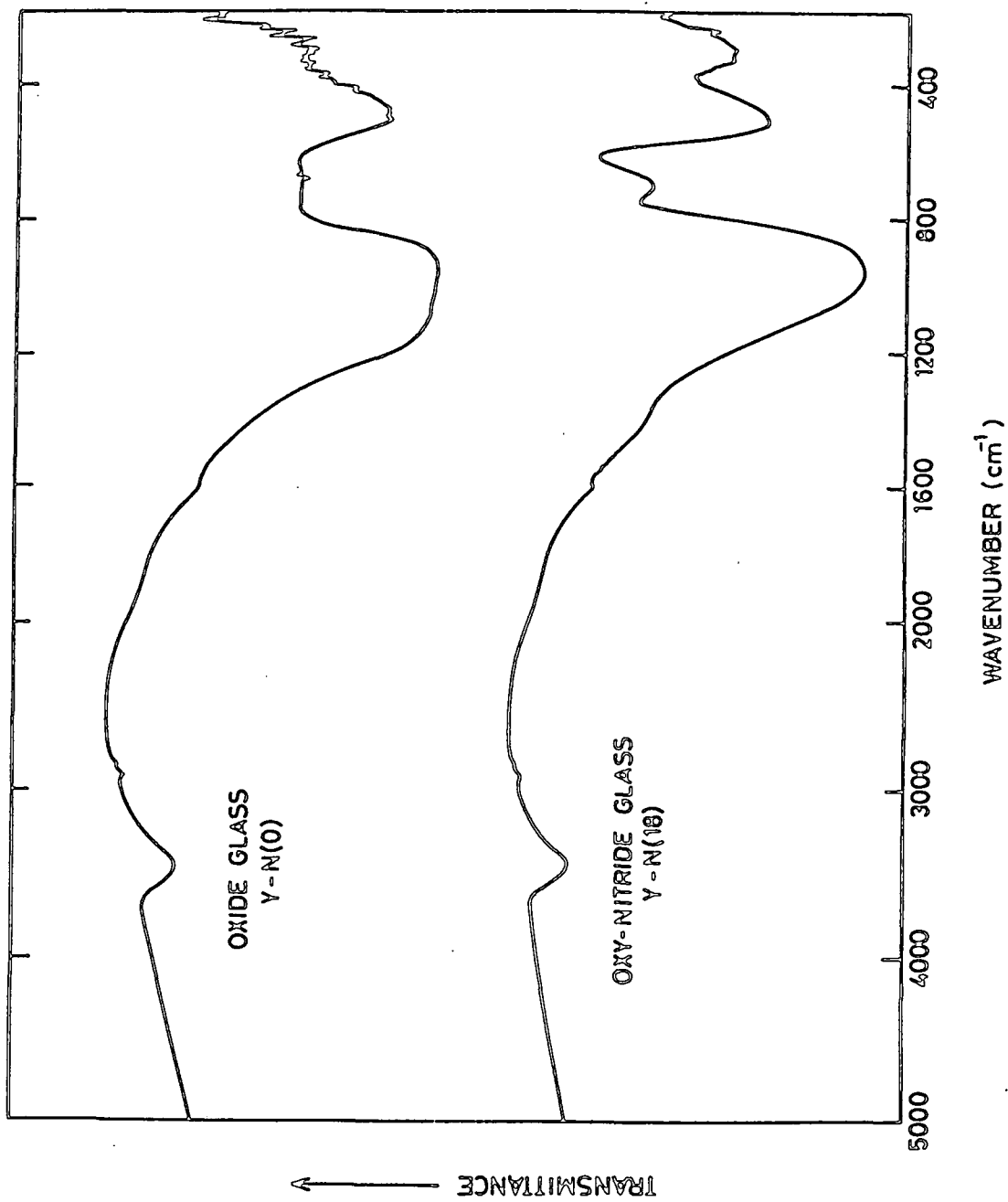


FIG. 7-8. INFRARED SPECTRA OF Y GLASSES

When considering the interpretation of the infra-red spectra it is helpful first to summarise some previous data on similar glass systems, in particular the recent work of Hutton and Thorp [ 7.1 ] on the vibrational spectra of  $\text{MgO-Al}_2\text{O}_3\text{-SiO}_2$  glasses containing  $\text{TiO}_2$ .

The glass batches were prepared from fine powders of  $\text{SiO}_2$ ,  $\text{Al}_2\text{O}_3$ ,  $\text{MgO}$  and  $\text{TiO}_2$ . The base glass components, i.e.  $\text{SiO}_2$ ,  $\text{Al}_2\text{O}_3$  and  $\text{MgO}$  were all of 4N purity, the 100 ppm of impurities being largely refractory oxides similar to the melt components. Total iron group impurities were less than 10 ppm. The  $\text{TiO}_2$  which was added to the base glass was of "specpure" quality with less than 1 ppm of any individual paramagnetic impurity. In all, five glass compositions were founded, four containing  $\text{TiO}_2$ , and a base glass without added titania. The melt compositions are given in Table 7.1.

Melt batches of 100g were founded at  $1600^\circ\text{C}$ , within Pt-Pt 10% Rh crucibles, for a period of 50 h. Periodic stirring in situ prevented fractioning of the melts into layers of varying composition, and seed-free homogeneous melts resulted. Homogeneity was confirmed by test specimens, which after careful annealing, showed only slight birefringence due to residual stress when viewed in a "strain" viewer, there being no indication of composition-induced birefringence.

The annealing temperature ( $T_g$ ) of the base glass was found by differential thermal analysis to be at  $790$  to  $800^\circ\text{C}$ , and since it has been established that optimum "nucleation" temperatures are some 20 to  $50^\circ\text{C}$  above the annealing temperature the samples studied here were heat-treated for 3 h at either  $750$ ,  $800$  or  $850^\circ\text{C}$ . As in the oxy-nitride studies described above, the glasses and ceramics were finely ground and prepared as KBr discs by a standard die-pressing

Reference number	Melt classification & nominal composition	Analytical data (wt%)			
		SiO <sub>2</sub>	Al <sub>2</sub> O <sub>3</sub>	MgO	TiO <sub>2</sub>
Melt 1	Base glass (BG)	60	20	20	0
Melt 2	BG + 0.2% TiO <sub>2</sub>	59.88	19.96	19.96	0.20
Melt 3	BG + 1% TiO <sub>2</sub>	59.41	19.80	19.80	0.99
Melt 4	BG + 5% TiO <sub>2</sub>	57.14	19.05	19.05	4.76
Melt 5	BG + 10% TiO <sub>2</sub>	54.55	18.18	18.18	9.09

TABLE 7.1: Compositions of glasses examined [after Hutton and Thorp]

technique. Room temperature absorption spectra between 2.5 and 40  $\mu\text{m}$ , (4000 to 250  $\text{cm}^{-1}$ ), were measured on a Perkin-Elmer model 475 double beam spectrometer. Fig 7.9 is a composite diagram of the infra-red absorption spectra from glasses 1, 3 and 5, both with and without pre-crystallization heat treatments. The absorption peaks are broad and ill-defined but it is clear that no substantial changes in the spectra have resulted from the addition of  $\text{TiO}_2$  to the base glass composition, or indeed within any particular composition due to pre-crystallization heat treatments. The main "high" and "low" frequency peaks occur at 1080 and 450  $\text{cm}^{-1}$  with shoulders on these peaks at  $\sim 1200$ ,  $\sim 930$  and  $\sim 550$   $\text{cm}^{-1}$ . The absorption on all traces at  $\sim 3500$   $\text{cm}^{-1}$  is due to O-H "group" vibrations [Banwell, 7.2].

The vibrational spectra of  $\alpha$  and  $\beta$  quartz have been successfully computed [Scott and Porto, 7.3, Etchepare et al 7.4] and, assuming a disordered quartz structure, i.e. a distribution of bond angles and strengths around those found in quartz, as a model of vitreous silica [Warren and Bisco, 7.5], the main features of the glassy spectrum have been derived [Borelli and Su, 7.6; Su and Bock, 7.7; Hass, 7.8]. Multicomponent glasses, however, contain silica tetrahedra with one, two, three, or four non-bonding oxygens (nbo), i.e. their basic structural units may be the  $[\text{SiO}_4]$ ,  $[\text{SiO}_4]^{2-}$ ,  $[\text{SiO}_4]^{3-}$ , or the  $[\text{SiO}_4]^{4-}$  groups. Theoretical studies (7.8) have shown that these units incorporated into a crystalline or vitreous material will have characteristic "group" frequencies [7.2]. Thus the existence of these silicate groups in a glass, can, in principle, be inferred by a comparison of the vibrational spectrum of the glass, and the vibrational spectra of crystalline silicates known to contain specific groups. This

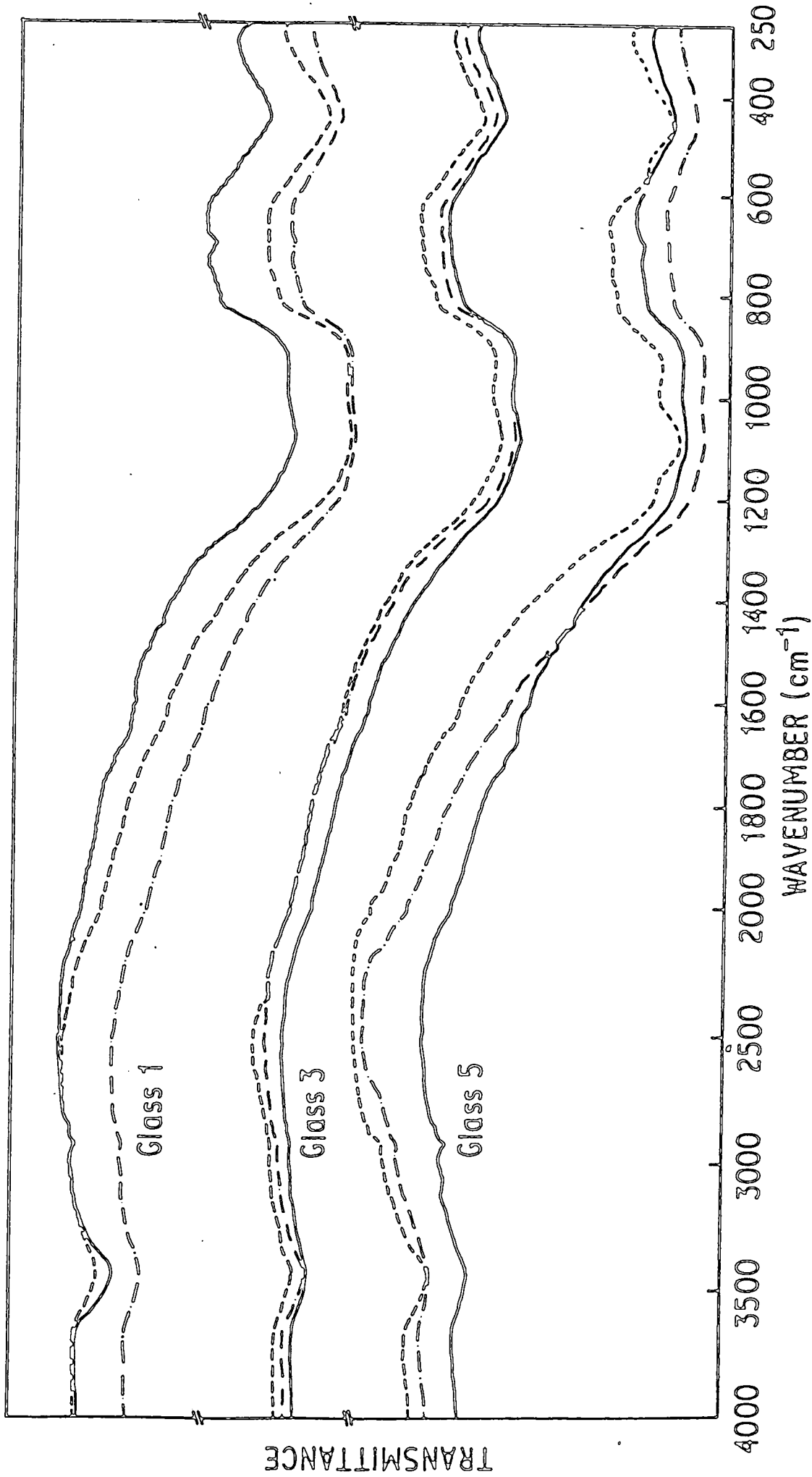


FIG.7.9. Infrared spectra of glasses: (a) no heat treatment —; (b) 750° C for 2½ h — · —; (c) 850° C for 2½ h — — —.

approach has been successfully employed by Konijnendijk [ 7.9 ] in identifying borate groups in borate and boro-silicate glasses.

Most crystalline silica polymorphs, fused silica, and many commercial high silica glasses such as Vycor, have been studied and the main infra-red bands catalogued, [Etchepare et al 7.4; Hass, 7.8; Konijnendijk, 7.9; Wong and Angell, 7.10; Ferraro et al 7.11]. The framework  $[\text{SiO}_4]$  tetrahedron has its main bands (in both glasses and crystals), in the 1070 to 1090  $\text{cm}^{-1}$  and 440 to 480  $\text{cm}^{-1}$  regions. The silicate glasses do mirror the "shift" to lower frequencies which is observed in the main high-frequency crystalline silicate bands when the number of nbos increase. Essentially, bands at frequencies lower than the 1070 to 1080  $\text{cm}^{-1}$  main peak of the framework tetrahedron, become more intense, e.g. in most crystalline metasilicates (  $[\text{SiO}_4]^{2-}$  units), there are three main high-frequency bands in the 850 to 1080  $\text{cm}^{-1}$  region, all of comparable intensity [Hass, 7.8; Estep et al 7.12].

The multiple high-frequency peaks of the crystalline silicates broaden to one or two main peaks in the glassy silicate spectra. At low concentrations of nbos a peak at  $\sim 950 \text{ cm}^{-1}$ , taken by many authors to be indicative of the Si-O terminal stretching mode [Tartre, 7.13; Manghrani et al 7.14; Estep et al 7.15] appears as a shoulder on the intense 1050 to 1080  $\text{cm}^{-1}$  vitreous silica peak. As the glass modifiers increase to the metasilicate ratio, these peaks assume approximately equal intensities. In some systems the above peaks merge to a single broad peak at  $\sim 980 \text{ cm}^{-1}$ .

In most binary silicate glasses and crystals of disilicate and metasilicate compositions, the infra-red absorption in the region of 1200  $\text{cm}^{-1}$  is very weak. Exceptions occur when the glass phases separate

into high silica and high alkali regions [Crozier and Douglas 7.16] ; it is suggested then that the high-frequency part of the spectrum, and in particular the high-frequency shoulder at  $\sim 1200 \text{ cm}^{-1}$  on the main  $\sim 1060 \text{ cm}^{-1}$  peak, is due to the high-silica region, and the band in the region of  $\sim 950 \text{ cm}^{-1}$  is due to the high-alkali phase. This explanation may be applied here, the  $\sim 1200$  and  $930 \text{ cm}^{-1}$  could be characteristic of a high-silica region and a region of disilicate or metasilicate composition. The  $1080 \text{ cm}^{-1}$  band would be common to each of these glass phases.

In conclusion it may be noted that the constancy of the experimental spectra throughout the compositional ranges examined both by Hutton and Thorp and in the present studies on the series of oxy-nitride glasses must be interpreted as a corresponding constancy in the nature of the silicate units within the glass; if there were significant changes in the number of non-bridged oxygen atoms per silica tetrahedron these would be reflected in significant intensity changes in the high-frequency bands. It is also clear that further studies near the  $250 \text{ cm}^{-1}$  region would be beneficial in order to establish firmly whether I.R.-spectroscopy can provide a means for assessing the degree to which nitrogen addition has been successfully accomplished during the preparation of the oxy-nitride glasses. There appears to be little information on the infra-red spectra of nitrogen ceramics in the literature and examination of materials such as silicon nitride, aluminium nitride and possibly magnesium nitride might provide useful reference standards.

## CHAPTER 7

### REFERENCES

- 7.1 W.Hutton and J.S.Thorp  
J.Mat.Sci 20, (1985), 542.
- 7.2 C.N.Banwell "Fundamentals of Molecular Spectroscopy",  
McGraw Hill, New York, 1972.
- 7.3 J.F.Scott, S.P.S.Porto  
Phys.Rev.161, (1967) 903.
- 7.4 J.Etchepare, M.Merian, L.Smetankin  
J.Chem.Phys. 60 (1974), 1873.
- 7.5 B.E.Warren, J.Biscoe  
J.Amer.Ceram.Soc.21 (1938), 49.
- 7.6 N.F.Borelli, G.J.Su,  
Mat.Res.Bull.3, 1968, 181.
- 7.7 G.J.Su, J.Bock  
J.Amer.Ceram.Soc. 53, (1970), 69.
- 7.8 M.Hass  
J.Phys.Chem.Solids 3 (1970), 415.
- 7.9 W.L. Konijnendijk  
Philips Res.Rept.Suppl.1 (1975), 143.
- 7.10 J.Wong, C.A.Angell  
Appl.Spectrosc.Rev.4a, (1971), 155.
- 7.11 J.R.Ferraro, M.H.Manghrani, A.Quattrochi  
Phys.Chem.Glasses 13 (4), (1972), 116.

- 7.12 P.A.Estep, J.J.Kovach, P.Waldstein, C.Karr,  
Geochim Cosmochim Acta Suppl.3, 3 (1972), 3047.
- 7.13 P.Tartre, Physics of Non-crystalline Solids,  
North Holland, Amsterdam, 1975.
- 7.14 M.H.Manghrani, J.R.Ferraro, L.J.Basile  
Appl.Spectrosc. 28, (1974), 256.
- 7.15 P.A.Estep, J.J.Kovach, C.Karr  
Geochim Cosmochim Acta Suppl. 2 (3), (1971), 2137.
- 7.16 D.Crozier, R.W.Douglas  
Phys.Chem.Glasses 6, (6), (1965), 240.

APPENDIX I

Publications Based on the Studies of Oxynitride  
Glasses Described in this Thesis

- I.1 Dielectric properties of some oxynitride glasses  
J.S.Thorp and S.V.J.Kenmuir  
Jour.Mater.Sic(Letters), 16 (1981), 1409.
- I.2 The Dielectric behaviour of Mg-Al-Si, Ca-Al-Si, Y-Al-Si  
and Nd-Al-Si oxynitride glasses  
S.V.J.Kenmuir, J.S.Thorp, B.L.J.Kulesza,  
Jour.Mater.Sci 18, (1983), 1725.
- I.3 High frequency dielectric properties of Mg-Al-Si, Ca-Al-Si,  
and Y-Al-Si oxynitride glasses  
J.S.Thorp, A.B.Ahmad, B.L.J.Kulesza and S.V.J.Kenmuir  
Jour.Mater.Sci 19, (1984), 3211.

APPENDIX II

Publications based on work on magnesium oxide undertaken in addition to the main researches on oxynitride glasses.

II.1 High frequency dielectric properties of MgO, Fe/MgO and Cr/MgO  
J.S.Thorp, B.L.J.Kulesz, W.E.Rad, S.V.J.Kenmuir,  
Jour.Mater.Sci.16, (1981), 1052.

II.2 Dielectric properties of single crystal Co/MgO  
J.S.Thorp, M.D.Hossain, S.V.J.Kenmuir,  
Sol.State Comm.38, (1981), 455.

Copies of these papers are included in this Appendix. The techniques used to make the measurements were the same as those described in detail in the main part of the thesis.

# High-frequency dielectric properties of Mg-Al-Si, Ca-Al-Si and Y-Al-Si oxynitride glasses

J. S. THORP, A. B. AHMAD, B. L. J. KULESZA, S. V. J. KENMUIR

*Department of Applied Physics and Electronics, University of Durham, South Road, Durham, UK*

Recently developed coaxial line techniques [1] have been used to determine, at room temperature, the values of the real ( $\epsilon'$ ) and imaginary ( $\epsilon''$ ) parts of the dielectric constants for some Mg-Al-Si, Ca-Al-Si and Y-Al-Si oxynitride glasses over the frequency range 500 MHz to 5 GHz. The frequency dependencies of  $\epsilon'$  and  $\epsilon''$  are consistent with the universal law of dielectric response in that  $(\epsilon' - \epsilon_\infty) \propto \omega^{(n-1)}$  and  $\epsilon'' \propto \omega^{(n-1)}$  for all glass compositions; the high experimental value of the exponent ( $n = 1.0 \pm 0.1$ ) suggests the limiting form of lattice loss [2] situation. In this frequency range, as previously reported [3] at longer wavelengths, the addition of nitrogen increases the dielectric constant, ( $\epsilon'$ ); in both the oxide and oxynitride glasses  $\epsilon'$  is also influenced by the cation, being increased with cation type in the order magnesium, yttrium, calcium as at lower frequencies.

## 1. Introduction

In 1981 Thorp and Kenmuir [4] reported initial measurements on the dielectric properties of Ca-Al-Si and Mg-Al-Si oxynitride glasses. Room temperature measurements of the dielectric constant and loss factor, using bridge techniques from 500 Hz to 10 kHz, showed that for each particular composition the data fitted well with the universal dielectric response law. It was also found that the addition of nitrogen in the glasses increase  $\epsilon'$  and furthermore that changing from magnesium to calcium increased  $\epsilon'$  in either the pure oxide or oxynitride glasses. Recently, these investigations have been extended by Kenmuir *et al.* [3] to new oxynitride glass systems. Low-frequency bridge techniques were again used to determine the room temperature values of the real ( $\epsilon'$ ) and imaginary ( $\epsilon''$ ) parts of the dielectric constant and also the conductivity ( $\sigma$ ) for some Y-Al-Si and Nd-Al-Si oxynitride glasses and for further compositions in the Mg-Al-Si and Ca-Al-Si systems. Over the range 500 Hz to 10 kHz the frequency dependencies of  $\epsilon'$  and  $\epsilon''$  are consistent with the universal law of dielectric

response,  $(\epsilon' - \epsilon_\infty) \propto \omega^{n-1}$  and  $\sigma(\omega) \propto \omega^n$ . For all compositions examined the experimental value of  $n$  was found to be  $n = 1.0 \pm 0.1$ . In all four systems the addition of nitrogen increased the dielectric constant ( $\epsilon'$ ) while, at each concentration of nitrogen (including the oxide glasses)  $\epsilon'$  increased with cation type in the order magnesium, yttrium, calcium, neodymium. Measurements on the same group of glasses have now been made in the 500 MHz to 5 GHz range in order to establish whether the trends of behaviour found at the lower frequencies were maintained in the higher frequency regions. These measurements were facilitated by the development of precision coaxial line techniques [1] which were themselves initiated by the need encountered in earlier work on doped magnesium oxide for greater precision in the dielectric constant measurements with low loss materials.

## 2. Experimental procedure

### 2.1. Glass compositions

The compositions of the glasses examined, all of which were prepared by the Crystallography

TABLE I Compositions of the Mg-Al-Si, Ca-Al-Si and Y-Al-Si oxynitride glasses examined

Sample	Composition (at %)							% oxygen replaced by nitrogen ( <i>R</i> )	$\epsilon_{\infty}$
	Mg	Ca	Y	Si	Al	O	N		
1	17.0	—	—	17.0	6.0	60.0	0	0	2.46
2	17.0	—	—	17.2	6.4	55.1	4.1	8.1	2.62
3	17.4	—	—	17.4	6.6	51.0	7.6	14.8	2.71
4	—	17.0	—	17.0	6.0	60.0	0	0	2.59
5	—	17.2	—	17.2	6.4	55.1	4.1	8.1	2.73
6	—	17.2	—	17.2	6.5	54.2	4.9	9.8	2.77
7	—	17.3	—	17.3	6.5	53.1	5.8	11.5	2.80
8	—	17.4	—	17.4	6.6	51.0	7.6	14.8	2.84
9	—	—	11.8	17.8	6.8	63.6	0	0	2.76
10	—	—	12.3	18.5	7.1	54.2	7.9	14.8	3.05

Laboratory, University of Newcastle upon Tyne [5], are given in Table I. The compositions were varied systematically and each of the three cation systems (magnesium, calcium and yttrium) included an oxide glass without nitrogen. The oxynitrides of the system were formed by substituting chemical equivalents of nitrogen for proportions of the oxygen of the oxide glass. The percentage of oxygen replaced in this way (*R*) is given in Table I for each of the oxynitride compositions. The proportions of other elements were held constant, and the same system was followed between the different cation series, which therefore contained equal chemical equivalents of either magnesium, calcium or yttrium. The ratio of (total positive valence)/(total negative valences) did not vary with either nitrogen concentration or cation type, and was equal to one for all the materials investigated. Table I also includes the limiting high-frequency dielectric constant,  $\epsilon_{\infty}$ , deduced from optical refractive index measurements [5].

## 2.2. Measurement methods

The measurements were made using coaxial line methods in which a disc-shaped sample is fitted in a coaxial holder terminated by either a short-circuit, a matched termination or a resonance circuit; the details of these techniques have been described recently by Kulesza *et al.* [1]. For these measurements circular samples of about 6.5 mm diameter and 0.5 mm thick were cut from the bulk oxynitride glasses using conventional diamond cutting methods and polished with diamond paste to 0.25  $\mu\text{m}$  finishes. The coaxial line with short-circuit termination proved most suitable for the determination of  $\epsilon'$  in the frequency range 500 MHz to 5 GHz while the coaxial line resonance

method was found to be preferable for  $\epsilon''$  determination. The matched termination method gave reliable answers only below about 1 GHz and was more suitable for the lower dielectric constant compositions. Above 5 GHz the voltage standing wave ratio (VSWR) measured by the coaxial line resonance method becomes very high, thus effectively setting an upper frequency limit of about 5 GHz for the loss measurements on these glasses. All the data were obtained at room temperature.

## 3. Results

The variations of  $\log(\epsilon' - \epsilon_{\infty})$  with  $\log(f)$  for the different compositions are given in Fig. 1. The values of  $\epsilon_{\infty}$  were calculated from the optical refractive index data given by Drew [5] and are included for reference purposes in Table I. Each composition showed a linear variation. The slopes of the plots were independent of composition and have the value  $1.0 \pm 0.1$  for all specimens. (It may be noted here that, since there are likely to be some other loss processes between the microwave and optical regions, the optical refractive index may not be the relevant value for the purpose of the present investigation.) At any given frequency the value of  $\epsilon'$  depended markedly on composition, increasing as nitrogen concentration increased and varying with cation type. The corresponding loss ( $\epsilon''$ ) behaviour is shown in Fig. 2 and this shows that over the extended frequency range from 0.5 to 9 GHz the loss for each particular composition is almost independent of frequency. The observed power law dependences of both  $\epsilon'$  and  $\epsilon''$  on frequency are consistent with the universal dielectric response law in solids [6–8] in that  $(\epsilon' - \epsilon_{\infty}) \propto \omega^{n-1}$  and  $\epsilon'' \propto \omega^{n-1}$ . For each composition the values of *n* found from Figs. 1 and 2 agree within

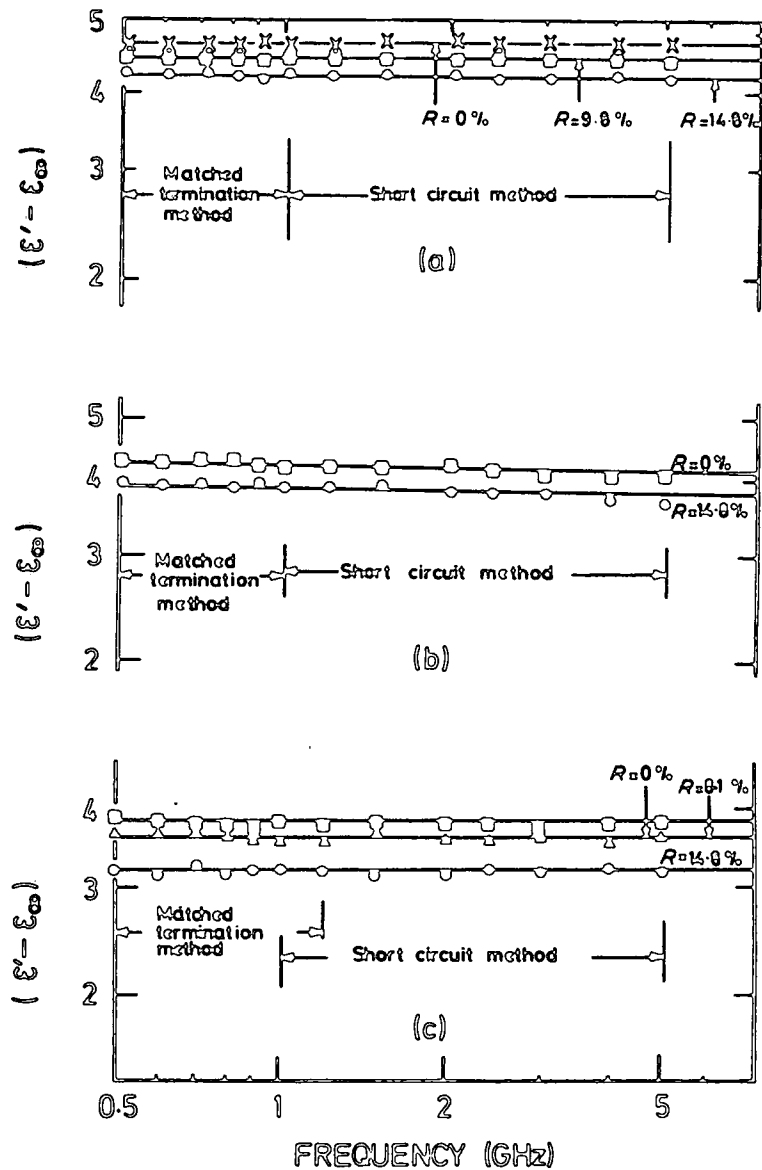


Figure 1 Variation of reduced dielectric constant ( $\epsilon' - \epsilon_{\infty}$ ) with frequency; (a) calcium glasses, (b) yttrium glasses, (c) magnesium glasses.

experimental error and the observation of the same value of  $n$  for all the specimens suggests that, at room temperature in this extended frequency range, the dielectric polarization and loss in all the compositions examined results from the same mechanism, and that this mechanism has not been changed by the substitution of nitrogen for oxygen.

The nature of the changes in dielectric behaviour caused by the substitution of nitrogen for oxygen becomes more apparent when the dielectric constant ( $\epsilon'$ ) and  $\tan \delta$  values are plotted

against the nitrogen concentration at a single frequency for all the compositions examined. In order to provide a more consistent comparison of the nitrogen dependence of different cation systems, the nitrogen concentration has been expressed as a percentage of the oxygen of the appropriate oxide glass for which nitrogen has been substituted ( $R\%$ ). Fig. 3 shows the variation of dielectric constant ( $\epsilon'$ ) with nitrogen concentration at a frequency of 1 GHz ( $\omega \approx 6.3 \times 10^9$ ). Fig. 4 shows the corresponding variation of  $\tan \delta$  with nitrogen concentration at 1 GHz and the

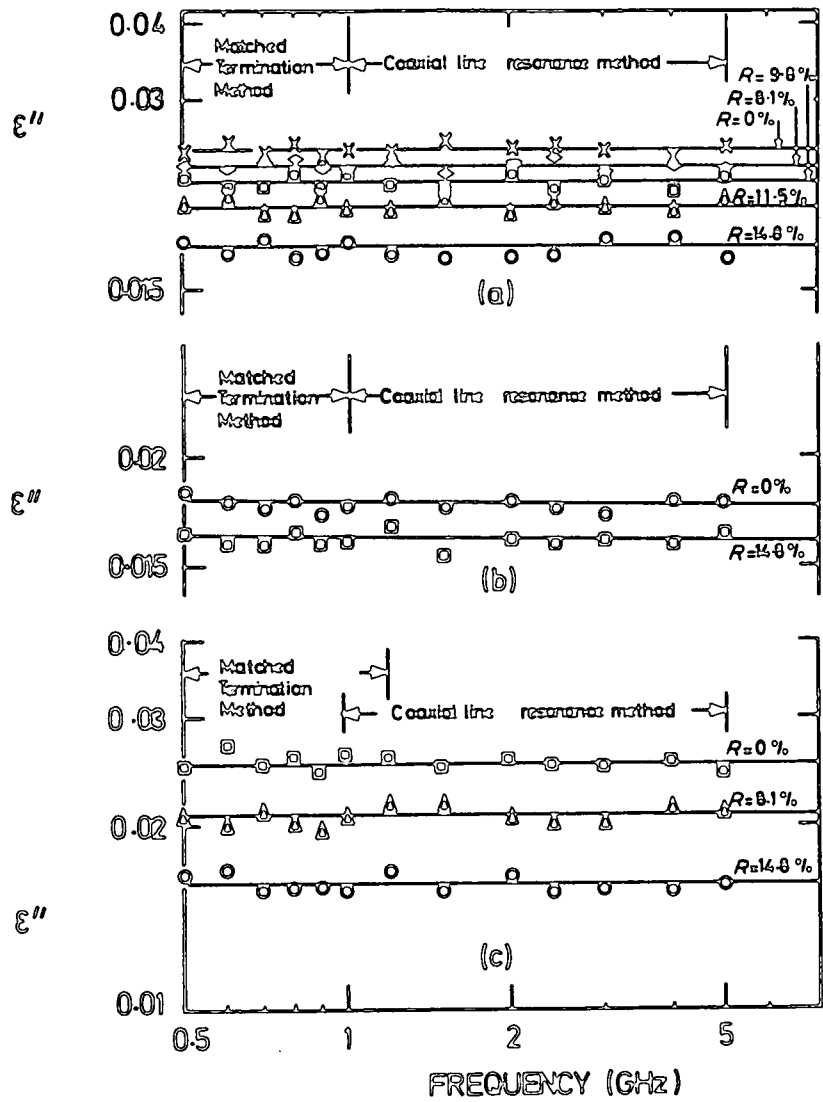


Figure 2 Variation of loss  $\epsilon''$  with frequency; (a) calcium glasses, (b) yttrium glasses, (c) magnesium glasses.

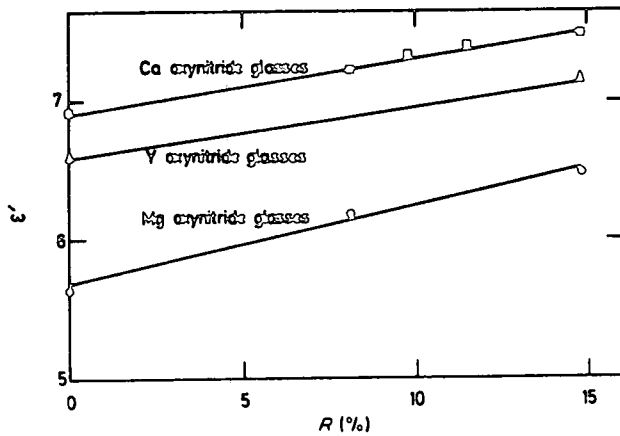


Figure 3 Variation of dielectric constant  $\epsilon'$  with % oxygen replaced by nitrogen in oxy-nitride glasses; 1 GHz data.

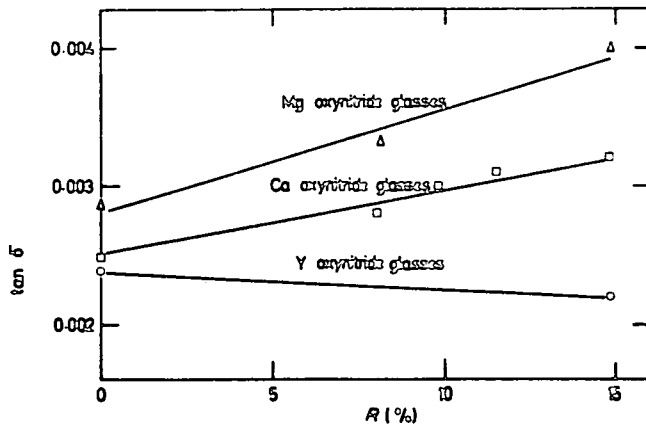


Figure 4 Variation of loss tangent with % oxygen replaced by nitrogen in oxynitride glasses; 1 GHz data.

results obtained for  $\epsilon'$ ,  $\epsilon''$  and  $\tan \delta$  are summarized in Table II.

#### 4. Discussion

Since the present measurements, made over the frequency range 500 MHz to 5 GHz, and the previous observations, made by Thorp *et al.* [3] over the lower frequency region from 500 Hz to 20 kHz, were all taken with the same series of oxynitride glass samples, a unique opportunity exists for assessing the dielectric behaviour over this very extensive frequency range. A number of important features are revealed.

For each individual glass composition the frequency dependencies of both the dielectric constant  $\epsilon'$  and loss  $\epsilon''$  are consistent with the universal law of dielectric response. Taking the results for all the individual compositions collectively reveals that this whole group of rigid ceramics gives dielectric behaviour corresponding to the limiting form of "lattice loss" [2] in which most dipolar processes have been eliminated and frequency inde-

pendent loss is expected. This is not common though it is interesting to note that similar properties have been reported both for doped magnesium oxide [9], a rigid refractory oxide ceramic and for several sialon materials [10], high frequency refractory ceramics containing oxygen and nitrogen.

A second point of interest is to note the range of values of  $\epsilon'$  which can be obtained by compositional changes in the glass system. At the lowest extreme one finds  $\epsilon' \approx 5.6$  at 1 GHz for magnesium oxide glass and at the highest  $\epsilon' = 11.6$  at 1 kHz for a neodymium oxynitride glass containing 8.8 at% nitrogen. This wide range suggests potential for the choice of special glasses where dielectric matching is important, e.g. in substrate materials for devices. In the oxide glasses  $\epsilon'$  is dependent on the cation type and increase in the order magnesium, yttrium, calcium, neodymium while in all the systems the addition of nitrogen increased  $\epsilon'$ . It should be noted, however, that there are limits to the latter method for increasing  $\epsilon'$  since, depending on the particular system, the maximum nitrogen solubility lies in the range 10 to 15 at%, the highest nitrogen-containing glasses so far produced [5] being in the Y-Si-Al-O-N system. It would be of interest to compare simpler oxide and nitride systems (e.g.  $\text{Al}_2\text{O}_3$  and  $\text{AlN}$ ;  $\text{SiO}_2$  and  $\text{Si}_3\text{N}_4$ ) to find whether there are generalized behaviour rules for nitrogen substitution or whether the effects described above are specific to the oxynitride glasses examined here. A similar increase in  $\epsilon'$  when 1.5 at% nitrogen was substituted for the same amount of oxygen in an yttrium oxynitride glass has been reported by Loehman [11] and by Leedecke and Loehman [12].

A third feature revealed by a comparison of the

TABLE II Dielectric properties of Mg-Al-Si, Y-Al-Si and Ca-Al-Si oxynitride glasses at 1 GHz

Oxynitride glass systems	% oxygen replaced by nitrogen (R)	$\epsilon'$	$\epsilon''$	$\tan \delta \times 10^3$
Mg	0	5.64	0.016	2.87
	8.1	6.18	0.021	3.32
	14.8	6.48	0.026	4.00
Y	0	6.60	0.017	2.51
	14.8	7.14	0.014	2.00
Ca	0	6.93	0.017	2.48
	8.1	7.22	0.020	2.81
	9.8	7.31	0.022	3.00
	11.5	7.39	0.023	3.10
	14.8	7.49	0.024	3.23

measurements in the different frequency ranges relates to the cation order found to give increasing values of the dielectric constant  $\epsilon'$ . This feature may most easily be demonstrated by reference to the oxide glasses. At low frequencies [3] it can be stated quite definitely that  $\epsilon'$  increases with change in the cation in the order  $Mg < Y < Ca < Nd$ ; here the differences in  $\epsilon'$  between compositions are very much greater than any possible experimental errors so that the trend is firmly established. A similar result has now been found at the higher frequencies (between 500 MHz and 5 GHz) and these coaxial line measurements confirm that  $\epsilon'$  increases in the order  $Mg < Y < Ca$ .

Some remarks may be made in conclusion regarding the influence of nitrogen substitution on the dielectric loss  $\epsilon''$ . Unlike the behaviour of the dielectric constant  $\epsilon'$  the dependence of dielectric loss on nitrogen concentration varied from system to system. The measurements in the lower frequency range showed that an increase in nitrogen concentration produced a relatively large increase in  $\tan \delta$  in the magnesium glasses and a smaller though definite increase in the calcium glasses; by contrast a small decrease was observed in the yttrium glasses. The difference in behaviour has been confirmed by the new measurements in the higher frequency range. Substitution of 14.8% oxygen by nitrogen increased  $\tan \delta$  by 39% for magnesium glasses, by 22% for calcium glasses and decreased  $\tan \delta$  by 16% for yttrium glasses (Fig. 4). These figures may be compared with those of Kenmuir *et al.* [3] where increases of 55% and 13% for magnesium and calcium glasses, and a decrease of 20% for yttrium glasses were observed between 500 Hz and 10 kHz for the same increase in nitrogen concentration. It is interesting to note the close similarity between the values obtained in the two frequency ranges and further that the contrast in behaviour between the yttrium glasses and the others has been confirmed. If the changes in dielectric loss are to be attributed to changes in the chemical bonding there seems no obvious reason why the yttrium ion should differ so markedly from both calcium and magnesium. It

must be borne in mind, however, that, at the present stage of development of the preparative techniques for making the oxynitride glasses, there may be other impurities present at low levels and that the measured dielectric loss may be determined by these rather than being a direct monitor of the changes in cation-oxygen or cation-nitrogen bonding schemes.

#### Acknowledgements

We wish to express our appreciation to Professor K. H. Jack and Dr D. Thompson (Crystallography Laboratory, University of Newcastle-upon-Tyne) for supplying the glasses and for many helpful discussions throughout the course of the research, and also to C. Savage, T. Harcourt, W. Mounsey and P. Richardson for their assistance with the preparation of test samples and the construction of sample holders. A. B. Ahmad wishes to thank the University of Malaya for support during study leave.

#### References

1. B. L. J. KULESZA, J. S. THORP and A. B. AHMAD, *J. Mater. Sci.*, 19 (1984) 915.
2. A. K. JONSCHER, *ibid.* 16 (1981) 2037.
3. S. V. J. KENMUIR, J. S. THORP and B. L. J. KULESZA, *ibid.* 18 (1983) 1725.
4. J. S. THORP and S. V. J. KENMUIR, *ibid.* 16 (1981) 1407.
5. R. A. L. DREW, PhD thesis, University of Newcastle-upon-Tyne (1980).
6. A. K. JONSCHER, *J. Phys. C Solid State Physics* 6 (1973) 235.
7. *Idem*, *Nature* 267 (1977) 719.
8. *Idem*, *Thin Solid Films* 36 (1978) 1.
9. J. S. THORP, B. L. J. KULESZA, N. E. RAD and S. V. J. KENMUIR, *J. Mater. Sci.* 16 (1981) 1052.
10. J. S. THORP and R. I. SHARIF, *ibid.* 12 (1980) 2274.
11. R. E. LOEHMAN, *J. Amer. Ceram. Soc.* 62 (1979) 49.
12. C. J. LEEDECKE and R. E. LOEHMAN, *ibid.* 63 (1980) 190.

Received 17 June

and accepted 29 November 1983

## DIELECTRIC PROPERTIES OF SINGLE CRYSTAL Co/MgO

J.S. Thorp, M.D. Hossain<sup>o</sup> and S.V.J. Kenmuir

Department of Applied Physics and Electronics, University of Durham, England

(Received 19 August 1980 by C.W. McCombie)

The dielectric constants of single crystal MgO doped with cobalt have been measured at room temperature from 500 Hz to 15 KHz. The cobalt concentrations varied from 310 to 9900 ppm. For all specimens the a.c. conductivity fitted well to the relation  $\sigma \propto \omega^n$  with  $n = 0.90 \pm 0.10$ . In contrast to the behaviour of single crystal MgO doped with trivalent iron or chromium, previously reported [1], the addition of divalent cobalt does not appear to increase the conductivity in the frequency range examined.

IN RECENT publications [1, 2] some results have been given of the dielectric behaviour of pure MgO single crystals and of crystals doped with iron or chromium. The first of these reported the room temperature variations of the real ( $\epsilon'$ ) and imaginary ( $\epsilon''$ ) parts of the dielectric constant with frequency at low frequencies while the second showed that the characteristic trends evident in the low frequency range held over the whole range to 9 GHz. Notable among these characteristics were that the a.c. conductivity ( $\sigma_{a.c.}$ ) varied as  $\sigma_{a.c.} \propto \omega^n$  with  $n = 0.98 \pm 0.02$  for both pure and doped crystals and that the addition of either of the trivalent ions  $\text{Fe}^{3+}$  or  $\text{Cr}^{3+}$  increased  $\sigma_{a.c.}$  (at any particular frequency). The change in  $\sigma_{a.c.}$  increased with dopant concentration (being more pronounced with  $\text{Fe}^{3+}$  than  $\text{Cr}^{3+}$ ) and it was suggested that this might in part arise from the introduction of additional vacancies created by the substitution of a trivalent ion for the divalent  $\text{Mg}^{2+}$ .

In order to test this hypothesis preliminary studies have now been made on a range of Co/MgO single crystals. Complementary electron spin resonance measurements made on the same crystals [3] showed that the cobalt entered the lattice as  $\text{Co}^{2+}$  occupying magnesium sites; consequently, no additional vacancies would be expected. The concentrations used ranged from 310 ppm, giving a light pink crystal, to 9900 ppm, giving a deep pink colouration. All the single crystals were grown by electro-fusion and were supplied (together with optical spectrographic determinations of cobalt concentrations) by W.C. Spicer (Cheltenham) Ltd. The measurements of  $\epsilon'$  and  $\epsilon''$  were made at room temperature using low frequency bridge techniques similar to those described previously [1, 2] and

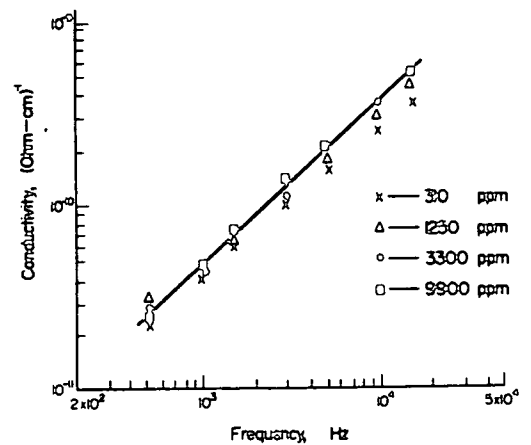


Fig. 1. The frequency dependence of conductivity;  $\text{Co}^{2+}/\text{MgO}$ , 293 K.

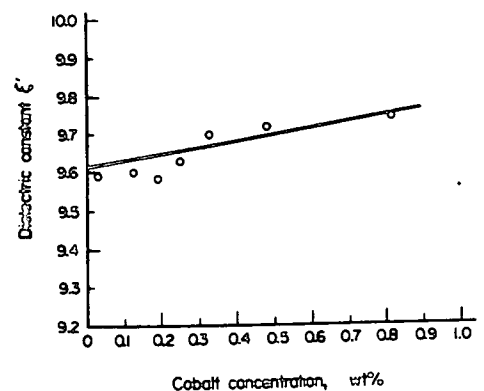


Fig. 2. The variation of dielectric constant  $\epsilon'$  with cobalt concentration for  $\text{Co}^{2+}/\text{MgO}$ ; 293 K, 1.592 KHz.

application of edge effect corrections enabled an overall accuracy of  $\pm 6\%$  to be obtained.

The variation of  $\log(\sigma_{a.c.})$  with  $\log \omega$  is shown in

<sup>o</sup> On study leave from Department of Applied Physics and Electronics, Rajshahi University, Bangladesh.

Fig. 1. It may be noted firstly that, for all the cobalt concentrations examined, the data fits the Universal dielectric law [4] in that  $\sigma_{a.c.} \propto \omega^n$  with  $n = 0.90 \pm 0.1$ ; this effect is similar to that observed in Fe/MgO and Cr/MgO and indicates that the same type of conductivity mechanism applies with all three dopants. The second feature of importance is that, at any particular frequency the values of conductivity for crystals of quite widely different cobalt concentration are constant to within experimental error; in this frequency range there is no evidence for significant increases in conductivity due to the addition of cobalt comparable to those due to iron and chromium and this supports the hypothesis outlined above.

Measurements of  $\epsilon'$  have also been made at room temperature, (Fig. 2) and these show that there is a small but systematic increase in  $\epsilon'$  as the cobalt concentration is raised. This is consistent with the fact that the value of  $\epsilon' = 12.9$  reported by Young and Frederikse for pure CoO, which corresponds to 100% of the available

magnesium sites being occupied by  $\text{Co}^{2+}$ , is significantly higher than the values reported for pure MgO [1, 2]. Although the concentrations at present available are too limited at the higher levels to enable accurate extrapolation to the point corresponding to pure CoO, extrapolation to zero concentration yields  $\epsilon' = 9.62$  which is in agreement with the value reported by Thorp and Rad [1, 2] for pure MgO.

*Acknowledgements* – S.V.J. Kenmuir wishes to thank the Science Research Council for the award of a post-graduate studentship.

#### REFERENCES

1. J.S. Thorp & N. Enayati-Rad, *J. Mat. Sci.* (to be published).
2. N. Enayati-Rad, Ph.D. Thesis, University of Durham (1980).
3. J.S. Thorp, M.D. Hossain, L.J.C. Bluck & T.G. Bushell, *J. Mat. Sci.* 15, 903 (1980).
4. A.K. Jonscher, *Nature* 267, 673 (1977).

